THESIS

This is to certify that the

dissertation entitled

Adsorption: A Study Adapting Cubic Equations of State

presented by

Ramkumar Subramanian

has been accepted towards fulfillment
of the requirements for

Ph.D. degree in Chemical Engineering

Carl T. Lira
Major professor

Date 10/10/95

MSU is an Affirmative Action/Equal Opportunity Institution O-12771

LIBRARY
Michigan State
University

PLACE IN RETURN BOX to remove this checkout from your record.
TO AVOID FINES return on or before date due.

DATE DUE	DATE DUE	DATE DUE
SEP 1 0 2000		
0 9 1 2 0 1		

MSU Is An Affirmative Action/Equal Opportunity Institution
c:\circ\datedue.pm3-p.1

ADSORPTION: A STUDY ADAPTING CUBIC EQUATIONS OF STATE

By

Ramkumar Subramanian

A DISSERTATION

Submitted to
Michigan State University
in partial fulfillment of the requirements
for the degree of

DOCTOR OF PHILOSOPHY

Department of Chemical Engineering

1995

ABSTRACT

ADSORPTION: A STUDY ADAPTING CUBIC EQUATIONS OF STATE

By

Ramkumar Subramanian

The Simplified Local Density (SLD) method is a new engineering approach to model adsorption based on spatial invariance of the chemical potential along with an equation of state. This work extends previous pure fluid applications to binary mixtures and more complex adsorbent geometries (slits, pores). Model predictions are compared to molecular simulations and experimental data. The SLD model can represent adsorption isotherms of Types I-V at subcritical conditions. Supercritical behavior has not been classified, however the SLD approach can accurately represent the complex behavior exhibited at supercritical conditions. In addition, clustering (molecular charisma) in supercritical fluids is modeled by representing infinite dilution by calculating the fluid density in the region around a single solute molecule.

Simple engineering models such as Langmuir and Freundlich cannot represent the variety of experimental adsorption isotherm shapes. On the other hand, molecular simulations represent the behavior, but are not suitable for routine process design. This SLD approach bridges the gap by retaining both the essential physics of the adsorption problem and the simplicity of an equation of state. The SLD approach is demonstrated to be a powerful engineering tool for prediction of adsorption, and requires fewer parameters than previous engineering models. In addition, the SLD approach can be

extended to non-ideal gas phase regions without additional parameters. The single parameter used for each adsorbate is temperature- and pressure-independent, permitting extrapolations and predictions of adsorption behavior.

Dedicated to my parents Krishnambal Subramanian & K. R. Subramanian, to my sisters Shyamala Nageswaran & Rama Ganesh, and to my late Kadayam grand father

Acknowledgments

First of all, I would like to thank my advisor, Dr. Carl Lira, for his guidance throughout my research, and also for his patience during tough times. I would like to thank Drs. D. J. Miller, R. E. Buxbaum and P. M. Duxbury for serving on my committee and for making appropriate suggestions to guide my research. I would like to thank Dr. Bharath Rangarajan for all the discussions that we have had during this research, and for his valuable suggestions.

I would like to thank Arvind and Shalini Mathur for helping me during times of need and for their wonderful company throughout my stay here in East Lansing. I would like to thank my wonderful roommates S. Iyer, and R. Easwar for being the best companions anyone could ask for. I would like to thank Sanjay Yedur for all the wonderful times we spent at coffee shops discussing worldly matters! I would like to thank Mike Bly, Sanjay Padaki, Valerie Adegbite, Satyadev Chilukuri, Kartik Pashupati, Nishant Rao and other unnamed friends for all their support and friendship during my stay at Michigan State. I would like to thank the secretaries, Faith, Julie, Beth and Candy for being so wonderful. I would like to thank my parents Mr. and Mrs. K. R. Subramanian, and my sisters, Shyamala and Rama for supporting me throughout my study. Finally, I would like to thank my wife Jayashree for her love and understanding for the last few months.

Michigan State is a great place to live and to study, and for the last six years I have had the greatest time of my life. Thank you Michigan State, and Go Spartans!

Table of Contents

Table of Contents (contd.)

List of Tables

List of Figures

Nomenclature (SLD Model)

a, b	Constants of the van der Waals or Peng-Robinson equation
f	fugacity
$g(r)$	radial distribution function
N_A	Avagadro's number
P	pressure
T	temperature
z	distance from surface of the wall. Intermolecular distance is $z+\sigma_{fs}/2$
Z	compressibility factor
k	Boltzmann's constant
ν	molar volume
n^{ex}	number of molecules
A_S	Surface Area

Greek

Γ^{ex}	surface excess
ϕ	fluid-fluid pair potential
μ	chemical potential
Ψ	fluid-wall potential (physical adsorption), fluid (solvent)-solute potential (clustering)
ρ	molar density
σ	molecular diameter
ε	pair interaction parameter

Subscripts

att	attractive property
rep	repulsive property
ff	contribution due to fluid-fluid interaction
f	fluid property
s	solid or solute property (in clustering)
fs	contribution due to fluid-solid interaction (physical adsorption) or fluid (solvent)-solute interaction (clustering)
b	bulk property (uniform fluid)
o	standard state

CHAPTER 1: INTRODUCTION

Physical adsorption is a separation process in which certain components of a fluid phase are transferred on to the surface of a solid adsorbent [McCabe, Smith & Harriott, 1984]. It is the result of intermolecular forces of attraction between the fluid and solid molecules. If the attractive force of the solid on the fluid is greater than the intermolecular forces among the fluid themselves, the fluid will condense upon the surface of the adsorbent [Treybal, 1983],and may be accompanied by the evolution of heat. In engineering applications, adsorption is usually used an alternate to extraction. Adsorption tends to have a smaller capacity but a higher selectivity than extraction. It can also be more gentle for e.g. proteins may be denatured by organic extraction but may be adsorbed. Separation processes using adsorption are on the increase while those using extraction are on the decrease [Belter, Cussler & Wu, 1988].

Physical adsorption is used in gas purification processes such as the removal of volatile organic compounds from stack gases, as a means of fractionating fluids that are difficult to separate by other methods, and in adsorbent regenerations using supercritical fluids [Tan and Liou, 1988, 1990]. Physical adsorption is also of interest in transportation and storage of fuel and radioactive gases, separation and purification of lower hydrocarbons, solid-phase extractions fluids, in supercritical extractions and chromatography [Findenegg, 1983; Barton, 1983; Strubinger and Parcher, 1989], and in critical point drying [Rangarajan and Lira, 1992]. Understanding the thermodynamics and

structure of the gas- solid interface is essential to the understanding of heterogeneous catalysis and wetting phenomena [Findenegg, 1983]. While there are a large number of theoretical and experimental studies of adsorption below the critical temperature, there are few studies of adsorption near or above the critical temperature of the fluid. Such studies are especially relevant to the storage of methane at ambient temperatures ($T_r = 1.57$) at reasonably high densities.

Theoretical approaches to understanding and predicting adsorption range from simple empirical fits (Freundlich/Toth isotherms) to theoretically-sound methods such as molecular dynamics (MD) and Monte-Carlo (MC) simulations. Computer simulations such as the grand canonical ensemble Monte-Carlo semi-quantitatively predict the cusp-like behavior near the critical point [van Megan and Snook, 1982]. However, such methods are computationally intensive. Simulations are difficult near the critical point due to fluctuations, and require a large number of molecules and consequently significant amounts of supercomputer time. Statistical mechanical theories such as the density functional theory are also computationally intensive although they are about two orders of magnitude faster than computer simulations [Gubbins, 1990]. On the other hand, the traditional empirical and semi-empirical methods which are computationally undemanding are unable to account for the wide variety of shapes of adsorption isotherms seen near the critical region. There is an engineering need for a model that bridges the gap between the simple and sophisticated models, and has predictive capability. Further, the development of processes utilizing supercritical fluids requires engineering models capable of spanning large pressure ranges. Experiments with supercritical fluids are more difficult and

expensive than experiments at atmospheric conditions, and a model that can predict supercritical behavior would be a well-received developmental tool.

The focus of this thesis is to develop the simplified local density (SLD) model, and demonstrate its application in predicting pure fluid adsorption isotherms over wide pressure and temperature ranges by comparing model predictions with experimental data from literature. The SLD model developed in this work superimposes the fluid-solid interaction potential on the van der Waals and Peng-Robinson equations-of-state. My intention is to present the concepts necessary to adapt common cubic equations of state for describing the adsorption phenomenon. The SLD model is intended to bridge the gap between the computationally intensive but more theoretically sound statistical mechanical models and the undemanding, empirical methods. The SLD concept should be a useful engineering supplement to other available models, and is not intended as a replacement for the statistical mechanical models.

With the above objectives, the thesis has been divided into the following chapters:

1) Introduction

2) Background, Literature Review and Preliminary Results.

3) Quantitative Modeling of Adsorption and Extension of the SLD Approach to Predict Clustering

4) Adsorption of Pure Gases in Slits and Pores, and Adsorption of Binary Mixtures

5) Conclusions and Recommendations

In chapter 2, a detailed literature survey of the various theories of adsorption is given, followed by the development of the van der Waals SLD model. High pressure experimental adsorption data that show fascinating behavior are also given in this chapter. The basic assumptions leading to the SLD model, and the model equations are described in this chapter..

In chapter 3, the van der Waals equation is replaced by the Peng-Robinson equation-of-state, thus making the model a quantitative predictive model. Model results for adsorption on flat walls are compared to experimental data. The model is modified to describe clustering in supercritical fluids, and model predictions are compared to experimental fluorescence spectra.

The model is extended to describe adsorption in slits and cylindrical pores in chapter 4. Model predictions for adsorption of pure fluids are compared to both experimental data and molecular simulations. The model is extended to describe adsorption of binary mixtures in slits. Model predictions of both the concentration and amount adsorbed are compared with experimental data.

Finally, the results of this model are summarized in chapter 5, followed by recommendations for future work.

CHAPTER 2: BACKGROUND, LITERATURE REVIEW AND PRELIMINARY RESULTS

DEFINITION

While several different methods are used to measure adsorption, adsorption is unambiguously defined by the surface excess, the excess moles per unit area.

$$\Gamma^{ex} = \frac{n^{ex}}{A_s} = \int_{z_o}^{\infty} [\rho(z) - \rho_b] dz \qquad [2\text{-}1]$$

where $\rho(z)$ is the density at a distance z from the wall, and ρ_b the bulk density. z_o is often defined as the plane above the surface of the solid where the fluid-solid potential is zero.

Before reviewing the theories for adsorption, some experimental results will be presented. Reliable experimental measurements of adsorption of fluids on well characterized solids are essential in order to test different theories of adsorption. While most commercial adsorbents are porous and heterogeneous, graphitized carbon black (g.c.b.) or exfoliated graphite or the basal planes of graphite provides an atomically smooth homogeneous and non-porous surface to study adsorption. Graphitized carbon black (or Graphon) provides the ideal surface to understand physical adsorption and wetting, and theories for adsorption on homogeneous surfaces can be extended to heterogeneous and porous materials. Some of the best data available are those of Findenegg and co-workers who have examined the adsorption of a variety of gases such as ethylene, propane, meth-

ane, krypton and argon on graphon [Findenegg, 1984; Specovius and Findenegg, 1978, 1980]. Some of their results are presented in Figures 2.1 - 2.3, where one sees the adsorption isotherms of subcritical propane and ethylene, near-critical propane and ethylene, and supercritical ethylene and krypton, on graphon.

CLASSIFICATION OF ADSORPTION ISOTHERMS

Adsorption isotherms (subcritical) are classified into six types [Sing et al., 1982; Sing 1983], as shown in Figure 2.4. Type I isotherms are normally seen in microporous adsorbents, Type IV & V on mesoporous adsorbents and Type II, III and VI on non-porous adsorbents. Types III & V are similar to Types II & IV respectively except for the stronger magnitude of the adsorbate-adsorbent interaction in the latter cases. Type VI isotherms indicate layering, and are observed for the adsorption of Ar/Kr on g.c.b. at low (liquid N_2) temperatures [Bienfait 1980 and references therein].

ADSORPTION MODELS

In this section some of the basic theories for physical adsorption will be briefly reviewed. There is an enormous amount of literature available on adsorption and the reader is referred to several monographs [Young and Crowell, 1962; Brunauer, 1945; de Boer, 1953; Defay and Prigogine, 1966; Nicholson and Parsonage, 1982; Yang, 1987; Lee, 1988].

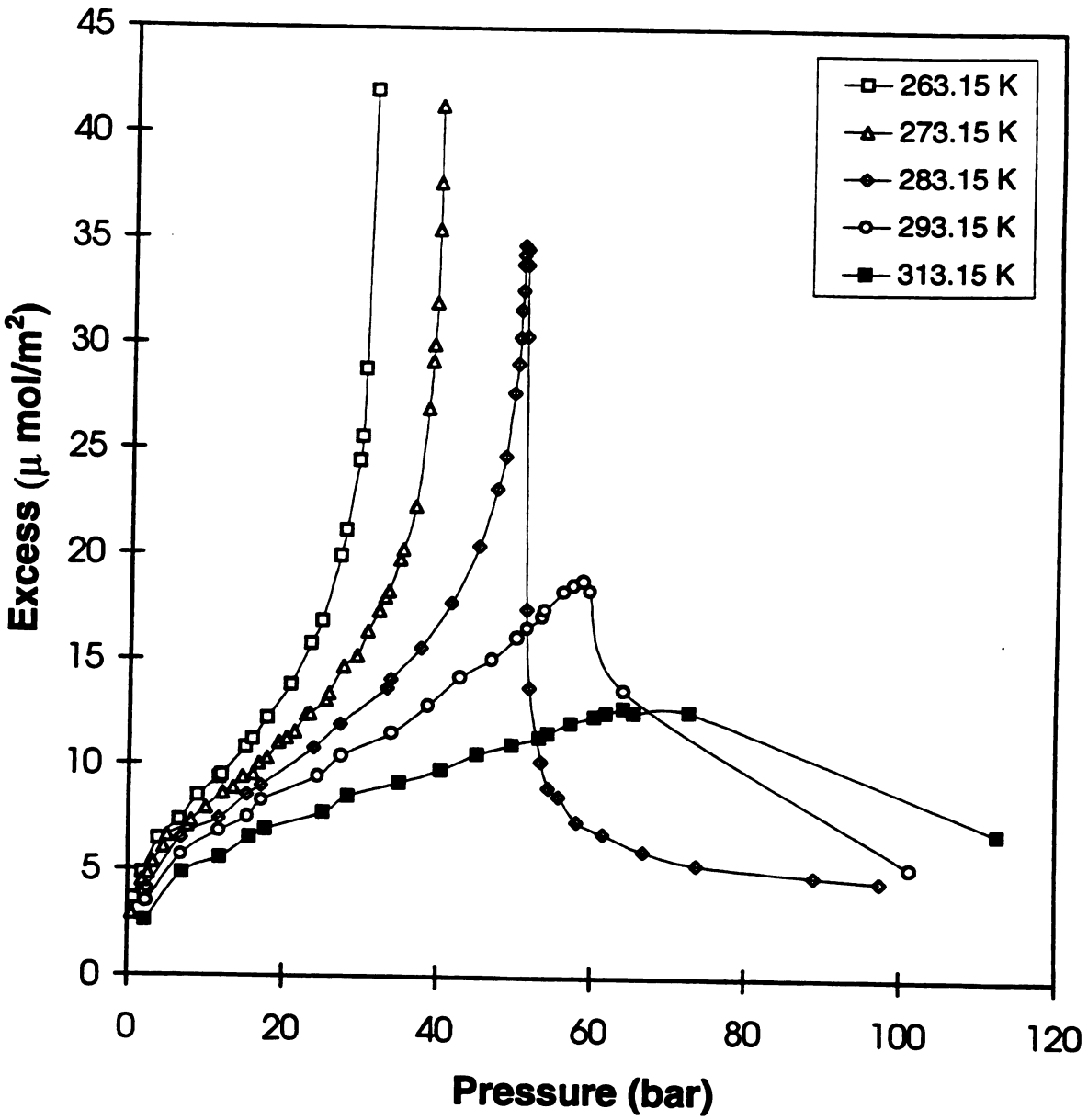

Figure 2-1: Adsorption of Ethylene on Graphon - Data of Findenegg (1983)

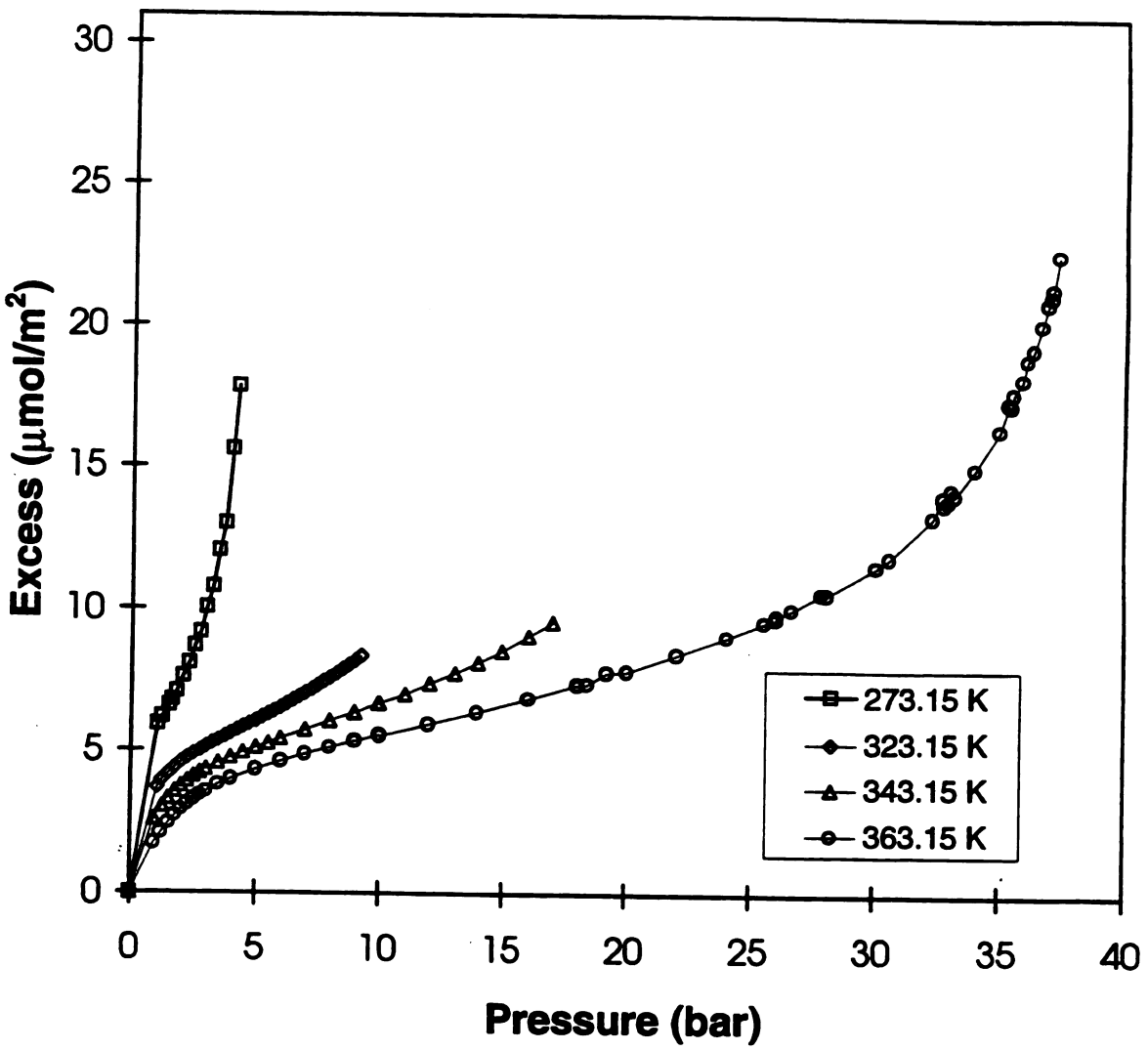

Figure 2-2: Adsorption of Propane on Graphon - Data of Findenegg (1983)

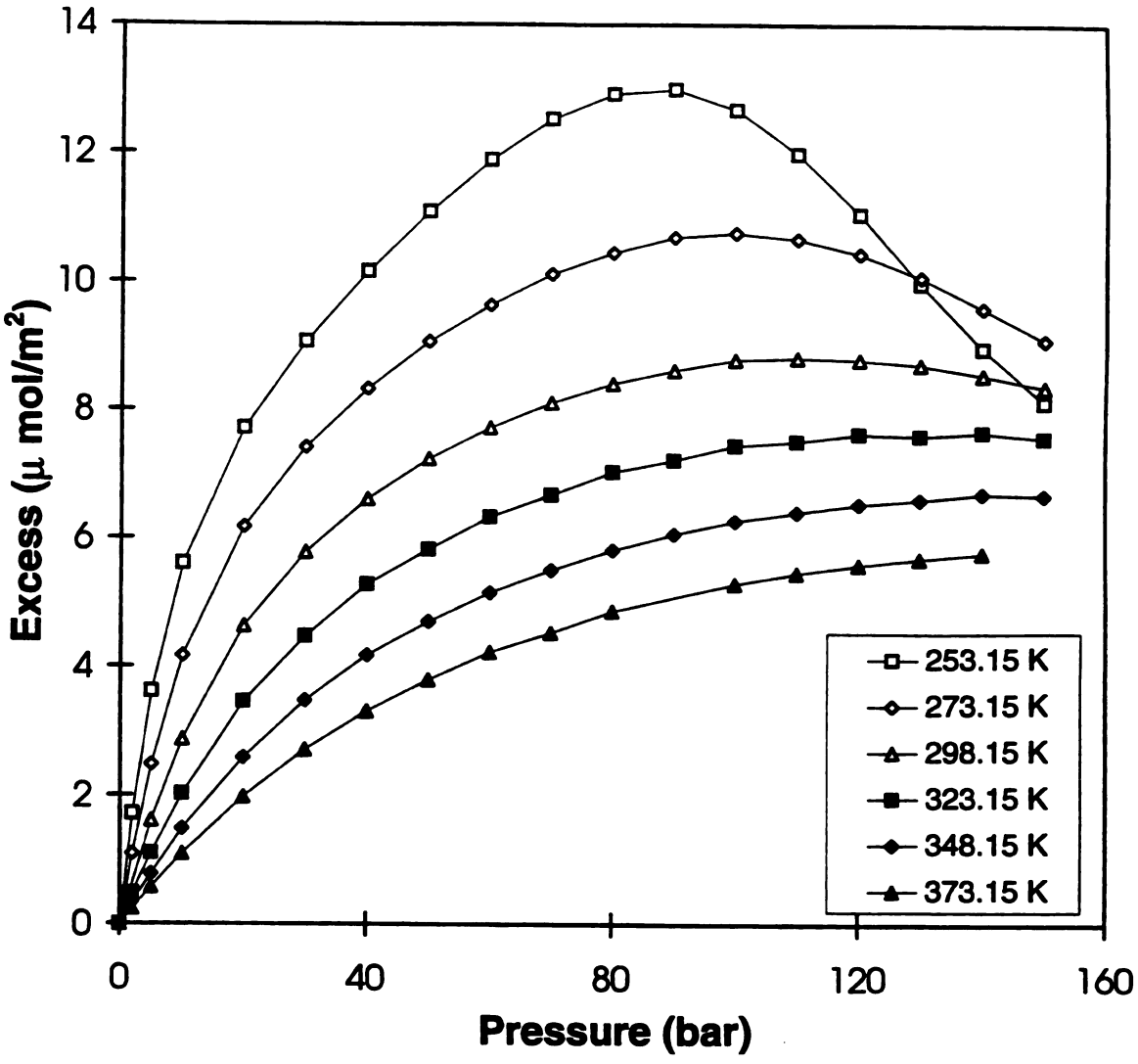

Figure 2-3: Adsorption of Krypton on Graphon - Data of Findenegg (1983)

Fig 9

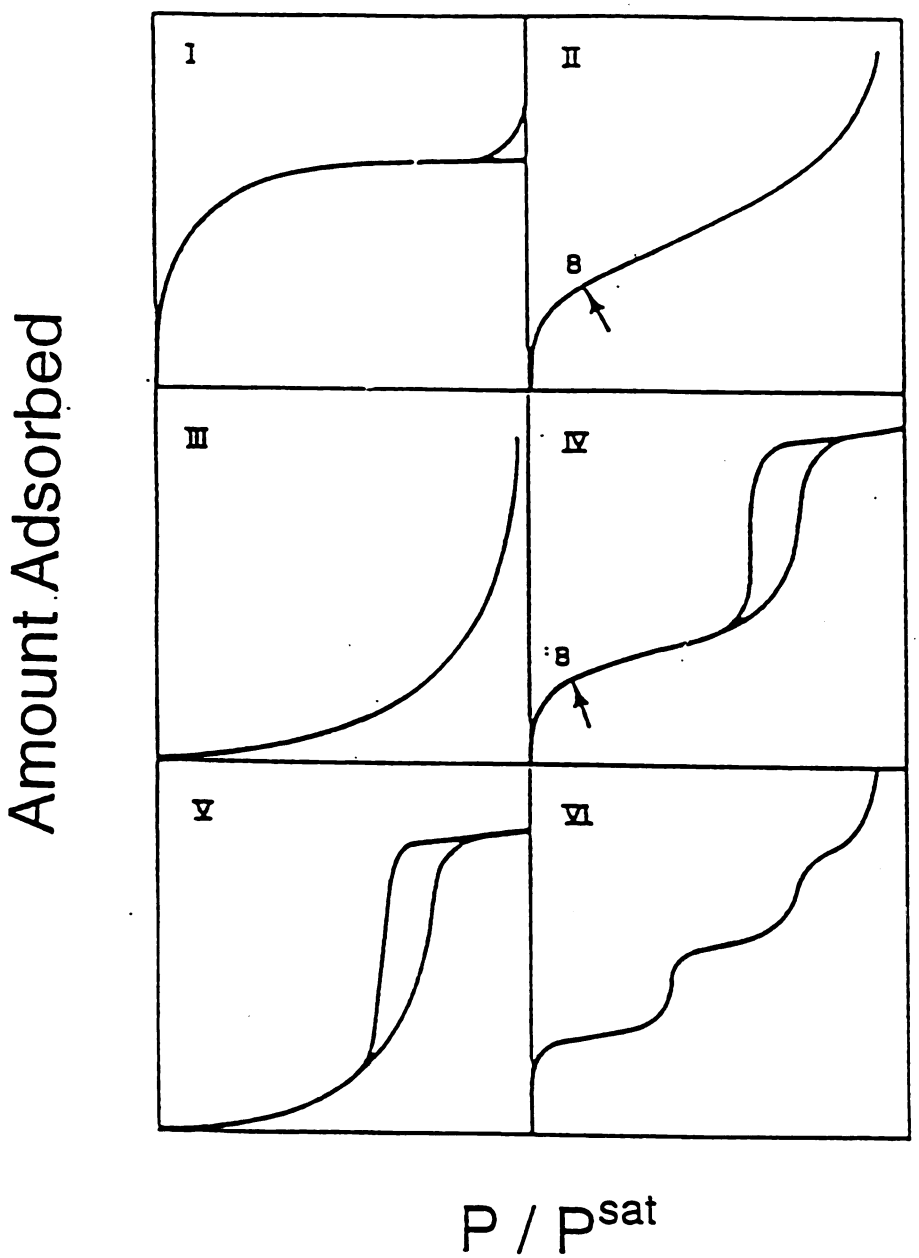

Figure 2-4: Variety of Behaviors at Subcritical Conditions

Henry's Law

In the low relative pressure region, the adsorption is linear, and the amount adsorbed (n) is proportional to the pressure (P). This region is often called the Henry's law region.

$$n = k\,P \qquad [2\text{-}2]$$

where k is the Henry's law constant. Sometimes the pressure at which this law is obeyed is below experimentally observable pressures. If the adsorption is measured at sufficiently low pressures discontinuities in the adsorption-pressure curve are sometimes noticed indicating phase transitions in the adsorbed phase as shown by the results of Ross and Clark [1954], Fisher and McMillan [1957], and more recently by a host of modern techniques by Thomy and Duvall [Bienfait 1980].

Langmuir Isotherm

One of the most popular empirically-adjusted models for adsorption is the Langmuir isotherm, a two parameter equation. This is one of the most popular isotherm due to its extreme simplicity, and is often expressed as

$$\Theta = \frac{W}{W_m} = \frac{kP}{1+kP} \qquad [2\text{-}3]$$

where W is the mass adsorbed, and W_m the amount adsorbed in a monolayer. The Langmuir equation is only derived for monolayer adsorption and therefore predicts only Type I isotherms. However, it is frequently applied to microporous materials. It is more suitable for describing chemisorption.

BET Isotherm

The Brunauer, Emmett and Teller (BET) theory extends the Langmuir theory to multilayers. It assumes that molecules adsorb in stacks or layers and that the uppermost molecules in the adsorbed stacks are in equilibrium with the vapor. The BET theory treats the first adsorbed layer separately and assumes that all layers above the first layer are condensed, and treats them identically as a liquid . This theory predicts that

$$\Theta = \frac{W}{W_m} = \frac{N}{N_m} = C\frac{P/P_o}{\left(1-\frac{P}{P_o}\right)\left(1-\frac{P}{P_o}+C\frac{P}{P_o}\right)} \qquad [2\text{-}4]$$

where P_o is the vapor pressure, N the number of moles adsorbed and C a constant related to the fraction of surface that is uncovered. The BET equation is often used in determining pore-size distributions and is often expressed as

$$\frac{1}{W\left(\frac{P_o}{P}-1\right)} = \frac{1}{CW_m} + \frac{C-1}{CW_m}\frac{P}{P_o} \qquad [2\text{-}5]$$

In pores where the number of layers are limited to n the BET equation is :

$$\Theta = \frac{W}{W_m} = \frac{N}{N_m} = \frac{C\left\{1-(n+1)\left(\frac{P}{P_o}\right)^n + n\left(\frac{P}{P_o}\right)^{n+1}\right\}}{\left(\frac{P_o}{P}-1\right)\left\{1+\frac{(C-1)P}{P_o}-C\left(\frac{P}{P_o}\right)^{n+1}\right\}} \qquad [2\text{-}6]$$

This equation reduces to the previous equation when n is infinity and the Langmuir isotherm for $n = 1$. The BET theory and its modifications are very popular since they show all the different types of subcritical isotherms. However, some of its limitations are due to the assumptions made in the developing the theory 1) the surface is energetically homogeneous; 2) there are no lateral adsorbate interactions; 3) adsorption is localized - adsorbed molecules are fixed on sites and do not laterally move; 4) the heat of adsorption in the second and higher layers is the same as the heat of condensation. Most of these assumptions are valid for pressures in the range $0.05 < P/P^S < 0.35$, where the high energy sites are filled but extensive multi-layer condensation has not commenced. The BET theory is limited to subcritical temperatures, and assumes an ideal gas vapor phase, although corrections can be applied.

Toth & UNILAN Equations

The Toth equation can be written as

$$n = \frac{mP}{\left(b + P^t\right)^{1/t}} \qquad [2\text{-}7]$$

This is a three parameter equation m, b, and t, where m is the saturation capacity (mol/kg), b and t are constants of the Toth equation, n is the specific amount adsorbed, and P is the pressure. A similar equation called the UNILAN equation can be written

$$n = \frac{m}{2s} \ln\left[\frac{c + Pe^{s}}{c + Pe^{-s}}\right] \qquad [2\text{-}8]$$

where s is a constant. Both these equations reduce to the Langmuir equation (Toth - t = 1, UNILAN - s = 0). Both these equations are empirical equations, but are for heterogeneous adsorbents. The constants needed are temperature-dependent and atleast two isotherms must be measured experimentally before calculating the temperature coefficient of adsorption. However, these theories seem to be the best overall for microporous adsorbents, and have been used as the basis for multicomponent adsorption models which will be discussed later in this chapter.

Two Dimensional Equations-of-State

The BET theory of multi-molecular adsorption is a generalization of Langmuir's unimolecular theory. Both theories are based on localized physisorption, and both neglect lateral interactions between fluid molecules, i.e. interactions between molecules in the same layer. A different approach treats the adsorbed phase as a two-dimensional fluid,

and uses a two-dimensional equation-of-state to represent the adsorbed layer [Hill, 1946, 1947, 1948; de Boer, 1953]. The two-dimensional equations-of-state allow for interactions between fluid molecules in the first adsorbed layer. Neither the Langmuir nor the BET theory allow for interactions between molecules, either on the surface, or between molecules in different layers. When a fluid is adsorbed onto a surface it exerts a pressure opposing the surface tension of a clean surface. If γ_0 is the surface tension of the clean surface and γ that of the surface with an adsorbed fluid, then the spreading pressure π is defined as

$$\pi = \gamma_o - \gamma \qquad [2\text{-}9]$$

The surface tension γ, or π can be related to the Gibb's surface excess

$$\Gamma^{ex} = -\frac{a}{RT}\frac{\delta\gamma}{\delta a} \qquad [2\text{-}10]$$

where a is the activity. For a dilute solution, the activity (a) may be replaced by the concentration C or pressure P, and a two-dimensional equation of state is used to give π. For an ideal gas the equation is

$$\pi A = RT \qquad [2\text{-}11]$$

where A is the area per mole. This equation implies no forces or interactions between the fluid molecules, which is what one would expect at low coverage. These two equations directly lead to the Henry's law isotherm. Such an approach along with activity coefficients has been used to model adsorption from gas mixtures and from solutions [Myers and Prausnitz 1965; Radke and Prausnitz 1972].

Several attempts have been made using a two-dimensional equation-of-state to represent the adsorbed layer which accounts for mobile interactions and includes lateral interactions in the first layer (The Langmuir and BET models account only for localized adsorption - i.e. they neglect lateral interactions between fluid molecules) [Hill, 1946, 1947, 1948; de Boer, 1953]. The two dimensional van der Waals equation predicts a two-dimensional critical temperature T_{c2} which is one half the bulk critical temperature (T_{c2} = 0.5 T_c) and a two-dimensional critical pressure $\phi_c = 0.361\ P_c\ (\ V_c / N\ )^{1/3}$. Here the subscript $c2$ is used to describe the critical constants for the two dimensional state. Similar results for T_{c2} are obtained with different systems. A Lennard-Jones Devonshire [1937] model gives $T_{c2} = 0.53\ T_c$. An excellent discussion of two dimensional critical temperatures and pressures from the van der Waals equation-of-state is given by de Boer [1953]. Typically $T_{c2}/\ T_c$ is about 0.4 with extremes of 0.36 and 0.56. This lies in-between mean field theory prediction of 0.5 and a 2-D Ising model prediction of 0.37 [Bienfait 1980]. The two-dimensional van der Waals model leads to the following equation

$$\frac{P}{P_o} = k_s \Theta \exp\left[\frac{\Theta}{1-\Theta}\right] \exp(-k_1 \Theta) \qquad [2\text{-}12]$$

The constant k_1 depends on a_2 and b_2 the two-dimensional van der Waals parameters, and therefore only the adsorbate. A high value of k_1 implies strong inter-molecular forces (fluid-fluid). The constant k_2 measures the strength of adsorption, and the stronger the adsorption the smaller the k_2.

This equation predicts phase transitions on the surface for weak adsorption forces and strong intermolecular attraction (i.e. large k_1 and k_2). If the fluid-fluid intermolecular attraction is weak, no condensation is seen. For strong adsorption forces, a tendency towards saturation (Type I isotherm) is seen, and the adsorbed fluid is either a compressed supercritical fluid or a condensed two dimensional liquid.

Relative to the BET equation, the Hill de-Boer model predicts lower pressures for coverage's below 0.8, but over-corrects the errors of the BET equation. This is due to the fact that lateral interactions are allowed, and not due to the mobility. If lateral interactions are allowed in a localized first layer, condensation takes place at very low pressures, and jumps from almost zero to near unity at a critical coverage Θ_c of 0.5. Such a result could probably be deduced by percolation on a lattice, since the similarity between the abrupt jump at Θc of 0.5 and a critical percolation probability of p_C of 0.5 does not seem coincidental.

Potential theories

Several other popular theories are the Polyani potential theory [Polyani 1932] and modifications of it such as the Dubinin-Radushkevich [Dubinin 1947, 1975], and the Frenkel-Halsey-Hill [Halsey 1948; Hill 1950] theory.

(i) Polyani Potential Theory

The Polyani potential theory assumes that a potential field exists at the surface of a solid that attracts the molecules of the surrounding fluid. These attractive forces are essentially London dispersion forces or van der Waals forces, which vary as $1/r^3$ (where r is the distance from the surface). The adsorption potential (ε_i), at a distance i from the surface is the work done in bringing a molecule from the gas phase at density ρ_x to that point where the density is ρ_i. Polyani noticed the similarity with gravitational potential, and used the equation of hydrostatics to calculate the adsorption.

$$\varepsilon_i = \int_{\rho_x}^{\rho_i} v\, dP \qquad [2\text{-}13]$$

It was assumed that the adsorbent potential at a given distance (or surface at) i is ε_i, regardless of the number and kind of molecules located between the i'th surface and the solid or gas, an assumption which was justified later by London's theory of van der Waals forces. Each of the potential surfaces along with the surface of the solid adsorbent encloses a volume ϕ_i. At the surface of the adsorbent ε_o is maximum and ϕ_i is zero. The

gas phase is assumed to be the region in which $\varepsilon = 0$, and limits the adsorption volume to $\phi = \phi_{max}$. In actuality, the potential never goes to zero but for practical purposes $\varepsilon = 0$ at a finite distance and therefore a finite volume from the surface. The theory assumes that $d\varepsilon_i/dT = 0$ implying that $d\phi_i/dT = 0$ and therefore that $\varepsilon = f(\phi)$ for all temperatures for a given adsorbent. This is used to form a *characteristic curve,* which is experimentally determined. The amount adsorbed (n) is given by

$$n = \int_0^{\phi_{max}} (\rho - \rho_x) d\phi \qquad [2\text{-}14]$$

In using the theory, first a characteristic curve $\varepsilon = f(\phi)$ is created. This curve should span the entire adsorption space, and is therefore typically evaluated at a moderate temperature. The second step consists of evaluating adsorption isotherms from these characteristic curves. The characteristic curve equations can be simplified if the temperature is significantly below or above the critical temperature. These equations ignore adsorption in vapor form, and the compressibility of the liquid layer, as well as assume ideal behavior. Near T_c these assumptions result in errors, but the different errors fortuitously cancel resulting in fairly accurate predictions. For high temperatures and pressures the Polyani theory has been modified by using empirical correction factors to account for the compressibility and thermal expansion of the adsorbed liquid [Berenyi 1923; Brunauer 1945].

(ii) Dubinin's Theory

An empirical relationship was found between ε_O of Polyani theory and the van der Waals constant 'a' of the fluid :

$$\varepsilon_o = k\sqrt{a} \qquad [2\text{-}15]$$

which originates from the mixing rules of Berthelot, who proposed that the attractive potential between two molecules at a fixed distance is proportional to $\sqrt{a_1 a_2}$ where a_1 and a_2 are their van der Waals constants. Using this, the potential theory was extended by Dubinin and co-workers to include adsorption of mixed gases onto a solid. They expressed the characteristic curve for all gases on the same adsorbent as :

$$\varepsilon = \beta f(\phi) \qquad [2\text{-}16]$$

where β is called the coefficient of affinity and is defined as the ratio of adsorption potentials ($\beta = \varepsilon / \varepsilon_o$) of a gas and a reference fluid, on the given adsorbent. They found that the molar volumes of the adsorbate in liquid state were closely proportional to the coefficient of affinity. The characteristic curves resembled the positive side of a Gaussian curve which lead Dubinin and Radushkevich to assume that the adsorption volume V occupied by the liquid adsorbate (and V_o by the reference) followed

$$V = V_o \exp\left[-K\left(\frac{E}{\beta}\right)^2\right] \qquad [2\text{-}17]$$

where K is a constant depending on the shape and size distribution of pores. This leads to

$$\ln(W) = \ln(V_o\rho) - K\left(\frac{RT}{\beta}\right)^2\left[\ln\left(\frac{P_o}{P}\right)\right]^2 \qquad [2\text{-}18]$$

Subcritical vapor pressure data have been extrapolated into the supercritical region and a good fit has been obtained using the extrapolated fugacities [Maslan et al., 1953].

(iii) Frenkel-Halsey-Hill Theory

This theory presumes that the adsorbed film consists of a liquid at a density ρ_l (density of bulk liquid at that temperature) with a thickness of h. The surface excess (Γ^{ex}) is given by

$$\Gamma^{ex} = h(\rho_l - \rho) \qquad [2\text{-}19]$$

where ρ is the density of the bulk gas. Assuming that the adsorbate and adsorbent interact through a 12-6 Lennard-Jones potential (and integrating to a 9-3 potential), this leads to

$$\ln\left(\frac{P}{P_o}\right) = -\frac{k}{\Gamma^3} \qquad [2\text{-}20]$$

where k is a constant.

In a further modification of the Frenkel-Halsey-Hill theory, multiple liquid like slabs and fugacities have been used to represent the adsorbed layer that has a density ρ_m for $z \leq z_1$ and ρ_1 for $z_1 < z < z_i$, where the fugacity is related to adsorption by :

$$\ln\left(\frac{f}{f_o}\right) = -\frac{\Delta\varepsilon}{kT}\left(\frac{z_i}{z_1}\right)^{-m} \qquad [2\text{-}21]$$

Here f_o is the fugacity of the saturated vapor, z_i the distance of the i'th statistical layer of molecules, $\Delta\varepsilon$ is the perturbation energy of a molecule in the first layer at a distance z_1. For a single step density profile if the density of the layer is ρ_1 for $z < z_i$ and ρ for $z > z_i$, then z_1 can be determined from experiments and

$$z_i = \frac{\Gamma^{ex}}{\rho_1 - \rho} \qquad [2\text{-}22]$$

and the parameter m fit from a plot of $\ln(z_i)$ vs. $\ln(-\ln(f_o/f))$. Such methods with multiple-step density profiles have been used to describe adsorption generally in the sub-critical range [Findenegg 1983].

van der Waals model of Barrer and Robins

This theory, developed by Barrer and Robins [1951], has been unrecognized for more than forty years. It uses the fact that the chemical potential is constant at all distances from a wall, and can be determined by the temperature and pressure far from the surface. This potential consists of two components - potential due to the interaction of the fluid molecules themselves, and a potential due to interaction of the fluid and the wall. Since the potential exerted by the wall and the bulk fluid potential are known the density profile and surface excess can be calculated. They assumed that the fluid obeyed the van der Waals equation-of-state and the fluid-wall interaction can be approximated by the 9-3 Lennard-Jones potential. This leads to the following equation

$$\frac{\theta}{1-\theta}\exp\left(\frac{\theta}{1-\theta}-\frac{2a\theta}{bRT}-\frac{CN}{r^3RT}\right)=\frac{\theta_b}{1-\theta_b}\exp\left(\frac{\theta_b}{1-\theta_b}-\frac{2a\theta_b}{bRT}\right) \qquad [2\text{-}23]$$

where a and b are the van der Waals constants, N and n are the total number of molecules and moles in the system respectively, $\theta = bn/V$, where V is the total volume occupied by closely packed molecules, r is the distance between the fluid molecule and the surface, C is an empirical constant and the subscript b stands for bulk properties. If v is the molar volume of the fluid being adsorbed on the surface of the adsorbent then equation 2-23 may be written as

$$\frac{1}{v-b}\exp\left(\frac{b}{v-b}-\frac{2a}{vRT}-\frac{CN}{r^3RT}\right)=\frac{1}{v_b-b}\exp\left(\frac{b}{v_b-b}-\frac{2a}{v_bRT}\right) \qquad [2\text{-}24]$$

This model predicted the different adsorbent isotherms whose magnitude could be manipulated by changing the empirical constant *C*. Hill [1952] suggested that this model can be improved by treating the fluid not as a bulk fluid as Barrer and Robins had done, but as an inhomogeneous fluid i.e. the chemical potential should not be calculated from the local density but from the entire density profile. He also suggested replacing the inaccurate van der Waals equation by a better equation.

Statistical Mechanical Models

There are different types of models derived from chemical physics, including the Lattice Gas model, Integral Equation theory, and Density Functional theory. The Lattice Gas model is a case of localized adsorption, where the molecules of the solid are large compared to the molecules of the fluid. This results in the formation of a lattice of adsorption sites that are separated from each other by high potential barriers. This model simplifies to the Langmuir or BET approaches and predicts several phase transitions on the surface.

Theoretical interpretations of adsorption include virial expansions in terms of bulk density at low pressures [Steele 1962]. A van der Waals theory for adsorption has been proposed by Sullivan [1979]. This approach has been generalized to examine wetting transitions at the solid-gas interface [Tarazona and Evans 1983], adsorption and wetting

transitions in binary fluid mixtures by Telo de Gama and Evans [1983]. The van der Waals density functional model for inhomogeneous fluids has also been used to study wetting transitions at surfaces [Kung et al., 1990; Teletzke et al., 1982a, b]. More recent applications of statistical mechanics have involved adaptation of integral equations developed for homogeneous fluids to inhomogeneous adsorbed fluids. These include integral equations for liquid state theories such as the BBGKY hierarchy for non-uniform liquids [Lee, 1987; Henderson, 1992] and density functional theory [Saam and Ebner, 1978; Fisher and Methfessel, 1980; Tan and Gubbins, 1990; Kierlik and Rosinberg, 1992].

(i) Integral Equation Theory

Statistical mechanical theories use distribution functions to describe the correlation between fluid molecules and hence the short range order. The primary cause of this short range order, or structure, of a uniform fluid are the repulsive forces, with attractive forces forming the background. In order to get a complete theory of liquid state an expression is needed for $g(r)$ the radial distribution function [McQuarrie, 1976; Rowlinson and Widom, 1982], or the pair correlation function.

$$g(r) = \frac{V^2 N!}{N^2 (N-2)!} \frac{\int \ldots \int e^{-\beta U_N} dr_3 \ldots dr_N}{Z_N} \qquad [2\text{-}25]$$

where, there is a system of N particles in a volume V and at temperature T, Z_N is the configurational integral, r_1, r_2, r_3 are coordinates in space. If the total potential of a N-body

system can be assumed to be pairwise additive, then all the thermodynamic properties of the system can be derived from the radial distribution function. For e.g. the pressure is related to *g(r)* by

$$\frac{P}{kT} = \rho - \frac{\rho^2}{6kT}\int_0^\infty ru'(r)g(r)4\pi r^2 dr \qquad [2\text{-}26]$$

A number of approximate equations have been used to solve Equation 2-26. These include the BBGKY hierarchy and Ornstein-Zernike equations with the Percus-Yevick and hypernetted-chain closures. These approaches are reviewed by McQuarrie [1976] and Henderson [1992], and are widely used in predicting clustering in supercritical fluids.

(ii) Density Functional Theory

The density functional approach was derived by Saam and Ebner [1978]. It is based on the fact that there exists a functional Ω of the local density $\rho(r)$, such that at equilibrium this functional is minimized.

$$F = F[f(r), \rho(r), c(r_1, r_2)] \qquad [2\text{-}27]$$

where $f(r)$ is the local free energy, $\rho(r)$ is the local density and $c(r_1, r_2)$ is the direct correlation function. Gubbins and co-workers have used this approach to describe adsorption is slits and cylindrical pores and have successfully compared their results to molecular simu-

lations. Kierlik and Rosinberg [1991, 1992] proposed a simplified version of the free energy functional for the inhomogeneous hard-sphere fluid mixture that requires four distinct weight functions and generates a triplet direct correlation function for the one component fluid.

Molecular Simulations

While there a large number of complicated theories they are not exact. The best solutions, for a given potential, are obtained by computer simulations where the equations of motion are solved for the particles of an ensemble. Observable macroscopic quantities are then calculated by time-averaging the appropriate microscopic equations. Such a calculation is called a molecular dynamics (MD) calculation. In the Monte-Carlo (MC) scheme a large number of configurations are sampled, and particles moved to find the most stable state, and averages are calculated to give a certain macroscopic property.

Computer simulations are difficult to perform near the critical point due to the large density fluctuations. However, these techniques are very powerful, and yield the best results for a given potential. van Megan and Snook [1982, 1985] have simulated the adsorption of fluids near the critical region using a grand canonical ensemble Monte-Carlo method. They compare the results of their simulation with experimentally measured [Specovius and Findenegg, 1978] isotherms of ethylene on graphite, just above the critical temperature and find reasonably good qualitative agreement with data (Figure 2.5). The simulation results show cusp-like maxima which are close in magnitude to experimental values, but the location of the cusp is off by 25% (~15 bar). Their results cannot be

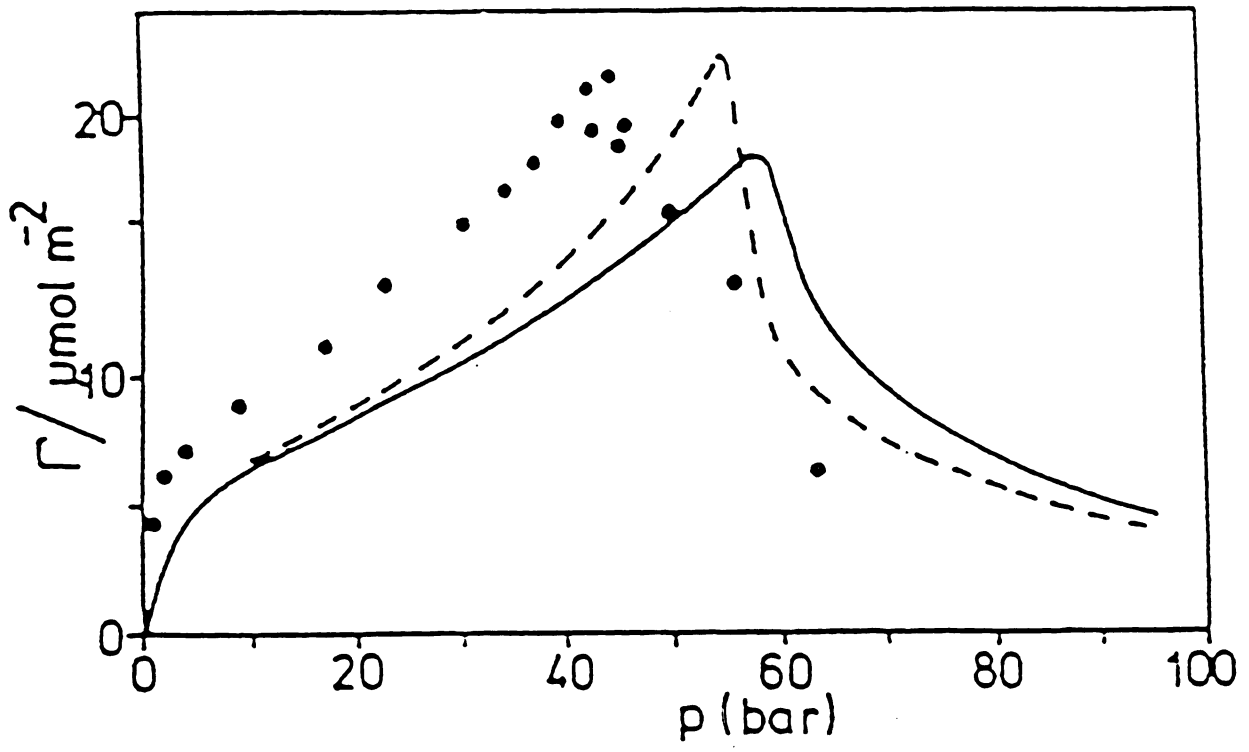

Figure 2-5: Comparison of Molecular Simulation (van Megen and Snook, 1982) to Experimental Data (Specovius and Findenegg, 1978)

•• Molecular Simulation ($T / T_c = 1.03$)

-- Experimental Data ($T / T_c = 1.02$)

– Experimental Data ($T / T_c = 1.04$)

quantitatively compared to experimental data because their simulation of bulk ethylene uses a shifted potential and does not represent the experimental bulk properties of ethylene; e.g. the simulation critical temperature ($T_{c,\,sim}$) of ethylene is 226 K, as opposed to an experimental value of 282.4 K. However, their results have been the basis for comparison for the density functional theory using the same shifted potential. Figure 2.6 and 2.7 show the adsorption of ethylene on a slit like pore at sub and supercritical temperatures. At low slit widths Type I isotherms are seen. There is also a slight decrease in the surface excess with increasing pressure. As the slit width increases type IV isotherms are seen. In flat walls, type II isotherms are seen. Figure 2.8 shows the density functional theory's prediction of van Megen and Snook's simulation [Tan and Gubbins, 1990], and it can be seen that the density functional theory does a very good job of reproducing the results of the molecular simulation. Snook and van Megen conclude that traditional adsorption theories will not be able to account for the wide variety of shapes of adsorption isotherms encountered in their computations.

Mixed-Gas Isotherms

Current models that predict mixed-gas isotherms use pure gas models such as the Toth or UNILAN equations. One such theory is the ideal-adsorbed-solution theory of Myers and Prausnitz [1965]. This theory is thermodynamically consistent and exact at the limit of zero pressure. The success of such theories depends of their ability to predict the pure gas isotherms accurately. Small errors in the prediction of pure-gas experimental data may cause large deviations in the mixed-gas predictions. Other sources may be the

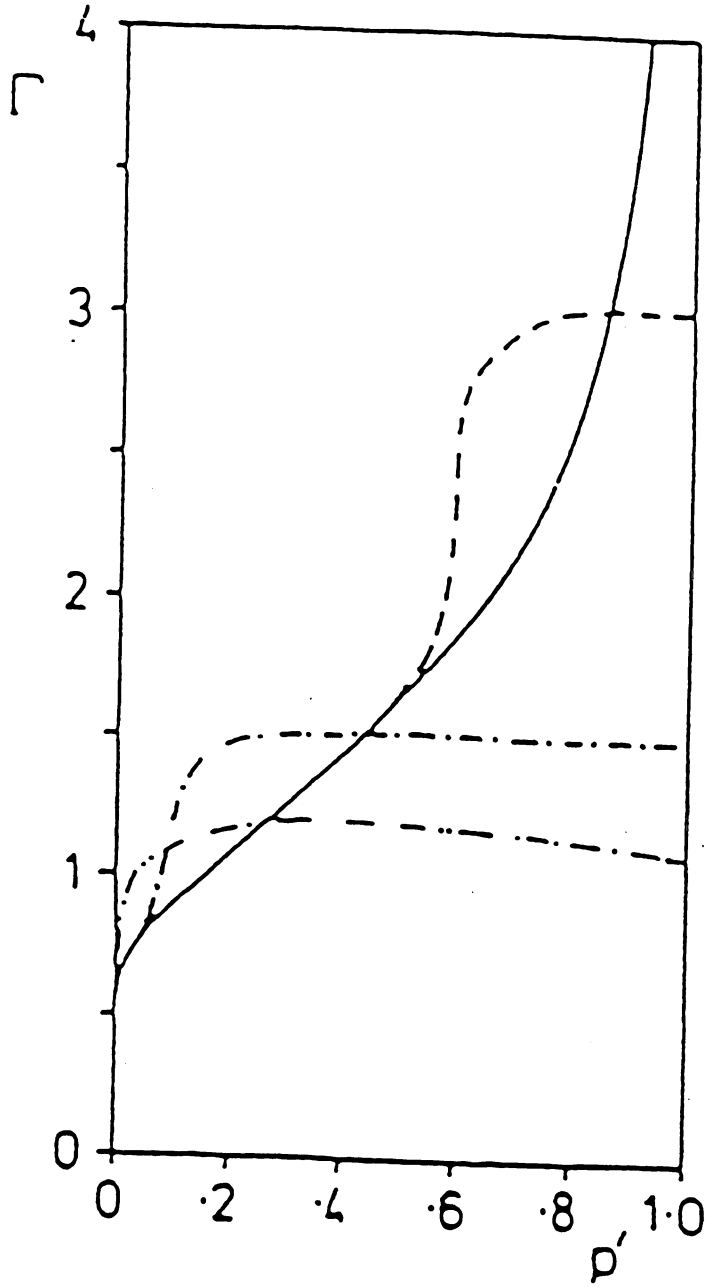

Figure 2-6: Grand Canonical Ensemble Monte Carlo Simulation of Ethylene in a Slit (T/T_c=0.85)

—h = ∞, - - - h = 10.0, ·-·-· h = 5.0, ·····h = 3.5

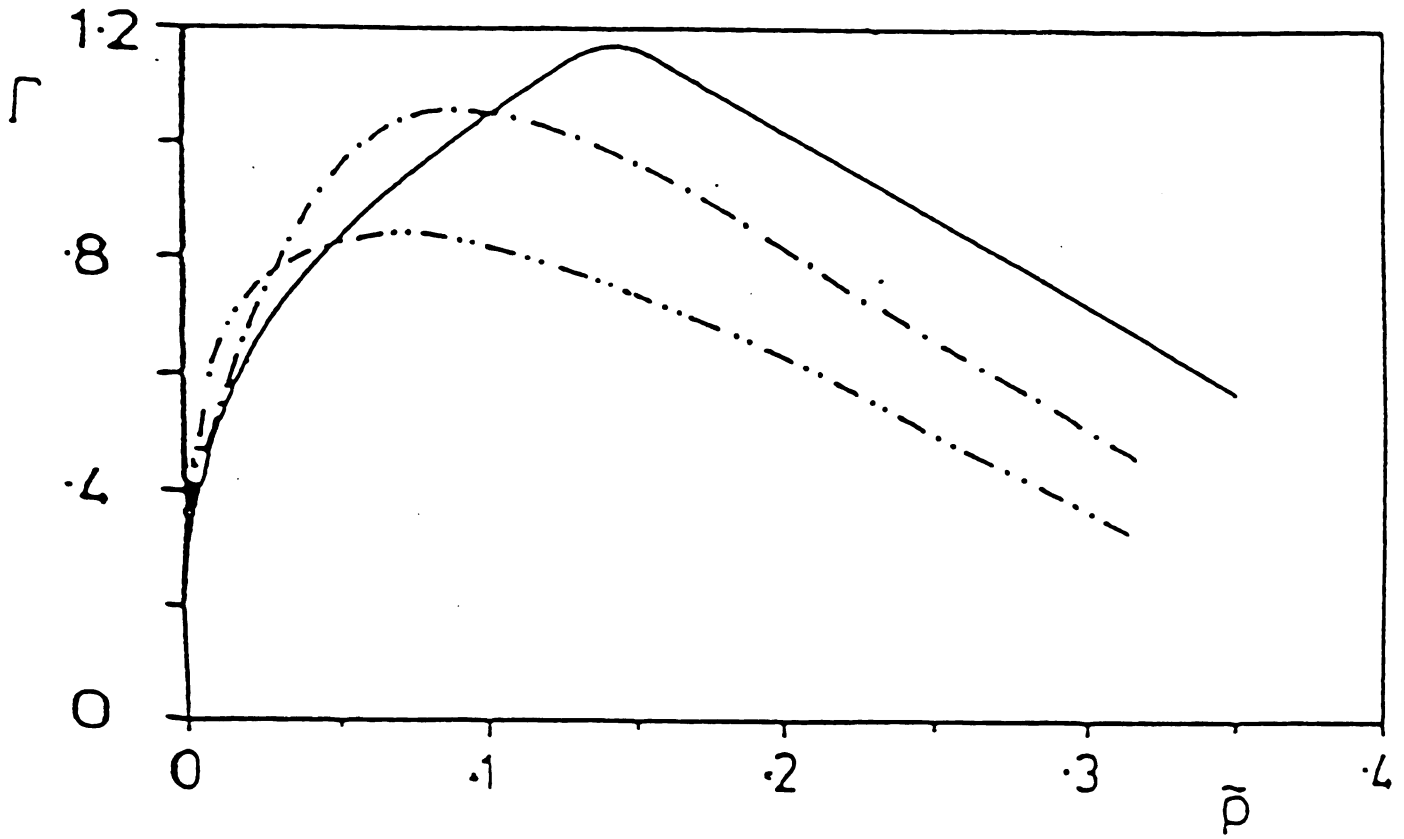

Figure 2-7: Grand Canonical Ensemble Monte Carlo Simulation of Ethylene in a Slit (T/T_c=1.2)

—h = ∞, ···· h = 5.0, ····· h = 3.5

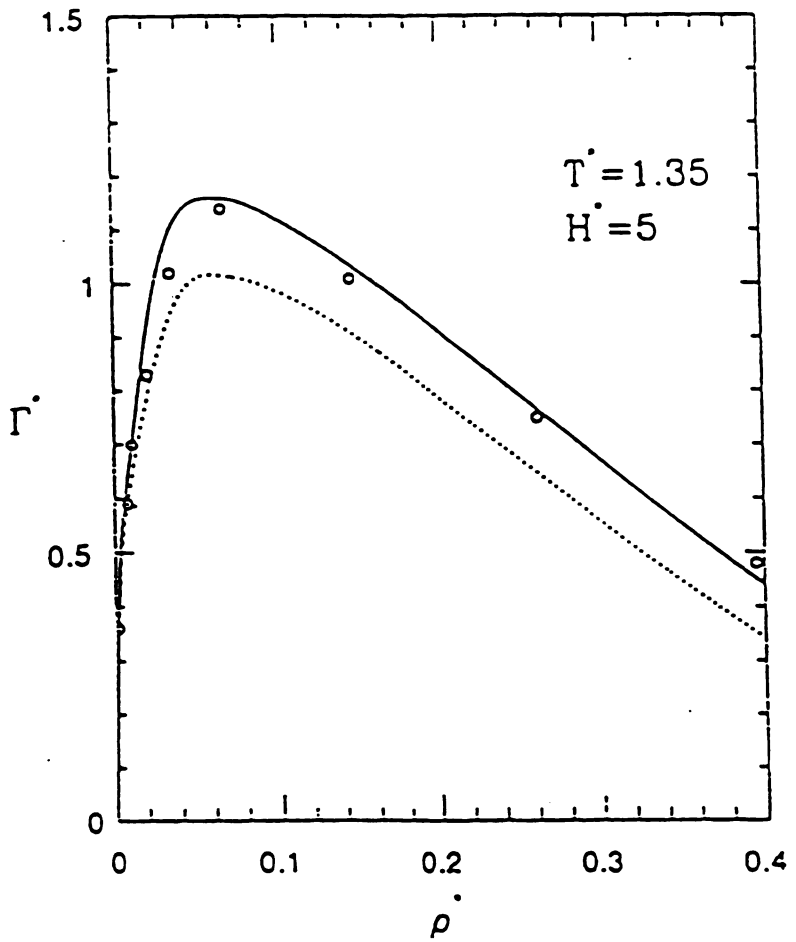

Figure 2-8: Density Functional Theory - Comparison to Grand Canonical Ensemble Monte Carlo Simulation

neglect of surface heterogeneity and adsorbate-adsorbent interactions, both of which may cause non-ideal behavior [Valenzuela and Myers, 1989]. Later models of this type, did not neglect these heterogeneities and were called non-ideal adsorbed solution theories. Since the basis of mixed-gas isotherm modeling is the IAS theory, we shall discuss it in more detail.

Ideal Adsorbed Solution (IAS) Theory

For a multicomponent system containing N adsorbates, the IAS equations for a perfect gas are

$$Py_i = P_i^o x_i \quad (i = 1,2,.....,N) \qquad [2\text{-}28]$$

where the adsorption isotherm of pure ith adsorbate is $n_i^o(P_i^o)$, y_i is the mole fraction in the gas phase and x_i is the mole fraction in the adsorbed phase.

$$\Psi_1^0\left(P_1^o\right) = \Psi_2^0\left(P_2^0\right) = ... = \Psi_N^o\left(P_N^0\right) \qquad [2\text{-}29]$$

$$\sum_{i=1}^{N} x_i = 1 \qquad [2\text{-}30]$$

The function $\Psi_i^o(P_i^o)$ is the integral for the spreading pressure ($\pi A/RT$) for the adsorption of pure ith adsorbate at the same temperature as the mixture.

$$\frac{\pi A}{RT} = \int_0^P \frac{n}{P} dP = \int_0^n \frac{d\ln(P)}{d\ln(n)} dn \qquad [2\text{-}31]$$

The independent variables are T, P, $y_1,...y_{N-1}$, leaving us with $2N$ unknowns (P_i^o, x_i) and $2N$ equations (2-28 - 2-30). After these three equations are solved, the total amount n_t and the amount of ith component are found as

$$\frac{1}{n_t} = \sum_{i=1}^{N} \frac{x_i}{n_i^0} \qquad [2\text{-}32]$$

$$n_i = n_t x_i \qquad [2\text{-}33]$$

The general algorithm for solving this theory is given in Valenzuela and Myers [1989]. Further development of non-ideal adsorbed solution theories, and the development of the fast-IAS theory, where the integrals for the spreading pressure are written as a series expansion in terms of the central moments of the adsorption energy distribution, are also given in Valenzuela and Myers [1989]. All these theories require the pure gas isotherm parameters (for Toth/UNILAN it is 3), and hence are not predictive models.

PRELIMINARY RESULTS - SIMPLIFIED LOCAL DENSITY MODEL OF RANGARAJAN, LIRA AND SUBRAMANIAN

This model, originally developed by Rangarajan [1992], and Rangarajan, Lira and Subramanian [1995] forms the basis for the rest of this dissertation, and hence will be discussed in detail. Some of the predictions of this model will also be presented and compared with experimental data. The model has a basis similar to the Polyani potential theory, where the adsorbent exerts an attractive potential on the adsorbate. The model is also similar to the approaches of Barrer and Robins [1951], Hill [1949], Sullivan [1979], and Kung et al. [1990].

Model Development

The attractive potential between the fluid and solid, at any point z, is assumed to be independent of temperature and the number of molecules at and around that point. At equilibrium, the molar chemical potential μ must be uniform throughout the system [Denbigh 1981; Guggenhiem 1967] and is calculated by contributions from fluid-fluid and fluid-solid interactions.

$$\mu = \mu_b = \mu_{ff}(z) + \mu_{fs}(z) \qquad [2\text{-}34]$$

where the subscript '*b*' refers to the bulk, the subscript '*ff*' to the fluid-fluid interactions and the subscript '*fs*' to the fluid-wall interactions. Equation 2-34 requires that at a distance z

from the wall, the sum of the chemical potential due to the fluid-fluid interactions and the attractive potential exerted by the solid on the fluid remains constant, and equal to the bulk chemical potential. While such an equation has been written from the principles of chemical equilibrium, this fundamental result for inhomogeneous systems has been derived by minimizing the grand potential [Evans 1979; Rowlinson and Widom 1982; Davis and Scriven 1982]. In using this equation care should be taken to ensure a consistent basis for chemical potential, whether it be per molecule or mole. If $\Psi(z)$ is the potential exerted by the wall on a fluid molecule , then on a molar basis,

$$\mu_{fs}(z) = N_A \Psi(z) \qquad [2\text{-}35]$$

where N_A is Avogadro's number. Therefore

$$\mu_{ff}(z) = \mu_b - N_A \Psi(z) \qquad [2\text{-}36]$$

For a non-ideal fluid :

$$\mu_b(T) = \mu_o(T) + RT \ln\left(\frac{f_b}{f_o}\right) \qquad [2\text{-}37]$$

where f_b is the bulk fugacity and f_o is 1 bar. For an inhomogeneous fluid,

$$\mu_{ff}(T) = \mu_o(T) + RT \ln\left[\frac{f_{ff}(z)}{f_o}\right] \qquad [2\text{-}38]$$

where $f_{ff}(z)$ is the fluid-fluid contribution to the fugacity of the fluid at a position z. The Equations 2-36 - 2-38 lead to

$$f_{ff}(z) = f_b \exp\left[\frac{-\Psi(z)}{kT}\right] \qquad [2\text{-}39]$$

It should be noted that Ψ is negative when attractive, leading to an increased fluid-fluid fugacity near the wall. The fluid chemical potential consists of a repulsive contribution μ_{rep} and an attractive contribution μ_{att} [Vera and Prausnitz, 1972]

$$\mu_{ff} = \mu_{rep} + \mu_{att} \qquad [2\text{-}40]$$

For a homogeneous fluid, using the van der Waals equation-of-state

$$\mu_{rep} = RT\left[\ln\left(\frac{RT}{v-b}\right) + \frac{b}{v-b}\right] \qquad [2\text{-}41]]$$

where v is molar volume and b is the van der Waals constant. The attractive potential is given by

$$\mu_{att} = \int_V \phi(r) \frac{g(r)}{v} dV \qquad [2\text{-}42]$$

where V denotes the volume of integration (all space occupied by the fluid), $\phi(r)$ the two-body interaction potential, $g(r)$ the radial distribution function, which is taken to be a constant outside the hard sphere diameter for a van der Waals fluid [McQuarrie, 1976]. In the case of a homogeneous fluid ($v \neq v(z)$) Equation 2-42 simplifies to the common form

$$\mu_{att} = -\frac{2a_b}{v} \qquad [2\text{-}43]$$

where a_b is the van der Waals constant. In order to evaluate the integral in Equation 2-42 for an inhomogeneous fluid, if the density changes with position more gradually than $\phi(r)$ does, then one needs to include density as a function of position. Equation 2-42 suggests that a feasible approximation might be to use a density at the local position for evaluation of the integral. In other words, the fluid at point z is treated as a homogeneous fluid at a density of $\rho(z)$ (such an approximation is the one used by Barrer and Robins [1951]). Since the two body potential $\phi(r)$ is short ranged ($\propto 1/r^6$), and the product of $\phi(r)$ and $\rho(z)$ appears in the configurational integral (Equation 2-42), it seems reasonable that most of the value of the integral (at z) results from contributions of $\phi(r)$ and $\rho(z)$ near z. Far from the given point z, where $\rho(z)$ changes, the two-body potential ($\phi(r)$) will approach

zero. Since the density of the fluid is larger closer to the attractive wall and smaller farther away from the wall, some of the errors introduced by this approximation cancel, although the approximation will not be as good near a phase transition. The term 'local' refers to the fact that all thermodynamic properties at point z are calculated using a single density value, $\rho(z)$, a 'local average' density, and are not calculated from gradients in density about the point z. This approximation is called the local density approximation.

Using an equation-of-state, an expression for fugacity in terms of the molar density or volume can be derived. The van der Waals equation-of-state leads to the following expression for fugacity for a homogeneous fluid:

$$f_b = \frac{RT}{v-b}\exp\left(\frac{b}{v-b} - \frac{2a_b}{vRT}\right) \qquad [2\text{-}44]$$

For an inhomogeneous fluid, the problem is one of calculating the density profile $\rho(z)$ which satisfies Equation 2-39. Following Hill [1951], Sullivan [1979], and Kung et al. [1990] we assume the short-range repulsive forces determine μ_{rep} by the local density. If we assume that μ_{att} is also determined by the density of $\rho(z)$, (local density approximation) then we can rewrite Equation 2-44 to calculate density as a function of z

$$f_{ff}(z) = \frac{RT}{v(z)-b}\exp\left(\frac{b}{v(z)-b} - \frac{2a(z)}{v(z)RT}\right) \qquad [2\text{-}45]$$

where $a(z)$ is evaluated from the integral given in Equation 2-42, in which the molar volume in the denominator is approximated by the local molar volume at z. In the model of Barrer and Robins [1951], the van der Waals a is independent of z ($a(z) = a_b$). In the present model, we exclude from the integral of Equation 2-42 that portion of space occupied by the solid adsorbent. This leads to the following expressions for $a(z)$ (see Appendix 1):

$$a(z) = a_b\left(\frac{5}{16} + \frac{6}{16}\frac{z}{\sigma_{ff}}\right) \quad for \quad 0.5 \le \frac{z}{\sigma_{ff}} \le 1.5 \qquad [2\text{-}46]$$

$$a(z) = a_b\left[1 - \frac{1}{8\left(\frac{z}{\sigma_{ff}} - \frac{1}{2}\right)^3}\right] \quad for \quad 0.5 \le \frac{z}{\sigma_{ff}} \le 1.5 \qquad [2\text{-}47]$$

The van der Waals constant a is related to the critical temperature (T_c) and the critical pressure (P_c) of the fluid. If the excluded volume does not change, then the b term remains constant. Since

$$a_b = \frac{27}{64}\frac{RT^2}{P_c} \qquad [2\text{-}48]$$

$$b = \frac{RT_c}{8P_c} \qquad [2\text{-}49]$$

The wall critical temperature is related to the bulk critical temperature as

$$\frac{a_{wall}}{a_b} = 0.5 = \frac{(T_{cwall} / T_c)^2}{P_{cwall} / P_c} \qquad [2\text{-}50]$$

and combined with the equation for b yields $T_{cwall} = T_c/2$. This is the mean-field theory prediction of a reduction of the critical temperature at the surface.

Outline of algorithm to solve for density profile

For a fluid at a given temperature and pressure, the bulk fugacity f_b can be evaluated. For a given adsorbent if the potential $\Psi(z)$ is known, then Equation 2-39 specifies the local fugacity. With the assumption of uniform local density, Equation 2-45 can be solved, at each point z, for $v(z)$ or its reciprocal the density. For a given temperature, bulk pressure (fugacity) and adsorbate-adsorbent system, the molar volume (or density) is specified at each point by Equation 2-39 and 2-45. However, below the critical point there may be three values of v which will satisfy Equation 2-45, and the question then becomes that of choosing the correct value of v. Since the fugacity rather than pressure is

specified, the Maxwell equal-area construction cannot be used to select the root. The different roots of Equation 2-45 give the same fugacity, but give different values of pressure P, where P is given by the van der Waals equation :

$$P(z) = \frac{RT}{v(z) - b} - \frac{a(z)}{v^2} \qquad [2\text{-}51]$$

This difference in pressure is used to select the correct root. A plot of fugacity versus pressure for a pure fluid is shown in Figure 2-9. Regions AB and BE represent the stable vapor and liquid phases respectively. Regions BC and DB are the meta-stable parts of the isotherm, and CD represents the unstable portion of the van der Waals isotherm. It may be noticed from the curve that for a given fugacity, the stable root is always at the highest pressure. The roots to the fugacity Equation (2-45) are substituted into the van der Waals equation and the root which gives the highest pressure is selected.

Equation 2-45 can be re-written in the following forms:

$$v(z) = b + \left\{\frac{RT}{f(z)}\right\} \exp\left[\frac{b}{v(z) - b} - \frac{2a(z)}{v(z)RT}\right] \qquad [2\text{-}52]$$

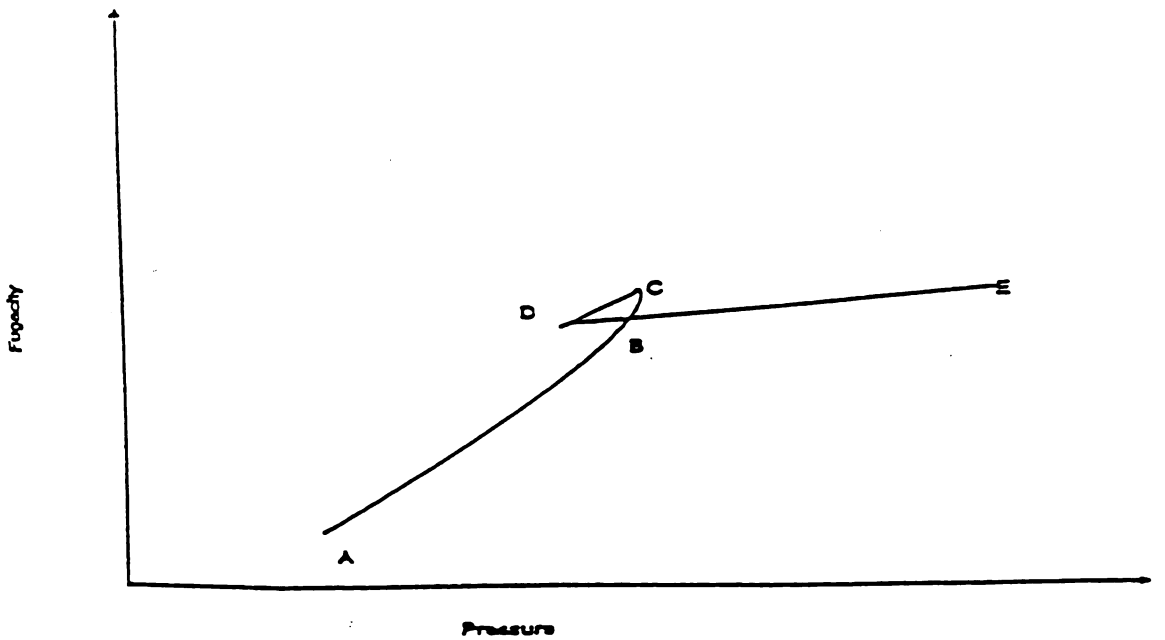

Figure 2-9: Fugacity vs Pressure for a Pure Fluid

$$v(z) = b + \frac{b}{\ln\left[\frac{f(z)\{v(z)-b\}}{RT}\right] + \frac{2a(z)}{vRT}} \qquad [2\text{-}53]$$

Equations 2-52 and 2-53 are solved by successive substitution. Equation 2-52 is written to provide an increasing value of $v(z)$, and for an initial guess the value of $v(z)$ is set equal to $RT/f(z)$. Equation 2-53 is started off with $v(z) = 1.1\ b$, and rapidly converges on the liquid root. Checks are placed to ensure that all the realistic roots at a point are obtained. The computer program used here is attached in Appendix 2. At a given temperature, this program utilizes the critical temperature of the fluid, the fluid-solid interaction parameter, and the size of the solid and fluid molecules to calculate the surface excess as a function of pressure, and the density as a function of position.

Results of the SLD Model

The SLD model discussed here, superimposes the attraction of the fluid molecules to the wall onto the attraction of fluid molecules to one another. The asymmetry of fluid-fluid interactions near an inert wall is incorporated into the equations for a, the attractive constant. Several limiting cases are discussed below and compared with theory, computer simulations and experiments.

1. Ideal Gas - Hard Wall

For an ideal gas and hard wall, there are neither fluid-fluid intermolecular attractions, nor fluid-wall attractive forces: Therefore $a = 0$, $b = 0$, and $\Psi(z) = 0$, $f = P$, and Equation 2-39 reduces to $P(z) = P_b$.. When combined with the ideal gas law, this reduces to $\rho(z) = \rho_b$, and as expected there is no adsorption.

2. Ideal gas - Attractive Wall

Here $a = 0$, $b = 0$, $f = P$. Equation 2-39 exactly reduces to $P(z) = P_b \exp[-\Psi(z)/(kT)]$. With the ideal gas law this gives $\rho(z) = \rho_b \exp[-\Psi(z)/(kT)]$. The surface excess is

$$\Gamma^{ex} = \int_{z_o}^{\infty} [\rho(z) - \rho_b] dz = \rho_b \int_{z_o}^{\infty} \left\{ \exp\left[-\frac{\Psi(z)}{kT} \right] - 1 \right\} dz \qquad [2\text{-}54]$$

Since the integral is constant, and ρ_b proportional to the pressure P_b, this leads to Henry's Law.

3. Attractive Fluid - Hard Wall

For an attractive fluid and hard wall, $a > 0$, $b > 0$, and $\Psi(z) = 0$, $f(z) = f_b$. The model predicts a reduced density near the wall, because of attraction of the fluid molecules near the wall to fluid molecules in the bulk. In fact a vapor-liquid phase transition is seen

adjacent to the wall for certain cases when the bulk fluid is liquid. This is similar to the observations of Abraham and Singh [1978].

4. Attractive Fluid - Attractive Wall

For this case, $a > 0$, $b > 0$, $\Psi(z) < 0$. In general, for an attractive fluid near an attractive wall an increase in density is exhibited near the wall depending on the magnitude of $\Psi(z)$. If the wall-fluid forces are stronger than the fluid-fluid forces, the fluid will wet the wall, otherwise there will be a rarefaction of gases near the wall. To represent the interactions of the adsorbate and adsorbent we have chosen the partially integrated 10-4 potential model [Lee, 1988]

$$\Psi(z) = 4\pi\rho_{atoms}\varepsilon_{fs}\sigma_{fs}\left(\frac{\sigma_{fs}^6}{5x_1^{10}} - \frac{1}{2}\sum_{i=1}^{4}\frac{1}{x_i^4}\right) \qquad [2\text{-}55]$$

where $\rho_{atoms} = 0.382$ atoms/ $\mathring{A}^2$, x_i is the intermolecular distance between fluid molecular centers and the ith plane of solid molecules, where we have truncated the interactions at the fourth plane of solid atoms, where the interplanar spacing is 3.35 $\mathring{A}$. ε_{fs} is the well depth of the fluid-solid potential, and is obtained from the Lorentz-Berthelot mixing rules which state that $\varepsilon_{fs} = (\varepsilon_{ff}\,\varepsilon_{ss})^{0.5}$ and $\sigma_{fs} = 0.5\,(\sigma_{ff} + \sigma_{ss})$. Table 2-1 summarizes other parameters used in this work. Note that ε_{ff} is not tabulated because the fluid-fluid contribution is calculated from Equations 2-46 - 2-48 and not directly from ε_{ff}. Steele [1974],

Table 2-1: Molecular properties used in SLD model

System	σ_{ff} (nm)	σ_{fs} (nm)	ε_{fs}/k (K)
Ethylene-Graphon	0.422	0.381	450, 23
Krypton-Graphon	0.35	0.345	225

Nicholson and Parsonage [1982], and Lee [1988] offer a further discussion of fluid-solid potentials.

Figure 2-10 shows adsorption isotherms that were calculated using the 10-4 potential of Equation 2-47 and the parameters for ethylene and graphon in Table 2-1. The curves are qualitatively similar to Figure 2-2. A knee is present, the magnitude of which can be increased by increasing the solid-fluid interaction energy ε_{fs} (Figure 2-10 also shows calculated adsorption isotherms for condensed phases at subcritical temperatures above the bulk vapor pressure which are not present in Figure 2-2). Some characteristic features of adsorption of near-critical fluids are the cusp-shaped isotherms seen near the critical point, and the 'cross-over' of adsorption isotherms at different temperatures. Consider the effect of temperature at a fixed pressure below the critical pressure. Below the critical pressure, adsorption decreases with increasing temperature, but this trend is reversed above the crossover region at pressures above the critical pressure. The crossover of the isotherms is eliminated by plotting the calculated surface excess with respect to calculated bulk density as shown in Figure 2-11. The reason for the cusp-like behavior of a supercritical isotherm in Figure 2-10 can be understood from the calculated density profiles shown in Figure 2-12. Below the critical pressure region, the adsorbed layer increases in thickness faster than the bulk density increases. Above the critical pressure region, the bulk fluid becomes increasingly incompressible, and the bulk fluid density approaches the density of the adsorbed fluid, causing the surface excess to decrease.

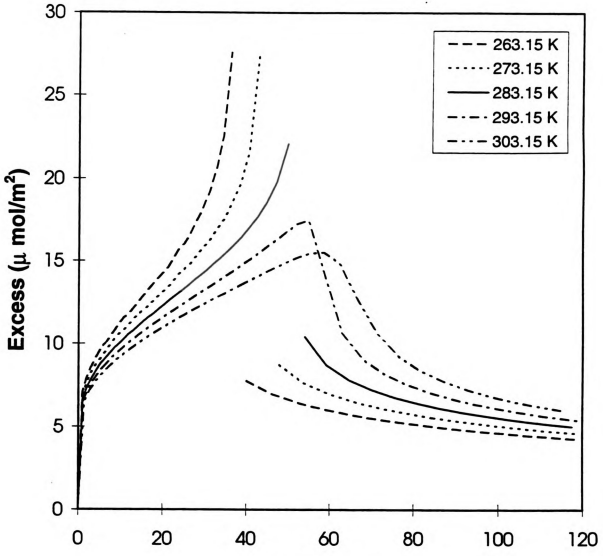

Figure 2-10: Adsorption of Ethylene on Graphon

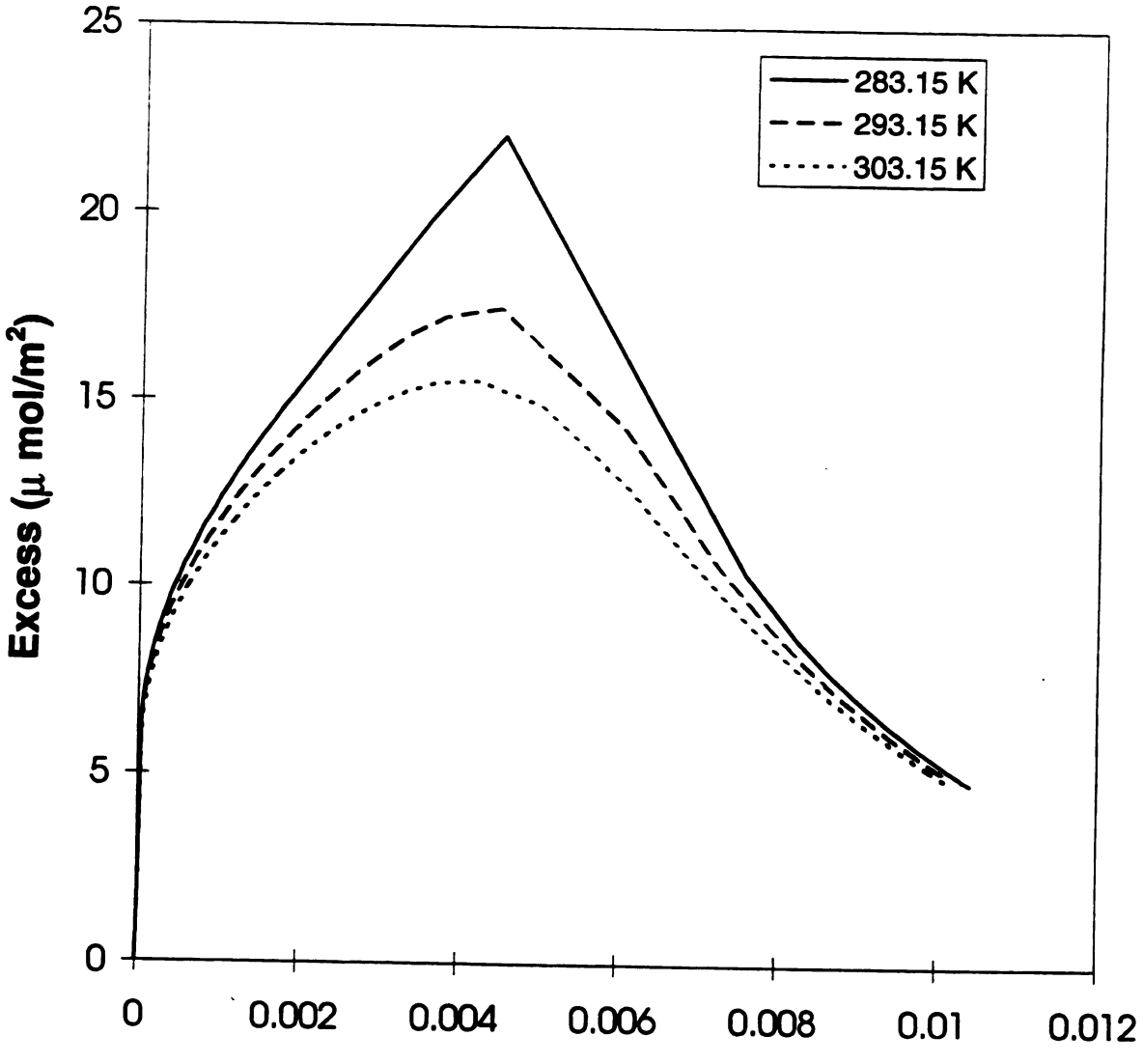

Figure 2-11: Adsorption of Ethylene on Graphon

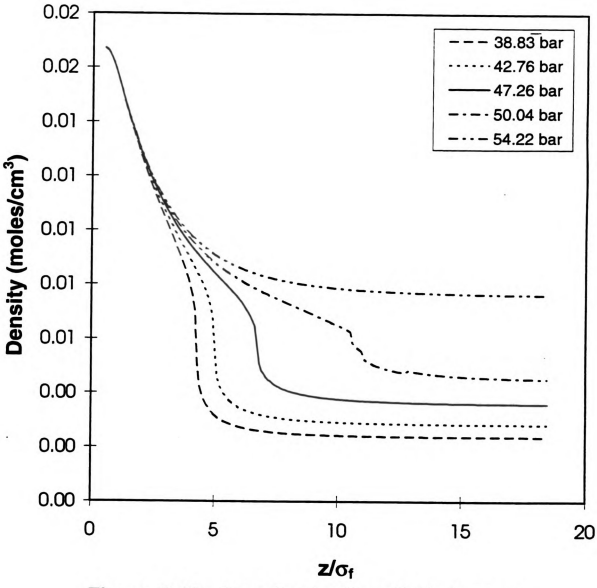

Figure 2-12: Density Profile of Ethylene on Graphon at 283.15 K

Type III isotherms are normally observed when the attraction between the solid and fluid is weak. Figure 2-13 demonstrates the capability of the SLD model for prediction of Type III isotherms. In this case, the fluid parameters are for ethylene, but the magnitude of the ε_{fs} has been decreased. The smaller ε_{fs} results in elimination of the knee and yields a Type III adsorption isotherm. At very low pressures and temperatures, a discontinuity in the adsorption isotherms is predicted (not shown here), indicating a phase transition in the adsorbed phase similar to those discussed for a two-dimensional model [Ross and Olivier, 1964]. At high pressures, when the bulk fluid exists as a liquid, the SLD model can predict a negative surface excess when ε_{fs} is small. Negative surface excesses have also been predicted by Sullivan [1979]. Figure 2-14 shows some predicted adsorption isotherms of krypton on graphon, at temperatures far above the critical temperature. When compared with experimental data shown in Figure 2-3, the predictions are again qualitatively correct. This model predicts some gas-liquid transitions on the surface, similar to the transitions seen in the experiments of Thomy [Bienfait, 1980].

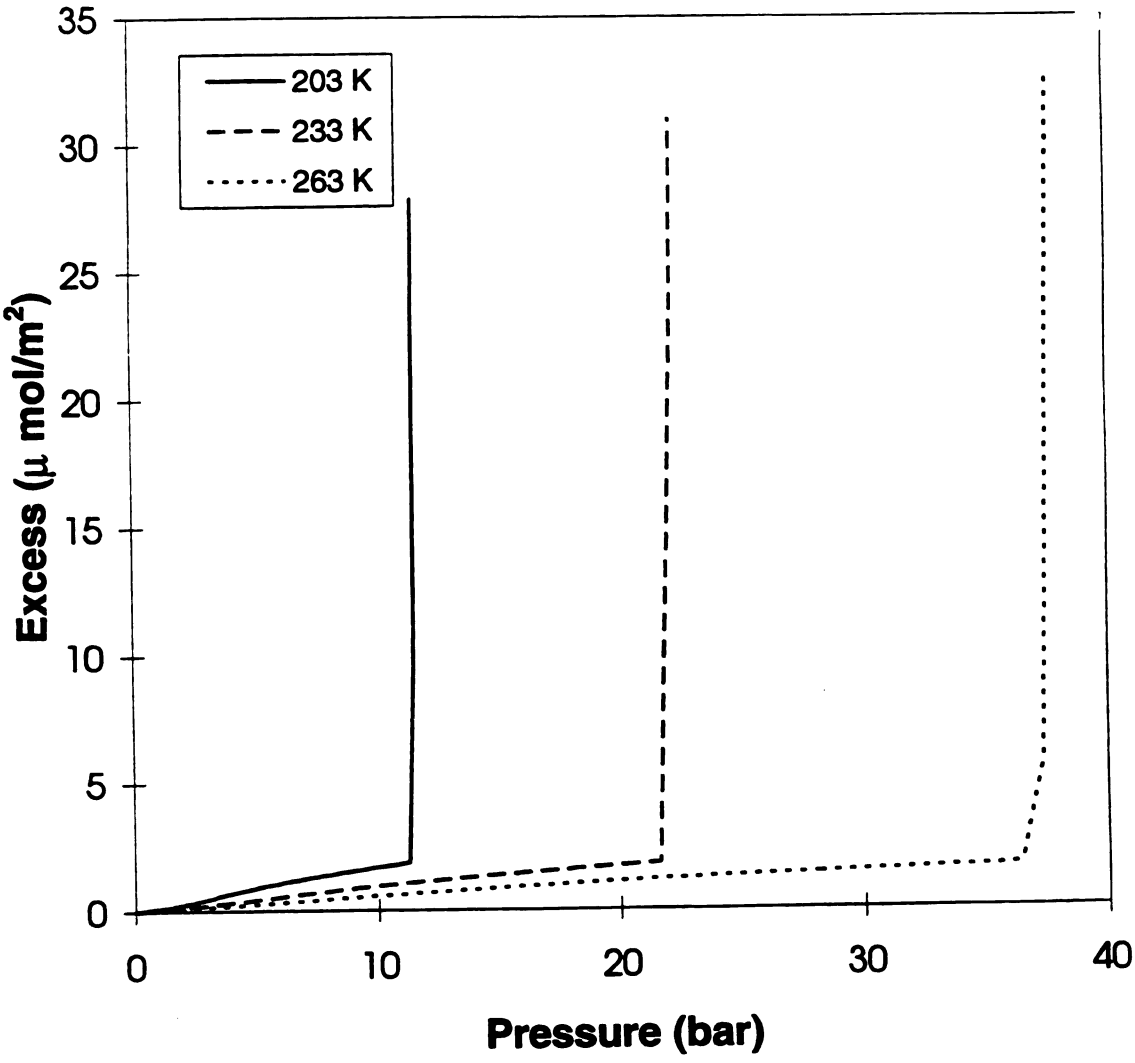

Figure 2- 13: Weak Adsorption of Ethylene on Graphon

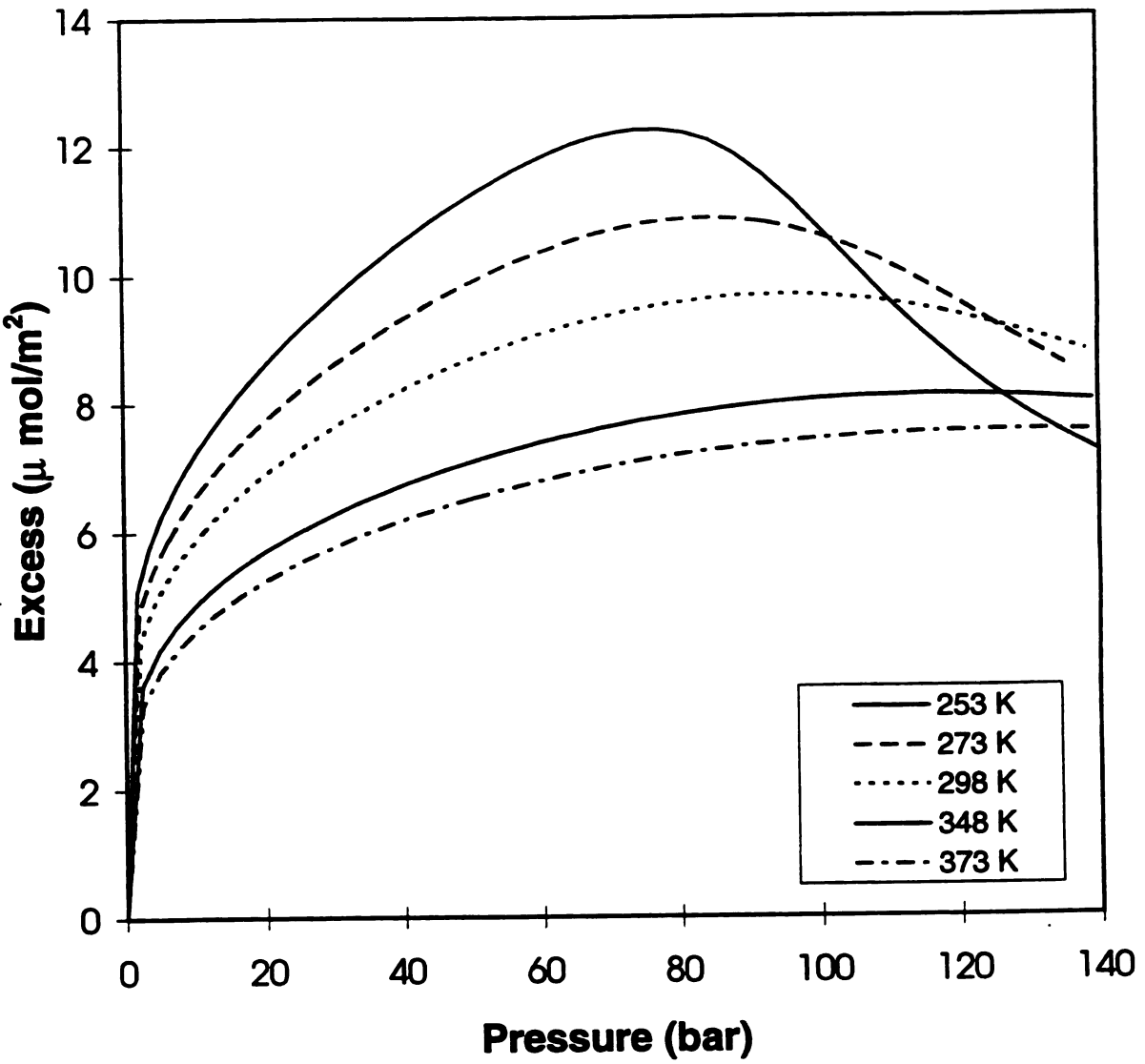

Figure 2-14: Adsorption of Krypton on Graphon

SLD Model - Discussion

The SLD model builds on the approaches of the simple theories such as Langmuir, BET, two-dimensional equations-of-state and the van der Waals approach of Barrer and Robins. By treating the fluid with a van der Waals equation with a suitably modified *a*, the SLD model allows for interactions between adsorbed molecules at various distances from the wall. All of the models mentioned above (including the SLD) assume an energetically homogeneous surface. The effect of heterogeneity will be pronounced at extremely low pressures and coverages, where the high energy sites are unfilled. To represent a heterogeneous surface, one could fit the potential to adsorption in the Henry's law region, and then work with a pseudohomogeneous surface.

The limitations of the model can be attributed to: (i) the lack of structure in the fluid; (ii) the use of the local density approximation; and (iii) the use of the van der Waals equation to describe the fluid properties. Since we are using the van der Waals equation and a mean field approach, we do not predict any of the fluid structure seen using either computer simulations or density functional theory [Snook and Henderson, 1978; Vanderlick et al., 1988; Kierlik and Rosinberg, 1991]. This model cannot describe discrete fluid structure or be used to study packing near a wall. The use of the local density approximation also results in the physically unrealistic prediction of abrupt vapor-liquid interfaces. Despite the fundamental theoretical limitations of the model, since model predictions mimic experimental trends, this model may be acceptable for engineering calculations. In order to estimate the errors introduced by the use of the local density approximation, Equation 2-42 was solved keeping the density inside the integral, leading to an integral

equation (IE) [Pyada, 1994]. When compared, solutions to the SLD model and IE approach showed differences which were dependent on pressure, temperature and magnitude of the gas-solid interaction potential. For the adsorption of ethylene on graphon, the SLD model tends to underpredict adsorption (relative to the integral equation (IE)) by about 10-20% between $0.9 < T_r < 1.1$, except where the surface excess increases steeply at high pressures. At pressures near 1 bar, the differences are less than 1%. These comparisons show that the local density assumption can provide a reasonably approximate solution to the adsorption problem.

A limitation of the van der Waals-based SLD model is the fact that predicted magnitudes of adsorption and vapor pressures are incorrect. For accurate prediction, the equation-of-state must be able to correctly predict the vapor pressure and liquid density. The inaccuracies of the van der Waals equation in this regard are well documented. In order to represent the fluid properties any equation-of-state can be used, provided the repulsive and configurational contributions can be separated for use in Equation 2-39. The selection of the van der Waals equation as the basis of this work was due to the fact that it is the simplest and most easily adapted equation-of-state with a theoretical basis. The objective of this work is to demonstrate that the proposed approach provides qualitative predictions with the van der Waals equation, and lay down the framework required to use a more accurate equation-of-state. A comparison of Figures 2-2 and 2-10 shows that the SLD model exhibits poor prediction of the vapor pressure for subcritical isotherms, but does better at predicting the pressure of the maxima in the supercritical isotherms. This is because the van der Waals parameters a and b were obtained from the critical temperature

and pressure. The ε_{fs} in Table 2-1 have been selected to provide semiquantitative fit to the magnitude of experimental adsorption.

Cubic equations are widely used in industry, and a method that adapts them to the adsorption problem could find widespread use in process calculations. In the next chapter we will see how changing the fluid equation-of-state significantly improves the quantitative modeling of adsorption. We will also show the extension of this model to predict Type I, IV and V isotherms, and multicomponent mixtures.

CHAPTER 3: QUANTITATIVE MODELING OF ADSORPTION AND EXTENSION OF THE SLD APPROACH TO PREDICT CLUSTERING

INTRODUCTION

In the previous chapter, we presented an engineering model that adapts the van der Waals equation-of-state to describe the fascinating behavior seen in the experiments of Findenegg [1983]. The fluid-solid potential was superimposed on the van der Waals equation-of-state, and the configurational energy integral in the inhomogeneous fluid phase is simplified with a local density approximation. While this model does a good job of qualitatively describing the adsorption behavior, quantitatively it does not predict the isotherms very well. The primary reason for this shortcoming was that the van der Waals equation does not predict accurately the vapor pressure and density of the adsorbing fluid. In this paper we use the Peng-Robinson equation to describe the fluid properties, which significantly improves the model predictions relative to the experimental results.

An adsorption model may also be adapted to describe clustering in supercritical fluids [Lee et. al, 1991]. Clustering is a phenomena that occurs in supercritical fluids whereby a large number of solvent molecules collapse around each solute molecule [Debenedetti, 1987; Eckert et. al, 1986], and the effect is most pronounced near the critical point. One of the first experimental studies on clustering involved the measurement of partial molal volumes near the critical point for solvents such as carbon dioxide and ethylene around solutes such as naphthalene [Eckert et. al., 1986], demonstrating that the partial molal volumes become extremely negative near the critical point. Debenedetti [1987],

using a fluctuation analysis converted these negative partial molal volumes to number of solvent molecules that cluster around the solute. Kim and Johnston [1987 a, b] state that at 300.5 K and 79.8 bar, the partial molal volume of naphthalene in supercritical carbon dioxide at infinite dilution is -7800 cc/mol, which corresponds to the condensation of 80 solvent molecules around a solute molecule. In a related study, Johnston et. al. [1987] show that there is a shift in the solvatochromic data of phenol blue in ethylene indicating an increase in the number of solvent molecules around a solute. Wu et. al. [1990] provide integral equation calculations on other supercritical systems that also suggest that clustering does occur in supercritical mixtures.

Brennecke and Eckert [1989] measured the intensity ratio of the fluorescence spectra to probe the local density of dilute organics in pure supercritical fluids. The intensity ratio for naphthalene in CO_2 at 4 K above the critical point was much greater than at 14 K above the critical point, indicating the clustering effect near the critical point. Such an increase was also demonstrated for systems such as pyrene-CO_2 and pyrene-ethylene. Lee et. al. [1991] have reviewed both the integral equation and spectroscopic measurements that give evidence of clustering in supercritical fluids.

Clustering is used to explain the unusual behavior in supercritical fluids such as increased solubilities, synergistic effects of mixed solutes and entrainer effects. The forces acting on the fluid molecule which result in this behavior are the fluid-fluid and fluid-solute intermolecular forces. On a molecular level, there is a similarity to the fluid-fluid and fluid-adsorbent intermolecular forces in physical adsorption on solid surfaces. In clustering, this leads to an increase in density of the fluid molecules in the region around the sol-

ute similar to the increase in density around the adsorbent in physical adsorption, and the fluid can be modeled in the inhomogeneous system.

In this chapter, the results of this simplified local density (SLD) model using the Peng-Robinson equation-of-state are given. The basic concepts of the SLD approach have been discussed in the previous chapter. The modifications made to this model to incorporate the Peng-Robinson equation, and model predictions of experimental results for adsorption on flat walls are discussed in detail in this chapter. The modifications made to this model to predict the clustering phenomenon are also discussed in detail. The model is capable of predicting the density profile and number of solvent molecules around a solute to indicate long-ranged interactions, giving evidence of clustering around a solute near the critical point. The model is shown to correlate with fluorescence spectroscopy measurements.

MODEL DEVELOPMENT

The approach of the model is the adaptation of a cubic equation-of-state to define the properties of a fluid that is in the external potential field of an adsorbent. First, we develop the model for flat solid adsorbents (incorporating the Peng-Robinson equation) and then generalize the results for clustering. A fluid molecule at any position from the solid interacts with both the solid and fluid molecules. Therefore, the chemical potential of the fluid may be written as a sum of the fluid-fluid and fluid-solid interactions

$$\mu(z) = \mu_b = \mu_{ff}(z) + \mu_{fs}(z) \qquad [3\text{-}1]$$

where $\mu_{ff}(z)$ and $\mu_{fs}(z)$ are the chemical potentials due to the fluid-fluid and fluid-solid interactions, and z is the distance normal to the surface of the solid, and the subscript b stands for bulk properties. If the fluid-solid potential is given by $\psi(z)$ on a molecular basis, then on a molar basis

$$\mu_{fs}(z) = N_A \Psi(z) \qquad [3\text{-}2]$$

For a non-ideal bulk fluid, the chemical potential μ_b of Equation 3-1 is related to the fugacity as

$$\mu_b = \mu_o + R\,T \ln\left(\frac{f_b}{f_o}\right) \qquad [3\text{-}3]$$

Details of the development of this model are given in the previous chapter.

Using the Peng-Robinson equation-of-state, can write an expression for the bulk fugacity in terms of molar volume.

$$\ln\left(\frac{f_b}{P}\right) = (Z_b - 1) - \ln(Z_b - B) - \frac{A_b}{2.828\,B}\ln\left(\frac{Z_b + 2.414\,B}{Z_b - 0.414\,B}\right) \qquad [3\text{-}4]$$

where

$Z_b = \frac{P\, v_b}{R\, T}$ is the compressibility factor

$$A_b = \frac{a_b P}{R^2 T^2}$$

$$B = \frac{bP}{RT}$$

$$P = \frac{R\, T}{v_b - b} - \frac{a_b}{v_b^{\,2} + 2bv_b - b^2}$$

where a, b are the constants of the Peng-Robinson equation [1976].

Rearranging Equations 3-2 - 3-4, the component of the fluid fugacity due to fluid-fluid interaction is

$$f_{ff}(z) = f_b \exp\left[-\frac{\Psi(z)}{kT}\right] \qquad [3\text{-}5]$$

Using the Peng-Robinson equation, the fluid-fluid fugacity at any point becomes

$$\ln\left[f_{ff}(z)\right] = \frac{b}{v(z)-b} - \frac{a(z)}{v(z)^2 + 2bv(z) - b^2}\frac{v(z)}{RT} - \ln\left[\frac{v(z)-b}{RT}\right] - \frac{a(z)}{2.828bRT}\ln\left[\frac{v(z)+2.414\,b}{v(z)-0.414\,b}\right] \qquad [3\text{-}6]$$

where $v(z)$ is the molar volume at any point z. $a(z)$ is calculated using the SLD approach, as given in the previous chapter, assuming a fluid-fluid pair potential $\propto r^{-6}$ and is given by

$$a(z) = a_b\left(\frac{5}{16}+\frac{6}{16}\frac{z}{\sigma_f}\right) \quad for \quad 0.5 \le \frac{z}{\sigma_f} \le 1.5 \qquad [3\text{-}7]$$

$$a(z) = a_b\left(1-\frac{1}{8(\frac{z}{\sigma_f}-0.5)^3}\right) \quad for \quad 1.5 \le \frac{z}{\sigma_f} \le \infty \qquad [3\text{-}8]$$

where σ_f is the diameter of the fluid molecule.

In modifying this model to arrive at Equations 3-6 - 3-8 for the Peng-Robinson equation assumptions are necessary to evaluate the configurational integral. Returning to the integral from which the equation-of state a parameter is based, the attractive chemical potential is given by

$$\mu_{att} = \int_V \phi(r)\frac{g(r)}{v}dV \qquad [3\text{-}9]$$

where V denoted the volume of integration, $\phi(r)$ is the two-body interaction potential, and $g(r)$ is the radial distribution function.

In the SLD model, the fluid at a point z is treated as a homogeneous fluid at a density of $\rho(z)$. Solving Equation 3-9, the attractive pressure term of the van der Waals equation for a homogeneous fluid becomes $-a/v^2$. In the case of the Peng-Robinson equation, the attractive pressure term for a homogeneous fluid is $-\frac{a}{v^2+2bv-b^2}$. The Peng-Robinson equation, as an empirical equation-of-state, has an unknown equivalent form of the integral given by Equation 3-9, and therefore some assumptions are necessary to approximate this integral. The term v^2 in the denominator of the attractive part of the van der Waals equation is a result of the volume derivative of Equation 3-9 . The term $v^2 + 2bv - b^2$ in the Peng-Robinson equation may be treated as an empirical equivalent of the term v^2 of the van der Waals equation, and can be subject to an analogous SLD approximation. If the density is uniform up to the surface of the adsorbent, then we know that at this limit $\mu_{wall} = \mu_b/2$, resulting in $a_{wall} = a_b/2$ for the van der Waals equation. The Peng-Robinson equation should have the same limits. Also, the functionality of the a/a_b should have the same qualitative curvature in both the van der Waals and Peng-Robinson equations. Since the true form of Equation 3-9 is not known for the Peng-Robinson equation, as a first approximation, we use the van der Waals ratio of $a(z):a_b$ for the Peng-Robinson SLD model, and retain $v^2 + 2bv - b^2$ as the denominator of the attractive pressure term, which results in Equations 3-6 - 3-8.

The other pair potential needed for this model is the fluid-solid potential. The adsorbate-adsorbent interactions are given by the integrated 10-4 Lennard-Jones potential [Lee, 1988] as

$$\Psi(z) = 4\pi\rho_{atoms}\varepsilon_{fs}\sigma_{fs}\left(\frac{\sigma_{fs}^6}{5x_1^{10}} - \frac{1}{2}\sum_{i=1}^{4}\frac{1}{x_i^4}\right) \qquad [3\text{-}10]$$

For modeling clustering in supercritical fluids, the approach is essentially similar, with the exception of the configurational integral calculation. The wall in adsorption onto a flat surface is replaced by a solute molecule with the solvent molecules clustering around it. Geometrically, this means replacing a planar surface with a spherical particle. The coordinate system is changed from rectangular geometry to spherical geometry and the fugacity, molar volume and the Peng-Robinson *a* term become functions of *r*, the radial distance from the center of the solute molecule. The corresponding *a(r)* become

$$\frac{a(r)}{a_b} = \frac{3}{16}\left[\begin{array}{l}\frac{8}{3}+\frac{2}{\sigma_f}(r-r')+\frac{2}{3}\sigma_f^3\left\{\frac{1}{(r+r')^3}\right\} \\ +\frac{\sigma_f^3}{r}\left\{\frac{1}{r'^2+r^2-2rr''}-\frac{1}{r'^2+r^2+2rr'}\right\}\end{array}\right] \quad for\ 0.5\sigma_f \le r-\frac{\sigma_s}{2} \le 1.5\sigma_f \quad [3\text{-}11]$$

$$\frac{a(r)}{a_b} = \frac{3}{16}\left[\begin{array}{l}\frac{16}{3}-\frac{2\sigma_f^3}{3}\frac{1}{(r-r')^3}+\frac{2\sigma_f^3}{3}\frac{1}{(r+r')^3} \\ +\frac{\sigma_f^3}{r}\left\{\frac{1}{r'^2+r^2-2rr'}-\frac{1}{r'^2+r^2+2rr'}\right\}\end{array}\right] \quad for\ 1.5\sigma_f \le r-\frac{\sigma_s}{2} \le \infty \quad [3\text{-}12]$$

where

$$r' = \frac{(\sigma_f + \sigma_s)}{2}$$

$$r'' = \frac{r'^2 + r^2 - \sigma_f^2}{2r'}$$

where the subscript *f* stands for fluid, and the subscript *s* for the solute. Details are given in the appendix 1.

The solute-solvent interactions are given by the Lennard-Jones potential

$$\Psi(r) = 4\varepsilon_{fs}\left(\frac{\sigma_{fs}^{12}}{r^{12}} - \frac{\sigma_{fs}^{6}}{r^{6}}\right) \qquad [3\text{-}13]$$

The component of the fluid-fluid fugacity due to fluid-fluid interactions, i.e. the equivalent form of Equation 3-5 for clustering is

$$f_{ff}(r) = f_b \exp\left[-\frac{\Psi(r)}{kT}\right] \qquad [3\text{-}14]$$

Using the Peng-Robinson equation-of-state, the fluid-fluid fugacity can be expressed similar to Equation 3-6, except that the molar volume, *a* and fugacity are functions of *r* instead of *z*.

Algorithm for solving density profile

To calculate the surface excess or cluster size, the density profile must be known. The density can be evaluated by first calculating the bulk fugacity and density from a given

temperature and pressure. Knowing the fluid-solid potential, the fugacity at any point can be calculated by Equation 3-5 (physical adsorption) or 3-14 (clustering). The density is then calculated iteratively using Equation 6 or by the modified form using *v(r)* and *a(r)* for clustering. Once the density profile is known the surface excess can be calculated by equation 2-1. Similarly, for clustering, the cluster size (N^{ex}) can be calculated as

$$N^{ex} = \int_{r_o}^{\infty} (\rho(r) - \rho_b) dV \qquad [3\text{-}15]$$

The FORTRAN programs for calculating the adsorption isotherms and cluster sizes are available in appendix 2.

RESULTS

The diameters of the fluid, solid and solute are the Lennard-Jones parameters as tabulated in Reid et. al [1987] and in Lee et. al. [1991]. The σ_{fs} is calculated as the arithmetic mean of the fluid and solid (or solute in clustering), while the fluid-solid potential (ε_{fs}) is used as an adjustable parameter to adjust the magnitude of adsorption. The values used for all the parameters are summarized in Table 2-1 or 3-1.

Figure 3-1 shows the surface excess of ethylene adsorbing onto graphon at various sub- and supercritical temperatures, and over a wide pressure range. This model is capable of quantitative fits for the adsorption isotherms over this entire pressure and temperature range, using a single parameter. The model also does a good job of accurately predicting the pressure at which the peaks occur, showing the characteristic cusp-like behav-

Table 3-1: Molecular properties used in the SLD model

System	σ_f(nm)	σ_s (nm)	σ_{fs} (nm)	ε_{fs} /k (K)
Ethylene - Graphon	.422	.34	.381	140
Krypton - Graphon	.3655	.34	.35275	95
Propane - Graphon	.5118	.34	.4259	110
Argon - Graphon	.3542	.34	.3471	68
Methane - Graphon	.3758	.34	.3579	107
Carbon dioxide - Naphthalene	.3794	.6199	.49965	800
Carbon dioxide - Pyrene	.3794	.714	.5467	850
Ethylene - Pyrene	.422	.714	.568	800

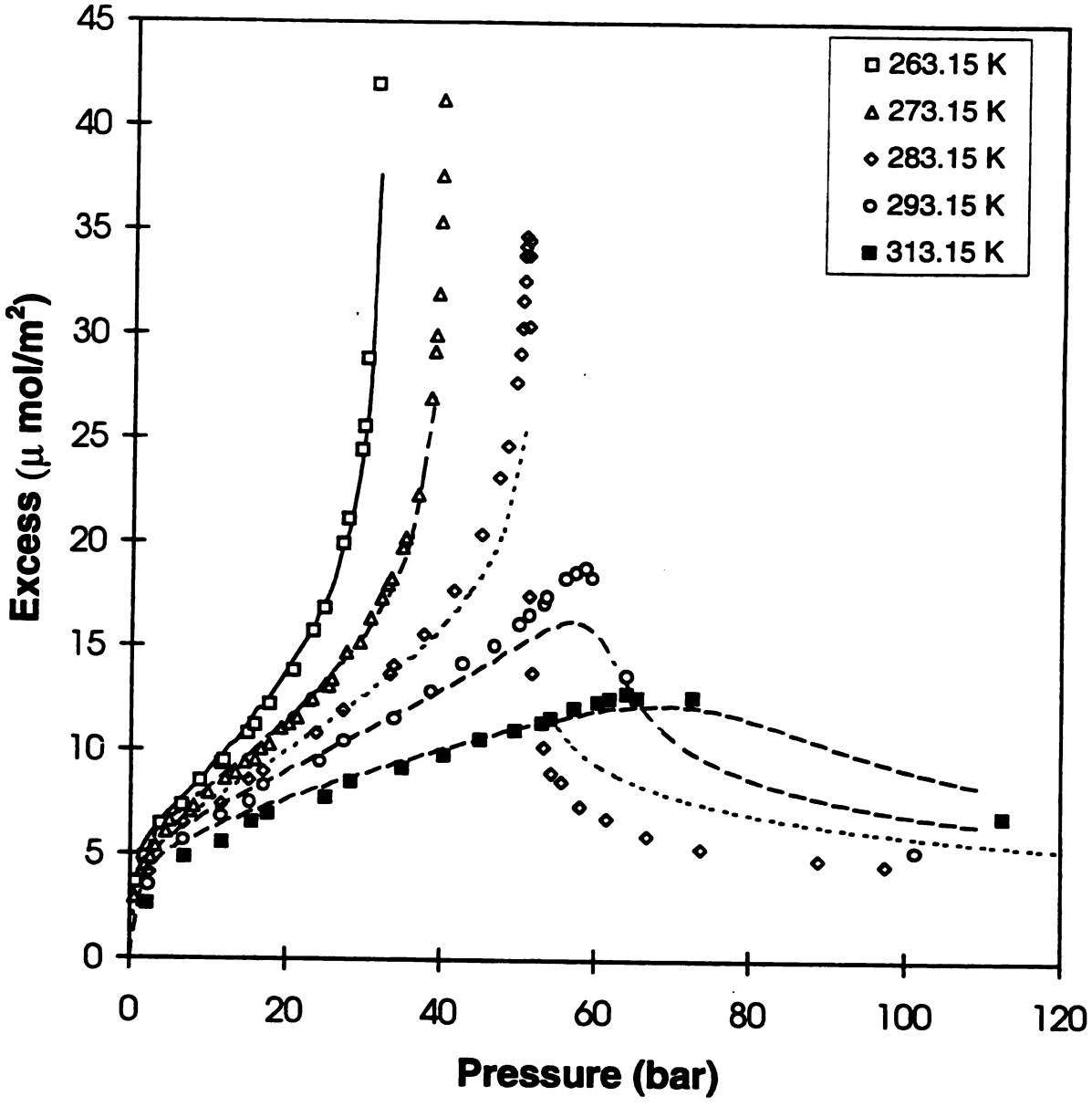

Figure 3-1: Adsorption of Ethylene on Graphon

ior seen near the fluid critical point. The model predicts the correct temperature-dependent crossover of adsorption isotherms in the supercritical region. One of the primary reasons that the Peng-Robinson SLD model does a better job than the van der Waals SLD model is that the Peng-Robinson equation predicts more accurate density values near the solid surface, and a more compressible adsorbed layer. A comparison of experimental saturation densities for ethylene [Angus et. al, 1974], and both these equations [Pyada, 1994] shows that while the van der Waals equation underpredicts the saturation densities by 80-90% between 211 and 260 K, the Peng-Robinson equation is within about 6%. van Megen and Snook [1982] have done Monte-Carlo simulations of Lennard- Jones molecules (that simulate ethylene) on graphon at supercritical temperatures [8] ($T/T_c = 1.03$) (see Figure 2-5). Their results significantly overpredict the experimental values of Findenegg, and their maxima is around 42 bar, as opposed to the experimental value of 58.7 bar, while the SLD model has a maxima at 57.8 bar.

Figures 3-2 and 3-3 show the adsorption isotherms of krypton onto graphon at supercritical temperatures, and propane at subcritical temperatures. The krypton isotherms 253 and 273 K crossover at around 140 bar. Once again, the model predicts this crossover at the correct pressure. This model was also tested on gases like argon and methane (Figures 3-4 and 3-5). While, the model predictions for argon were good, the model did not do a very good job of predicting the isotherms for methane, the reason maybe that the Peng-Robinson equation does not do a good job of predicting the fluid properties of liquid methane [Prausnitz, 1980]. The PVT behavior of these different gases and the error in predicting density values is shown in appendix 3.

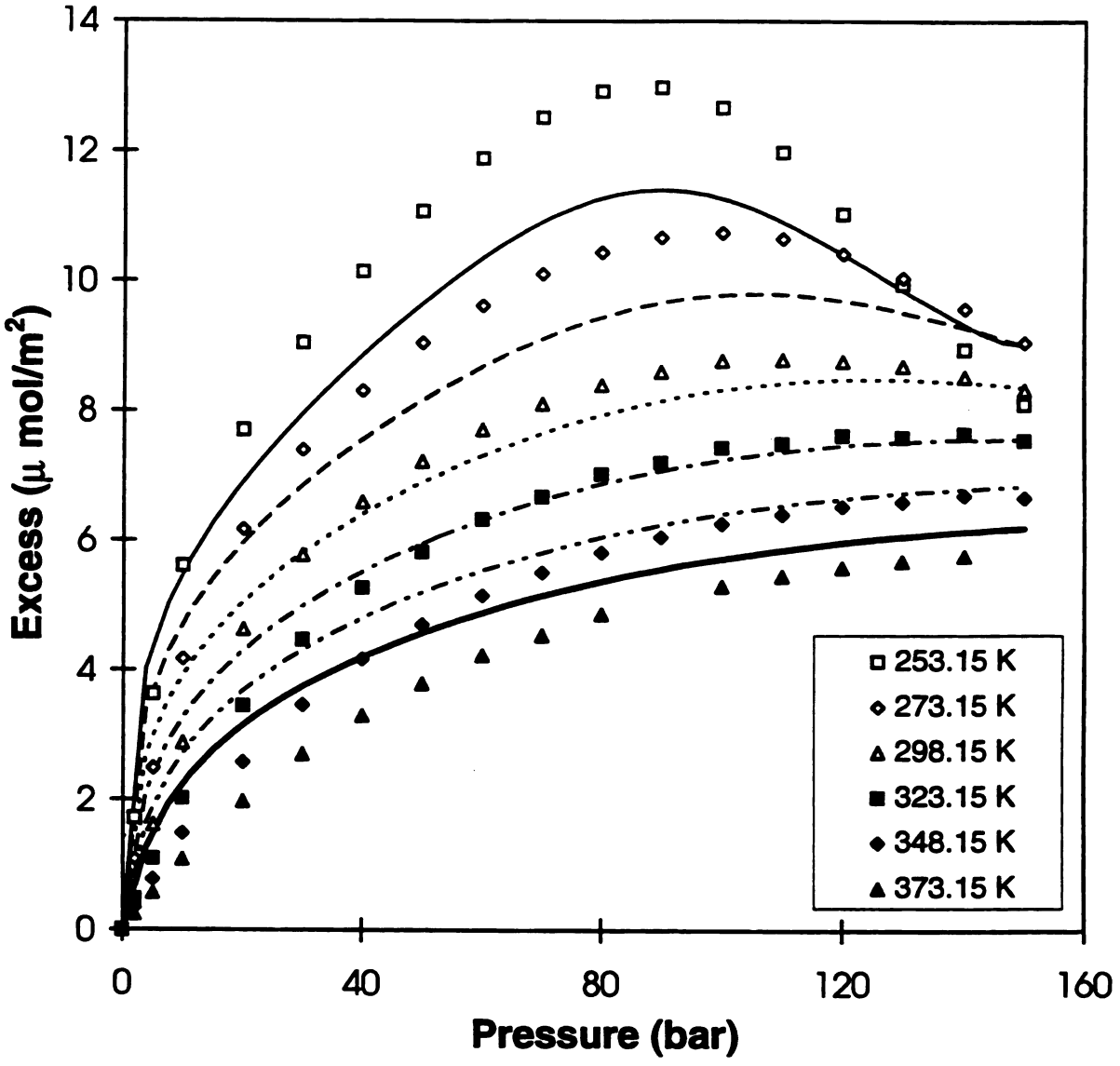

Figure 3-2: Adsorption of Krypton on Graphon

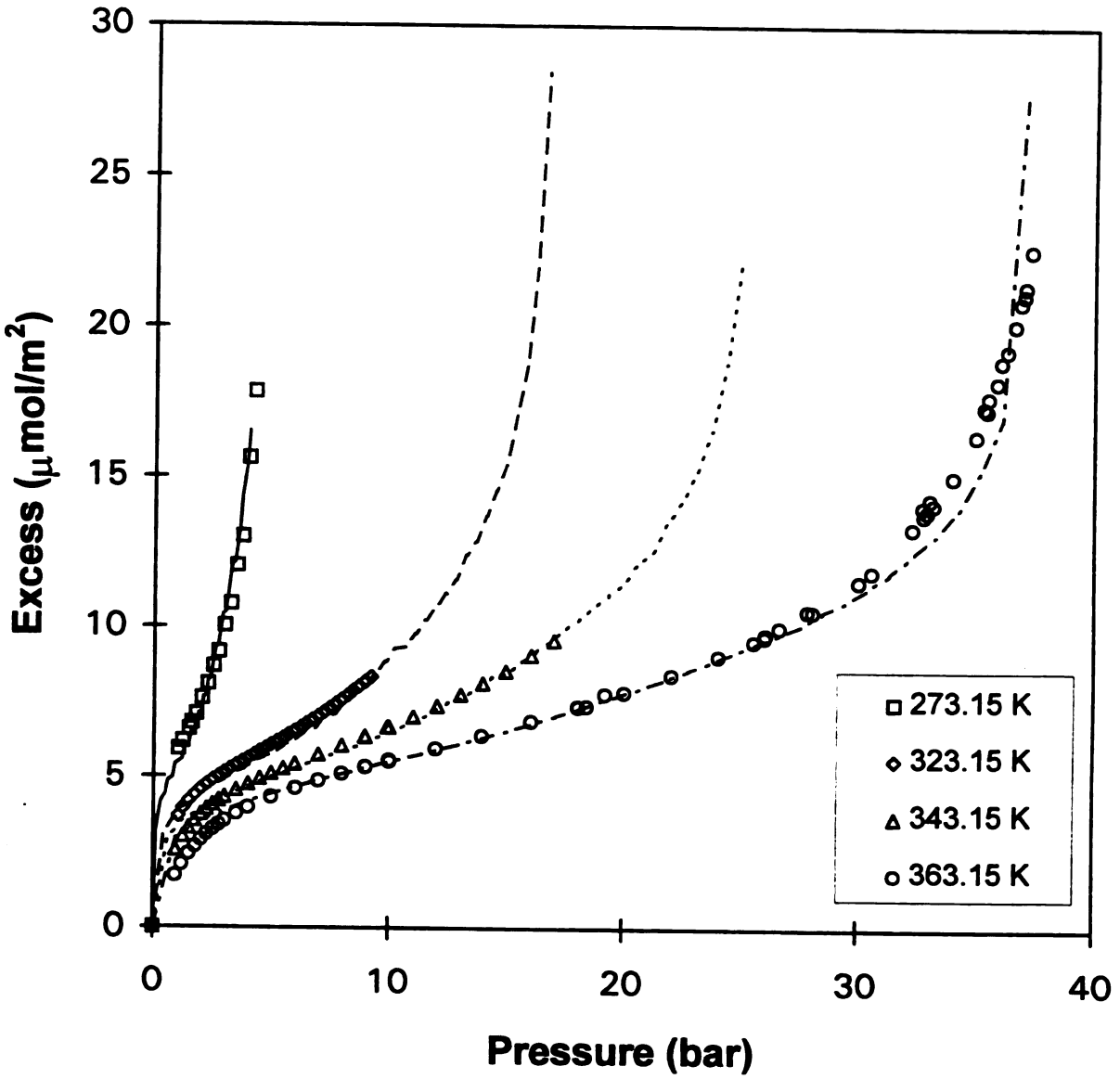

Figure 3-3: Adsorption of Propane on Graphon

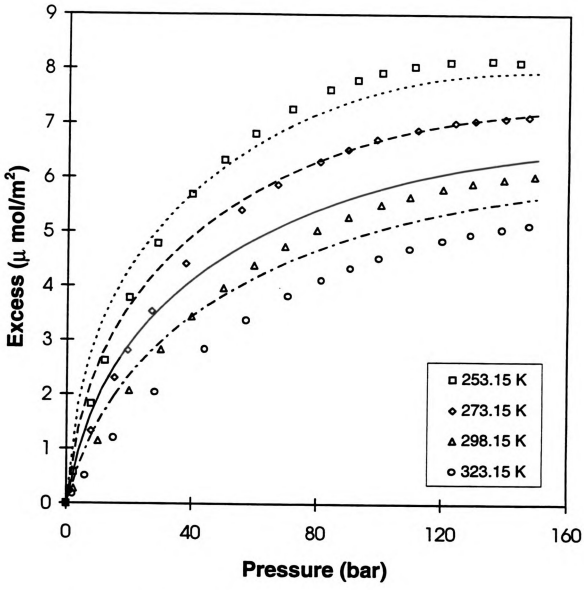

Figure 3-4: Adsorption of Argon on Graphon

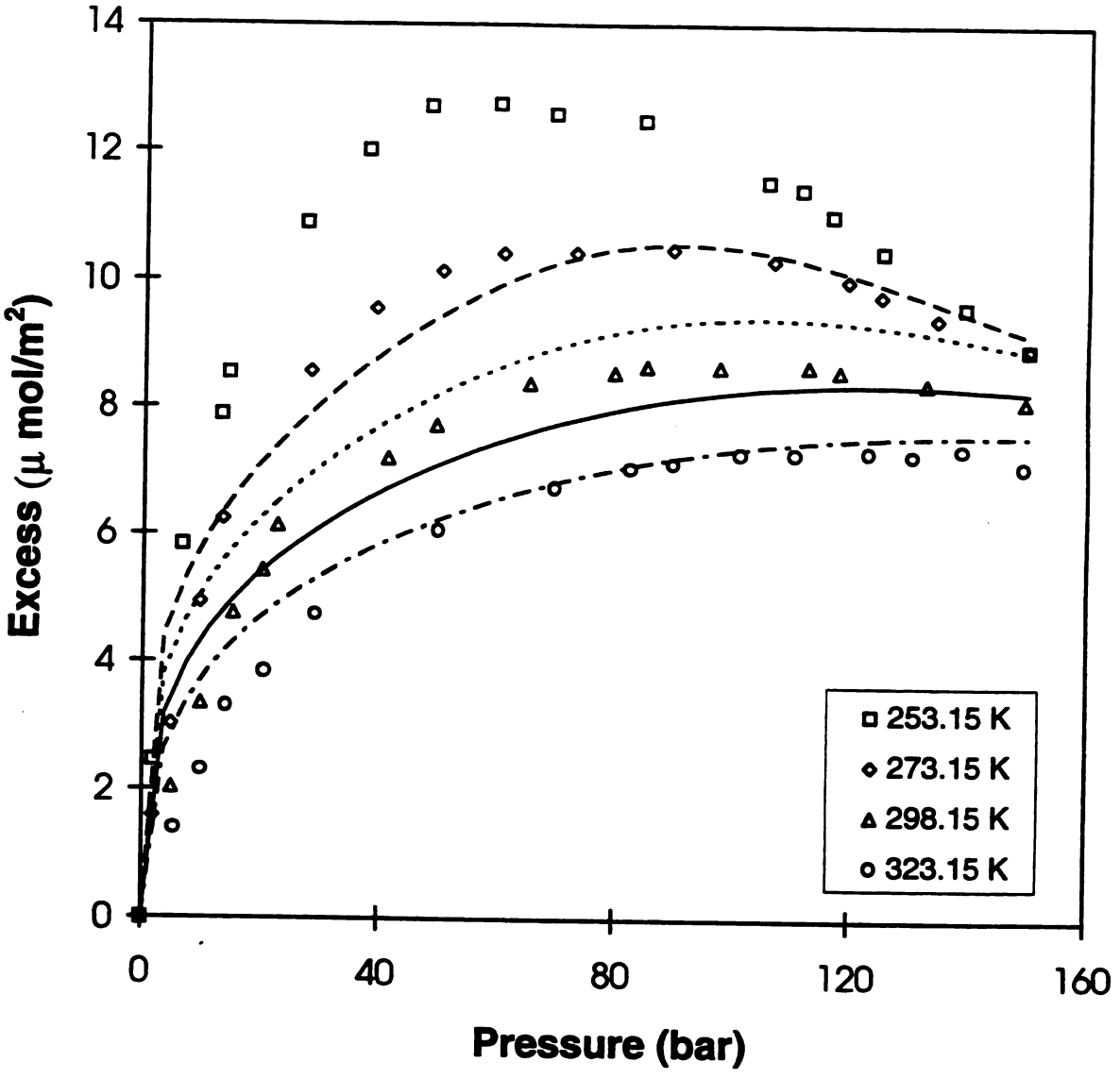

Figure 3-5 : Adsorption of Methane on Graphon

Figures 3-6 - 3-12 describe the clustering phenomenon. The density profile and the excess number of solvent molecules within a sphere of radius R around a solute are plotted in Figure 3-6. As shown in the figure, the density goes through a sharp increase near the surface of the solute but quickly drops to the bulk value. The excess number of solvent molecules is slightly negative very near the surface before increasing sharply. Such a trend has been shown in the integral equation calculations of xenon in neon [Wu et. al, 1990] (Figure 3-7). The figure also shows that the excess number of solvent molecules increases sharply up to 5 molecular diameters, and then slowly till 9 or 10 molecular diameters, showing the long-ranged effect of this clustering phenomenon. This trend has also been reported by Wu et. al [1990].

Figures 3-8 & 3-9 shows the results for clustering of CO_2 molecules around naphthalene at 2 K, 4 K and 14 K above its critical point. As seen in Figure 3-8, the cluster size increases sharply near the critical point, but drops quickly as we move away from the critical point. The results of the fluctuation calculation of Debenedetti [1987] on the same system at 308 K are also plotted in Figure 3-8. The model predicts the correct density at which maximum number of CO_2 molecules cluster around naphthalene, and does a fair job of predicting the number of CO_2 molecules. The model also predicts a slightly broader density range over which this clustering phenomenon occurs. However, the model does accurately predict the increase in the number of CO_2 molecules around a single naphthalene molecule as the critical point is approached, and also the variation of this peak with temperature and pressure. When this cluster size is plotted against bulk density, cross-

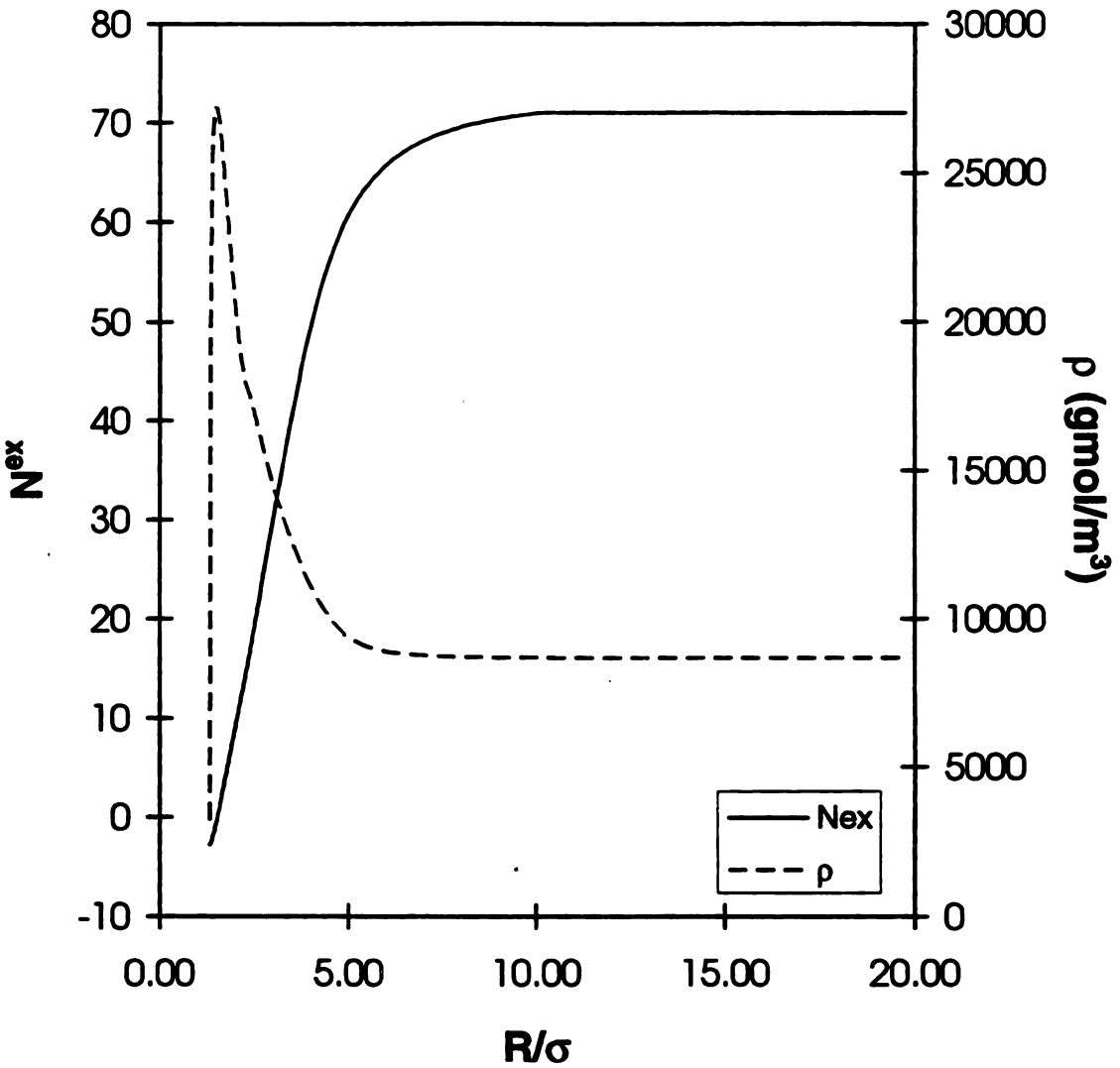

Figure 3-6: Density and Excess number of solvent molecules within a Sphere of Radius R around a Solute

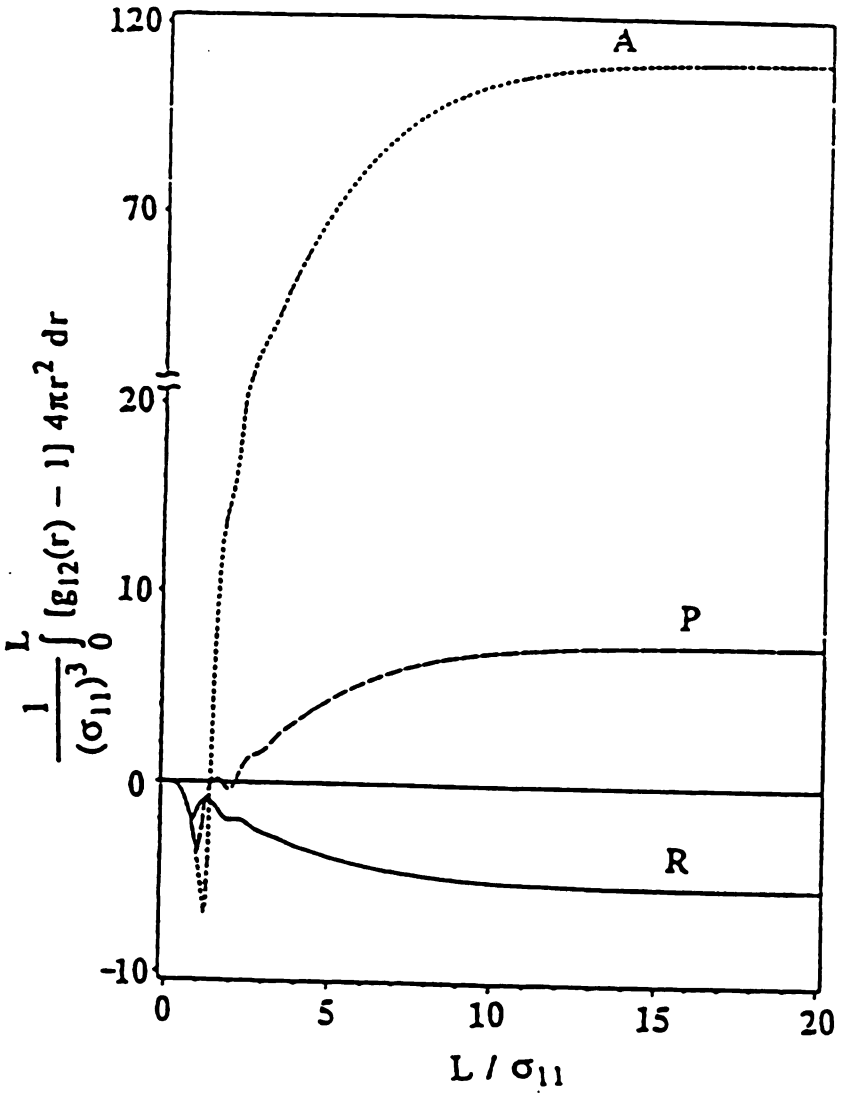

Figure 3-7: Number of Excess Solvent Molecules Within a Sphere of Radius L Around a Solute

A: Xenon in Neon (Attractive)
R: Neon in Xeonon (Repulsive)
P: Pure Lennard-Jones

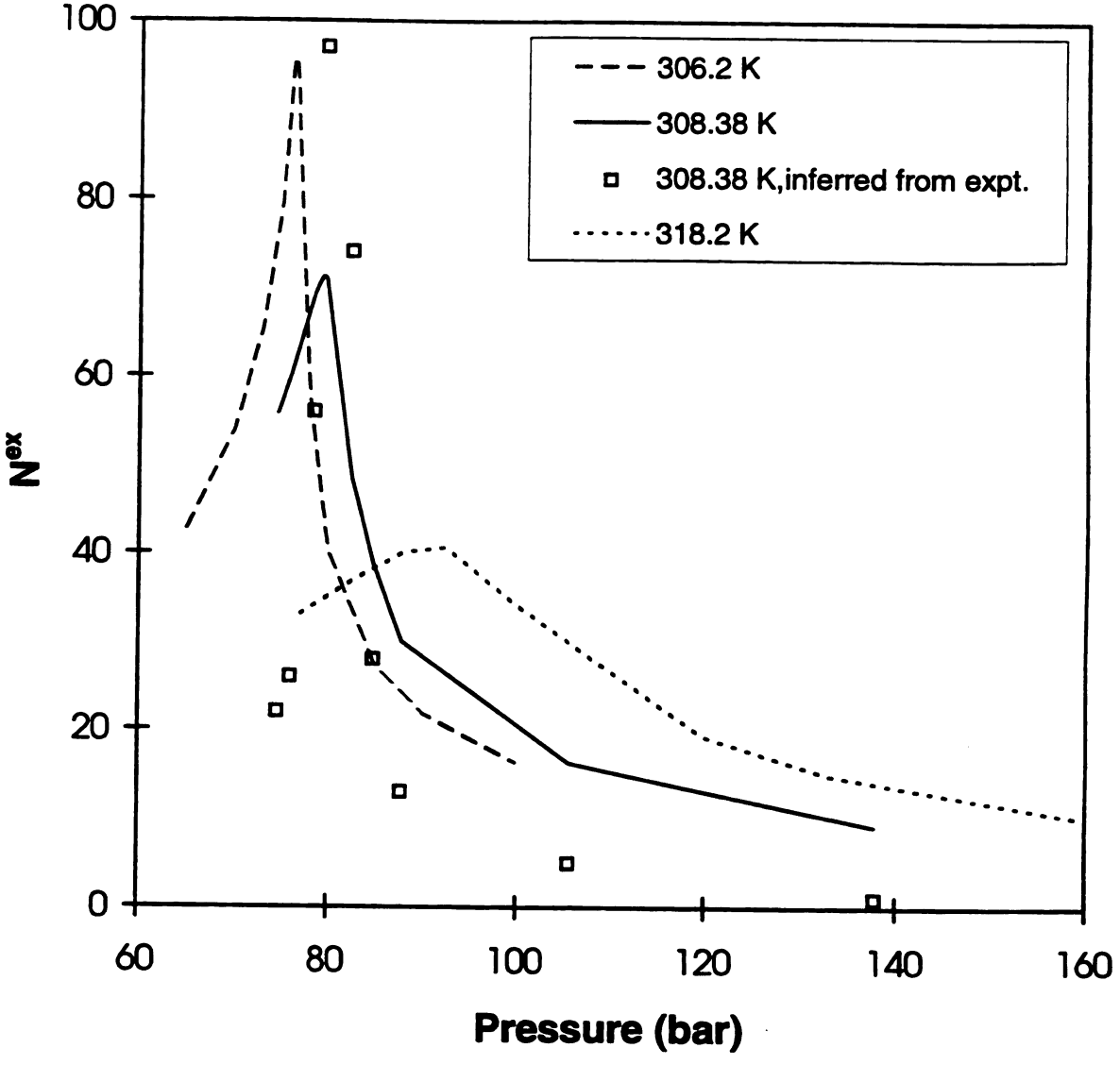

Figure 3-8: Clustering of CO_2 around Naphthalene

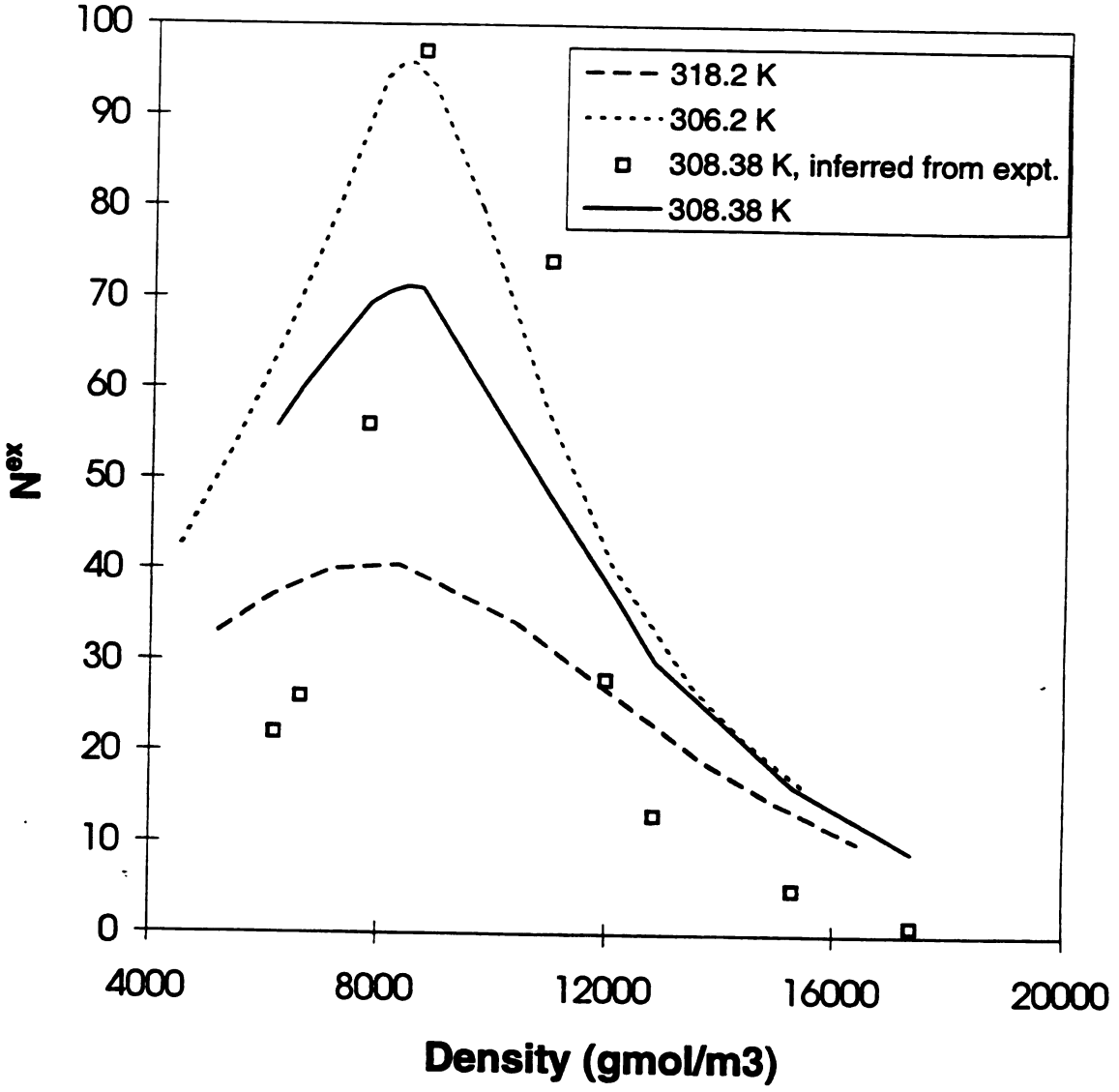

Figure 3-9: Clustering of CO2 around Naphthalene

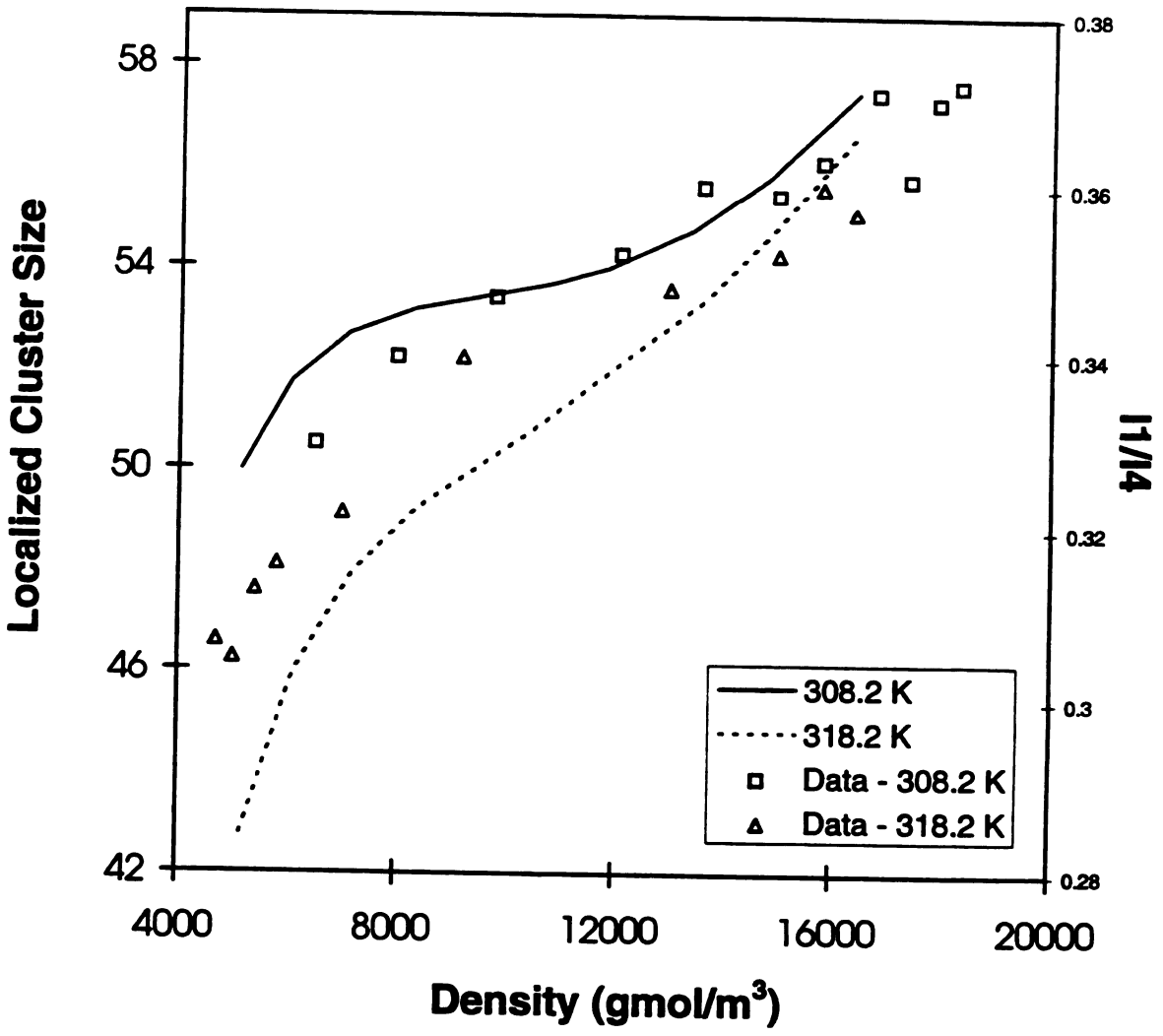

Figure 3-10: Comparison of Cluster Size with Fluorescence Spectroscopy - CO_2 around Naphthalene

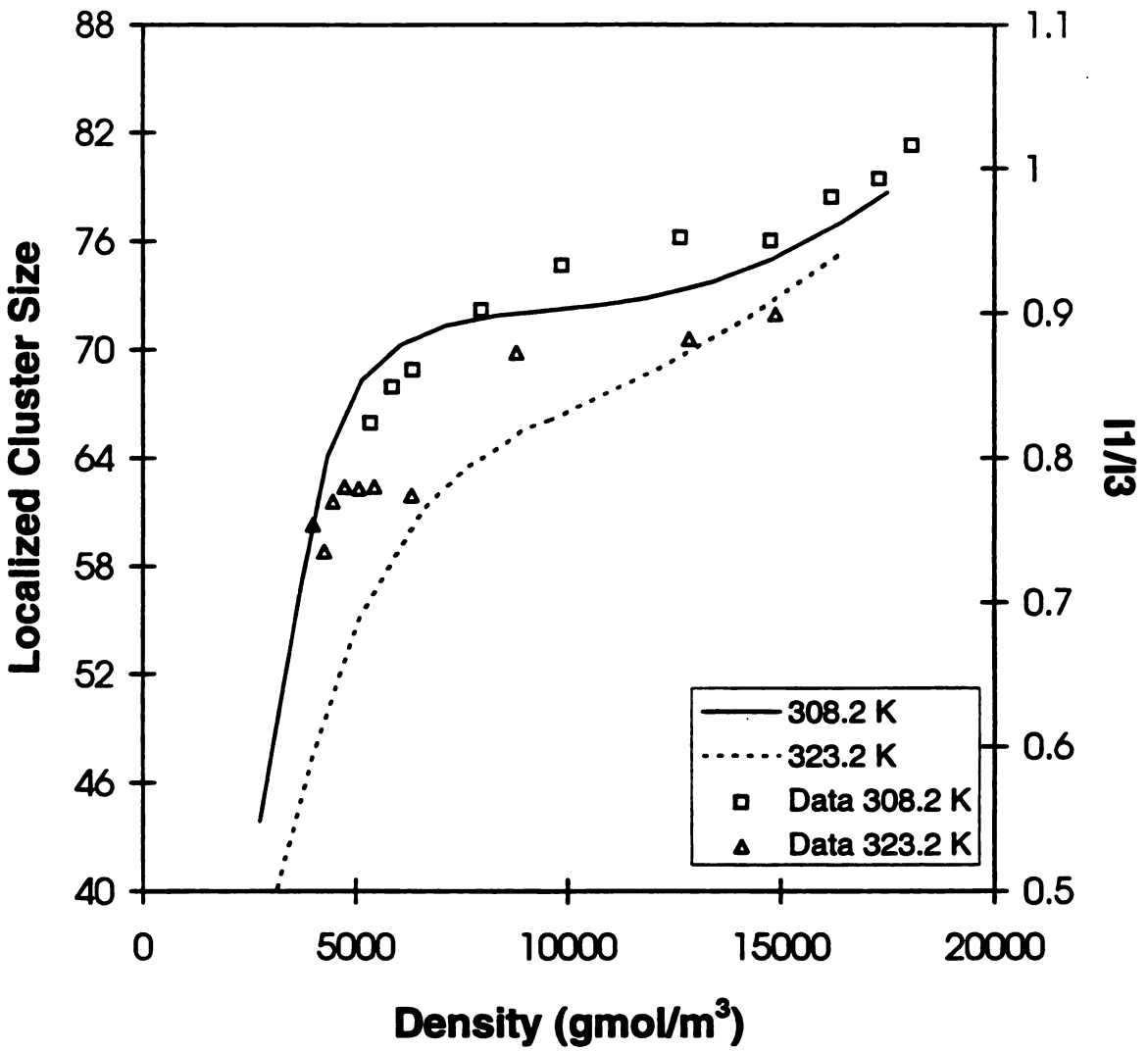

Figure 3-11: Comparison of Cluster Size with Fluorescence Spectroscopy - CO_2 around Pyrene

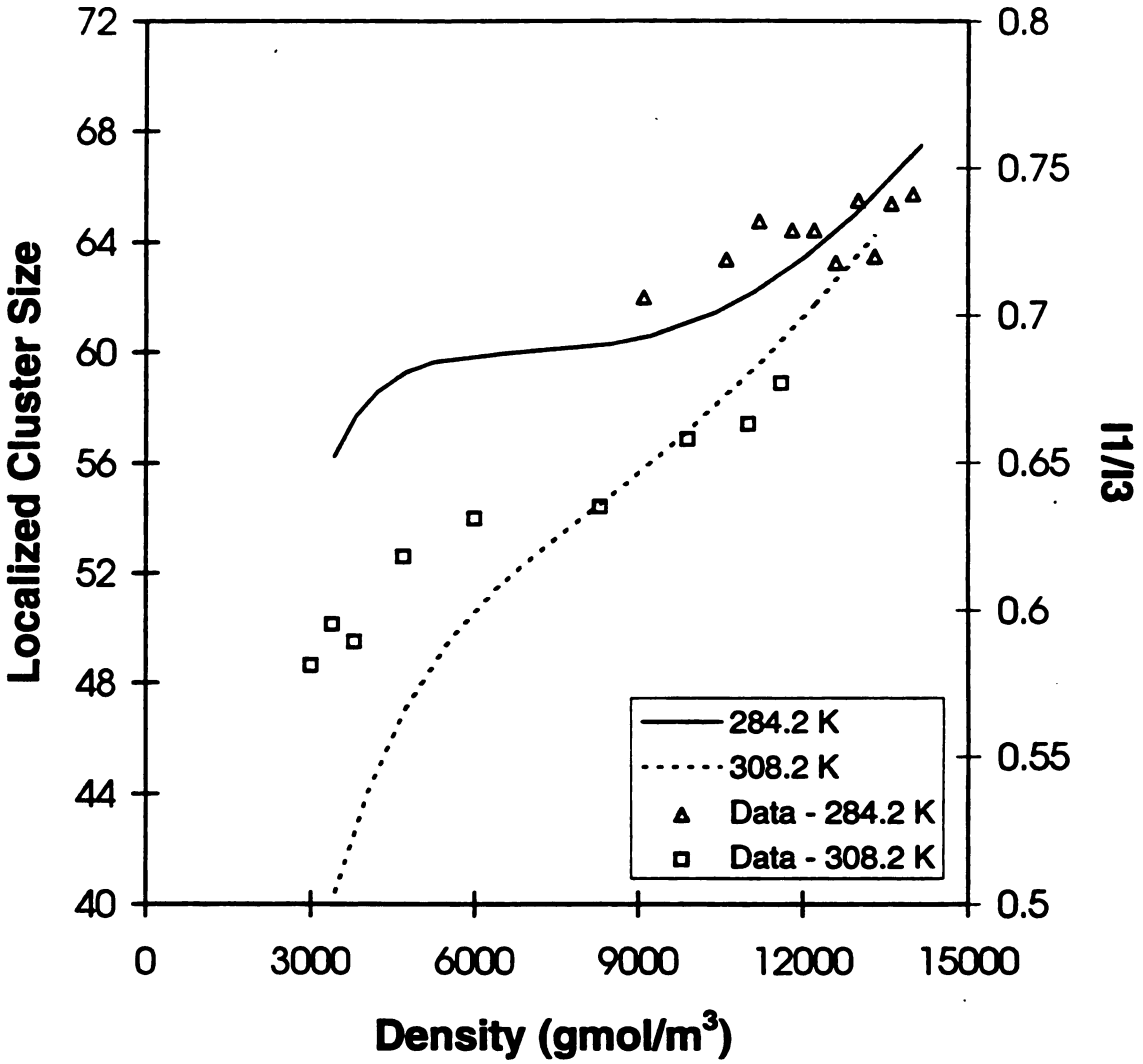

Figure 3-12: Comparison of Cluster Size with Fluorescence Spectroscopy - Ethylene around Pyrene

overs of Figure 3-8 disappear, and the maxima appear at the same bulk density (Figure 3-9).

The fluorescence intensity ratios are an indication of the total number of molecules around the solute within a short range, and hence the total amount within the first two molecular diameters [$\frac{\sigma_s}{2} \le r \le \frac{\sigma_s}{2} + 2\sigma_f$] outside the solute was chosen as a measure of the local density. Figures 3-10 - 3-12 show the total number of molecules around a solute within the first two molecular diameters against bulk density. This is cross-plotted against the fluorescence signal of Brennecke [1989], Brennecke and Eckert [1989] and Brennecke et. al. [1990]. The increase in the intensity of the signal near the critical point suggests that the solvent molecules cluster around the solute. For naphthalene, the stable signal is the ratio between fluorescence peaks 1 and 4, while for pyrene it is 1 and 3. These figures show the predicted total number of CO_2 molecules clustering around naphthalene and pyrene, and ethylene clustering around pyrene. The model predicts the trends seen in the fluorescence spectra. For CO_2 clustering around pyrene and naphthalene at 308.2 K, the data show a sharp increase at low densities, then becomes rather flat before increasing again at high densities. Also, at higher temperatures, the flat region is rather small. Once again this trend is captured by the model. This difference is the trend of the fluorescence spectra is even more pronounced for ethylene clustering around pyrene. The figures also show that the intensity of the ratio of the fluorescence spectra and the excess number of CO_2 molecules around pyrene is more than around naphthalene. The fluid-solvent interaction parameter is higher for pyrene than for naphthalene, and pyrene being a larger molecule provides a larger surface area for the solvent molecules to collapse upon. Com-

paring the CO_2-pyrene and ethylene-pyrene systems, pyrene attracts a larger number of CO_2 molecules than ethylene. The reason may be because of the bigger size of the ethylene molecule which sterically limits the number of ethylene molecules that can surround the solute. In all the cases presented here, the model predicts greater clustering near the critical point which is in agreement with the spectroscopic data.

DISCUSSION

The SLD model uses the fluid-fluid and fluid-solid interaction parameters to model adsorption over wide pressure and temperature ranges. It characterizes the fluid molecules using cubic equations-of-state. Predictions of the SLD model using the van der Waals model were shown earlier [Rangarajan et. al, 1995, chapter 2]. Here, we use the Peng-Robinson equation to describe the fluid, thus significantly improving the predictions of the fluid properties. By comparing Figures 3-1 - 3-2 with the results seen in chapter 2, the significant improvement is obvious. However, for any particular system, the equation-of-state that does the best job for representing its properties may be chosen, and the SLD approach adapted for that purpose.

The fluid-wall potential is used as an adjustable parameter in this approach. It is fitted to any one of the different temperatures given in the data, and then the same potential is retained for the other temperatures. This makes the model a semi-predictive model, in that, while one of its parameters needs to be fitted to experimental data at a particular temperature, it then becomes a predictive model to describe the adsorption characteristics at other temperatures. The geometric mean of the Lennard-Jones potentials tends to un-

derpredict the values of the surface excess. We have consistently used a fluid-solid interaction parameter that is about 1.8 to 2.2 times the geometric mean.

The SLD model superimposes the Lennard-Jones potential for solute-solvent interactions on the Peng-Robinson equation of state that describes the properties of the supercritical solvent. If the solute is attractive, then the density of solvent molecules near the solute increases resulting in the phenomenon of clustering. This is very similar to the adsorption of a fluid on to a flat wall, except that the wall-fluid interactions are slightly different than the solute-solvent interactions. As shown by the results of both these two cases, there are many similar behaviors between the two cases. The crossover of the adsorption isotherms is also seen in the case of clustering (Figure 3-8). This crossover disappears when the excess is plotted against bulk density (Figure 3-9). The peak in the supercritical adsorption isotherms decreases as we move to higher reduced temperatures. This phenomenon is also seen in clustering, where the number of excess solvent molecules drops sharply as the temperature is increased from 2 to 4 K above the critical point. One of the differences is that below the critical pressure, the surface excess of a fluid adsorbing on a flat wall increases gradually and then drops sharply as seen at 283 and 293 K for ethylene (Figure3-1). However, in clustering, as the fluctuation calculation of partial molal volume data indicates, the number of molecules increases sharply as the critical pressure is approached and decreases rapidly past the critical pressure. This model's predictions for clustering are more in line with the adsorption data on a flat wall i.e., the excess number of solvent molecules increases more gradually below the critical pressure, and then drops sharply after the critical pressure. This may be an artifact of the SLD assumptions.

Wu et. al. [1990] showed that for the attractive mixture of neon clustering around xenon, there is a negative N^{ex} close to the surface of the xenon molecule (Figure 3-7). The SLD model also predicts such a negative value close to the surface. At the surface, the attractive and repulsive parts of the Lennard-Jones potential cancel, and the solvent molecules are not attracted to the solute, and this negative value is the result of the solvent-solvent interactions. By choosing the correct solute-solvent potential parameter, this model may be used to describe a repulsive mixture where there is depletion of solvent molecules e.g. xenon molecules cavitating around neon.

The SLD model serves as a good first approximation of the adsorption problem. The use of the Peng-Robinson equation helps resolve one of the limitations of the previous SLD model *viz.* use of an equation that can better represent the fluid properties, thus significantly improving the capabilities of this model.

High-pressure adsorption and clustering in supercritical fluids are phenomena that are of importance in various industries. A simple engineering model to describe these different phenomena will enhance their applications in industry. Modifications of this model to predict adsorption in slits and pores, and for describing adsorption of mixtures onto different surfaces are discussed in the next chapter.

CHAPTER 4 ADSORPTION OF PURE GASES IN SLITS AND PORES, AND ADSORPTION OF BINARY MIXTURES

INTRODUCTION

In two previous chapters, we presented a new model, called the Simplified Local Density (SLD) model, for describing physical adsorption of gases on flat walls using cubic equations-of-state. In this model, the fluid-solid potential is superimposed on a cubic equation-of-state, and the configurational energy in the inhomogeneous fluid phase is simplified with a local density approximation. In the first chapter, we used the van der Waals equation, which gave qualitative predictions of the experimental data of Findenegg [1984]. The van der Waals equation was used because it is the simplest fundamentally sound equation-of-state and provided a basis for qualitative studies. This model predicts Type II and III isotherms for adsorption on flat walls, shows the characteristic cusp-like behavior and crossovers seen near the critical point. In the second chapter, we modified the model to incorporate the Peng-Robinson equation-of-state, which represents the fluid properties more accurately, including vapor pressure and compressibility, and showed dramatic improvement in the quantitative representation of experimental measurements of Findenegg.

Most commercial adsorbents are porous, activated carbon being one of them. Adsorption in pores and the phenomenon of pore filling among carbon based adsorbents has received considerable attention [Dubinin, 1975]. Gregg and Sing [1982] have classified pores into three categories, macropores (50 - 100 nm), mesopores (2 - 50 nm) and micro-

pores (<2 nm). Adsorption properties of microporous solids enjoy wide spectrum of applications including chromatography and other separation processes, filtration, industrial effluent cleanup, ion exchange, biological applications etc. [Gubbins, 1990; Pendleton and Zeetllemoyer, 1984]. In microporous solids, adsorbed fluids show many unusual properties such as preferential adsorption of certain fluid components, chemisorption at particular sites, hysterisis effects and a variety of new and unusual phase transitions [Gubbins, 1990]. Dubinin [1975] says that all existing theories of physical adsorption proceed with the same physical image in describing adsorption in porous and nonporous adsorbents.

Design of columns for thermal swing adsorption and pressure swing adsorption require the simultaneous solution of partial differential equations for the material, energy and momentum balances describing the dynamics of adsorption in columns, in conjunction with the kinetic and equilibrium properties of the adsorbents [Sircar and Myers, 1985]. The models for multicomponent adsorption isotherms are discussed in chapter 2. There are plenty of experimental and molecular simulation data available for adsorption of pure gases and mixtures onto slits and pores at low pressures [van Megen and Snook, 1982, 1985; Barton et al., 1984; Powles et al., 1988; Valenzuela and Myers, 1989; Tan and Gubbins, 1990; Kierlik and Rosinberg, 1992]. In this paper, we extend the SLD model to describe adsorption of pure gases and binary mixtures in confined spaces, i.e. slits - two infinite parallel flat surfaces and cylindrical pores.

MODEL DEVELOPMENT - PURE GAS

Slit-like Pores

These can be thought of as two parallel semi-infinite plates separated by a small distance (Figure 4-1). Any particle in between the walls will be subjected to attractive forces from the two walls. The distance between the two walls may be quite small (<2 nm), which implies that only particles smaller than this will be adsorbed i.e. exclusion will be important.

The chemical potential of the fluid in the vicinity of a wall may be written as a sum of the fluid-fluid and fluid-solid interactions, as described in the previous two chapters.

Recapping from the last chapter, using the Peng-Robinson equation-of-state, we can write an expression for the bulk fugacity in terms of molar volume [Sandler, 1989]. The fluid-fluid fugacity at any point is an analogous expression

$$\ln[f_{ff}(z)] = \frac{b}{v(z)-b} - \frac{a(z)}{v(z)^2+2bv(z)-b^2}\frac{v(z)}{RT} - \ln\left[\frac{v(z)-b}{RT}\right] - \frac{a(z)}{2.828bRT}\ln\left[\frac{v(z)+2.414\,b}{v(z)-0.414\,b}\right] \qquad [4\text{-}1]$$

where $v(z)$ is the molar volume at any point z, a and b are the constants of the Peng-Robinson equation [Sandler, 1989; see previous chapter also]. $a(z)$ is calculated using the SLD approach after suitable modifications, and details are given in appendix 1. The equations for $a(z)$ in slits are

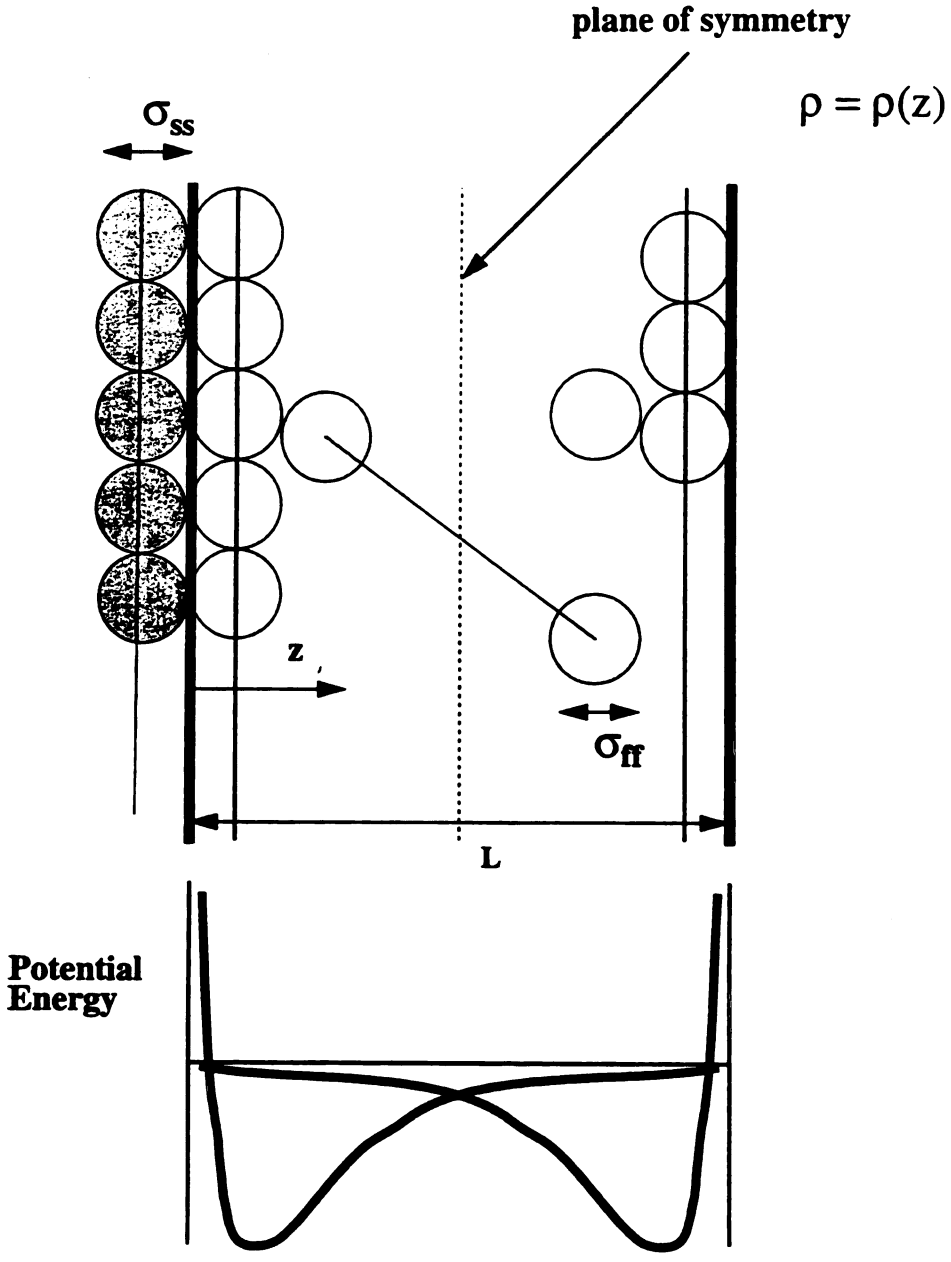

Figure 4-1: Slit-Like Pores

$$\frac{a(z)}{a_b} = \frac{3}{8}\left[\frac{z}{\sigma_{ff}} + \frac{5}{6} - \frac{1}{3\left(\frac{L-z}{\sigma_{ff}} - 0.5\right)^3}\right], \quad for \ 0.5 \le \frac{z}{\sigma_{ff}} \le 1.5 \qquad [4\text{-}2]$$

$$\frac{a(z)}{a_b} = \frac{3}{8}\left[\frac{8}{3} - \frac{1}{3\left(\frac{z}{\sigma_{ff}} - 0.5\right)^3} - \frac{1}{3\left(\frac{L-z}{\sigma_{ff}} - 0.5\right)^3}\right], \qquad [4\text{-}3]$$

$$for \ 1.5 \le \frac{z}{\sigma_{ff}} \le \frac{L}{\sigma_{ff}} - 1.5$$

$$\frac{a(z)}{a_b} = \frac{3}{8}\left[\frac{L-z}{\sigma_{ff}} + \frac{5}{6} - \frac{1}{3\left(\frac{z}{\sigma_{ff}} - 0.5\right)^3}\right], \quad for \ \frac{L}{\sigma_{ff}} - 1.5 \le \frac{z}{\sigma_{ff}} \le \frac{L}{\sigma_{ff}} - 0.5 \qquad [4\text{-}4]$$

where $L+\sigma_s$ is the distance between the centers of the atoms of the two surfaces. Note that L has to be at least 3 σ_{ff} in length for the above equations to be used. If $L < 3\ \sigma_{ff}$ then, the equations will have to be slightly modified and the corresponding equations are

$$\frac{a(z)}{a_b} = \frac{3}{8}\left[\frac{L}{\sigma_{ff}} - 1\right], \quad for \ 0.5 \le \frac{z}{\sigma_{ff}} \le 1.5, \ and \ if \ z + \sigma_{ff} > L - \frac{\sigma_{ff}}{2} \qquad [4\text{-}5]$$

$$\frac{a(z)}{a_b} = \frac{3}{8}\left[\frac{z}{\sigma_{ff}} - \frac{\sigma_{ff}^3}{3\left(L - \frac{\sigma_{ff}}{2} - z\right)^3} + \frac{5}{6}\right], \quad \text{for } 0.5 \le \frac{z}{\sigma_{ff}} \le 1.5 \text{ and if } z + \sigma_{ff} \le L - \frac{\sigma_{ff}}{2} \qquad [4\text{-}6]$$

$$\frac{a(z)}{a_b} = \frac{3}{8}\left[\frac{L-z}{\sigma_{ff}} - \frac{\sigma_{ff}^3}{3\left(z - \frac{\sigma_{ff}}{2} - (L-z)\right)^3} + \frac{5}{6}\right], \quad \text{for } 1.5 \le \frac{z}{\sigma_{ff}} \le L - \frac{\sigma_{ff}}{2} \qquad [4\text{-}7]$$

The adsorbate-adsorbent interactions in slits are given by the partially-integrated 10-4 Lennard-Jones potential [Lee, 1987] (Equation 3-10), where the interactions are summed over the two walls.

Cylindrical Pores

Any molecule in a cylindrical pore is subject to a force from all sides of this cylinder (Figure 4-2). The configuration integral in pores is given by

$$\frac{a(r_1)}{a_b} = \frac{3}{\pi}\sigma_{ff}^3 \int_z \int_\theta \int_{r_1} \frac{r}{(r^2 + z^2)^3}\, dr\, d\theta\, dz \qquad [4\text{-}8]$$

where r and z are the radial and axial distances. Using the SLD approach, the region inside the pore is divided in three parts: 1) at the pore surface; 2) near the pore surface; and 3) far from the pore surface, and the details of these calculations are given in appendix 1.

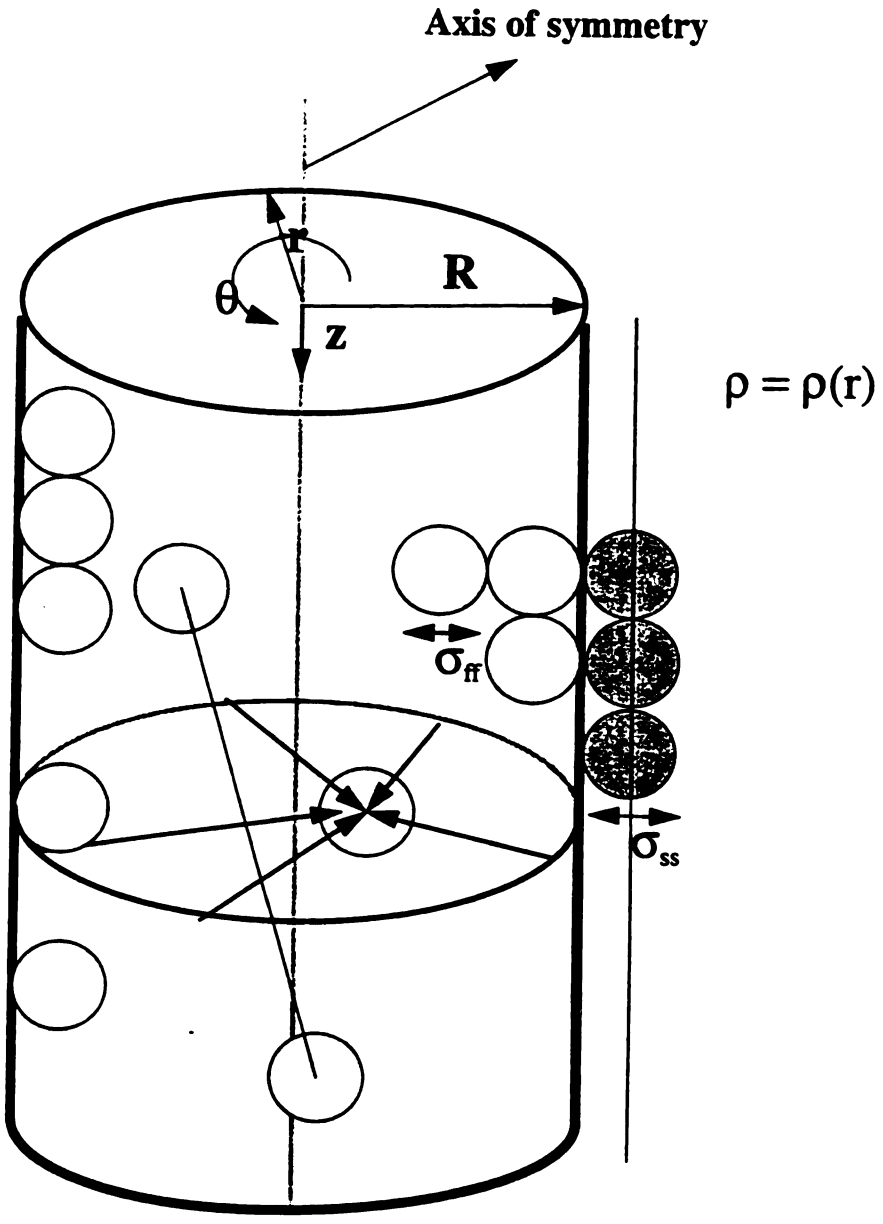

Figure 4-2: Cylindrical Pores

The resulting solution leaves us with an integral to be solved for $a(r_1):a_b$, and it is the longest part in the calculation of the amount adsorbed. The results can be summarized as follows:

$$\frac{a(r_1)}{a_b} = \frac{3\sigma_{ff}^3}{\pi}\left[\begin{array}{l}\displaystyle\int_0^{\sigma_{ff}} \frac{1}{4\sigma_{ff}^4}\cos^{-1}\left(\frac{\sqrt{\sigma_{ff}^2 - z^2}}{2r_1}\right)dz - \int_{\sigma_{ff}}^{\infty} \frac{\pi}{2}\frac{2r_1^2 + z^2}{z^3\left(4r_1^2 + z^2\right)^{3/2}} \\ \displaystyle -\frac{1}{4}\int_0^{\sigma_{ff}}\int_0^{\cos^{-1}\nu} \frac{1}{4r_1^2\cos^2\theta + z^2}\,d\theta\,dz + \frac{\pi}{24\sigma_{ff}^3}\end{array}\right], \qquad [4\text{-}9]$$

$$for\ r_1 = R - \frac{\sigma_{ff}}{2}$$

$$\frac{a(r_1)}{a_b} = \frac{3\sigma_{ff}^3}{\pi}\left[\begin{array}{l}\displaystyle\int_0^{\sigma_{ff}} \frac{1}{4\sigma_{ff}^4}\cos^{-1}(\nu)\,dz - \frac{1}{4}\int_0^{\sigma_{ff}}\int_0^{\cos^{-1}\nu} \frac{1}{\left(w^2 + z^2\right)^2}\,d\theta\,dz \\ \displaystyle -\frac{1}{4}\int_0^{\pi}\left(\frac{\pi}{4w^3} - \frac{\sigma_{ff}}{2w^2\left(w^2 + \sigma_{ff}^2\right)} - \frac{\tan^{-1}(\sigma_{ff}/w)}{2w^3}\right)d\theta + \frac{\pi}{12\sigma_{ff}^3}\end{array}\right], \qquad [4\text{-}10]$$

$$for\ R - \frac{3\sigma_{ff}}{2} \le r_1 < R - \frac{\sigma_{ff}}{2}$$

$$\frac{a(r_1)}{a_b} = \frac{3\sigma_{ff}^3}{\pi}\left[\frac{\pi}{3\sigma_{ff}^3} - \frac{\pi}{16}\int_0^{\pi}\frac{1}{w^3}d\theta\right],\ for\ 0 \le r_1 < R - \frac{3\sigma_{ff}}{2} \qquad [4\text{-}11]$$

where $\nu = \dfrac{r_1^2 + \sigma_{ff}^2 - z^2 - \left(R - \frac{\sigma_{ff}}{2}\right)^2}{2r_1\sqrt{\sigma_{ff}^2 - z^2}}$, *and* $w = r_1\cos\theta + \sqrt{\left(R - \frac{\sigma_{ff}}{2}\right)^2 - r_1^2\sin^2\theta}$, $R+\sigma_{ff}/2$ is the pore radius, and r, θ, and z are the cylindrical coordinates.

If the fixed particle is near or at the wall, then the configurational energy calculation at each point takes about 45 seconds for the fortran calculation. If the fixed particle is away from the wall, the calculation takes about one second to compute the configurational integral. Note that the calculation has to be done only once for a given z/σ_f. Similar to the slits, if the pore radius is smaller than 3 σ_{ff} + σ_{ss}, then $r_1 > R - \frac{3\sigma_{ff}}{2}$ in all cases and Equation 4-11 is not required.

In cylindrical pores the adsorbate-adsorbent interactions are given by the potential of Tjatopolous et al. [1988]

$$\Psi(x,R_{fs}) = n\sigma_{ff}^2\pi^2\varepsilon_{fs}\left\{\frac{63}{32}\frac{\sigma_{fs}^{10}}{x^{10}\left(2-\frac{x}{R_{fs}}\right)^{10}}F\left[\frac{-9}{2},\frac{-9}{2},1,\left(1-\frac{x}{R_{fs}}\right)^2\right] - 3\frac{\sigma_{fs}^{4}}{x^{4}\left(2-\frac{x}{R_{fs}}\right)^{4}}F\left[\frac{-3}{2},\frac{-3}{2},1,\left(1-\frac{x}{R_{fs}}\right)^2\right]\right\} \quad [4\text{-}12]$$

where x is the distance of closest approach between the fluid molecule and the pore surface, R_{fs} = R+σ_s/2 is the pore radius, $F[\alpha, \beta; \gamma; \delta]$ is the hypergeometric series with parameters α, β, γ, and n is the number density of carbon atoms.

Algorithm for solving the density profile

The algorithm for solving the density profile and calculation of surface excess are given in the previous chapters. In slits and pores the only difference is the calculation of

a/a_b, which is given by Equations 4-2 - 4-7 for slits and 4-8 - 4-11 for pores. The amount adsorbed in slits is calculated as

$$Amt = \int_{z=\sigma_{ff}/2}^{L-\sigma_{ff}/2} \rho(z)(S.A.)dz \qquad [4\text{-}13]$$

and in pores as

$$Amt = \int_0^{R-\sigma_{fs}} 2\pi r L\rho(r)\,dr = \int_0^{R-\sigma_{fs}} r\frac{S.A.}{R-\frac{\sigma_s}{2}}\rho(r)\,dr \qquad [4\text{-}14]$$

where *S.A.* is the experimental surface area (for e.g. BPL activated carbon has a surface area of 988 m^2/g) and *L* is the length of the cylinder. It was assumed that the experimental surface area was $2\pi L(R\text{-}\sigma_s/2)$.

MODEL DEVELOPMENT - BINARY MIXTURES

In binary mixtures, the van der Waals mixing rules are used to determine the properties of the mixture [Prausnitz et al., 1986]

$$a = \sum_{i=1}^{m}\sum_{j=1}^{m} y_i y_j a_{ij} \qquad [4\text{-}15]$$

$$b = \sum_{i=1}^{m} y_i b_i \qquad [4\text{-}16]$$

$$a_{ij} = a_{ji} = \sqrt{a_{ii}a_{jj}}(1-k_{ij}) \qquad [4\text{-}17]$$

where y_i is the mole fraction of component i, and k_{ij} is the binary interaction parameter, a constant introduced to obtain better agreement in mixture equation-of-state calculations. Equation 4-1 may be written for the fugacity of each component as

$$\ln\left(\frac{f_i}{y_i P}\right) = \frac{B_i}{B}(z-1) - \ln(z-B) - \frac{A}{2\sqrt{2}\mathbf{B}}\left[\frac{2\sum_j y_i A_{ij}}{A} - \frac{B_i}{B}\right]\ln\left[\frac{z+(\sqrt{2}+1)B}{z-(\sqrt{2}-1)B}\right] \qquad [4\text{-}18]$$

where A, B and z are as discussed in chapter 3.

$$\sum_{i=1}^{m} y_i = 1 \qquad [4\text{-}19]$$

Algorithm to solve density profile

For a binary mixture, the above equations result in solving two simultaneous equations (fugacity of each component) for both composition and density with position, subject to the constraint that the sum of the mole fractions of the two components is 1. A technique developed by Asselineau et al. [1979] for calculating VLE data has been adapted for this purpose. In this method, Equations 4-17 - 4-19 are written such that the right hand side equals zero. These equations are called the objective equations, G_1, G_2 and G_3.

$$G_1 = \frac{y_1 \phi_1 P}{f_1} - 1 \qquad [4\text{-}20]$$

$$G_2 = \frac{y_2 \phi_2 P}{f_2} - 1 \qquad [4\text{-}21]$$

$$G_3 = 1 - y_1 - y_2 \qquad [4\text{-}22]$$

Partial derivatives with respect to the independent variables (pressure and local composition) are then written in matrix form, which are then inverted to recalculate the objective functions such that $G = \sqrt{G_1^2 + G_2^2 + G_3^2}$ is minimized. Further details of this method may be obtained from Asselineau et al. [1979], and the resulting computer program is attached in the appendix 2.

RESULTS

The diameters of the fluid, solid and solute are the Lennard-Jones parameters as tabulated in Reid et al. [1987], and are given in chapter 3. The σ_{fs} is calculated as the arithmetic mean of the fluid and solid, while the fluid-solid potential parameter (ε_{fs}/k) is adjusted to match the magnitude of adsorption.

van Megen and Snook have done Monte-Carlo simulations of Lennard- Jones molecules (that simulate ethylene) on slit-like pores [1985] (Figure 4-3). Their simulation results cannot be quantitatively compared to either experimental or SLD model results because their simulation of bulk ethylene does not represent the experimental bulk properties of ethylene; e.g. the simulation critical temperature ($T_{c,sim}$) of ethylene is 226 K, as opposed to T_c = 282.4 K seen experimentally. Figure 4-4 shows the corresponding model

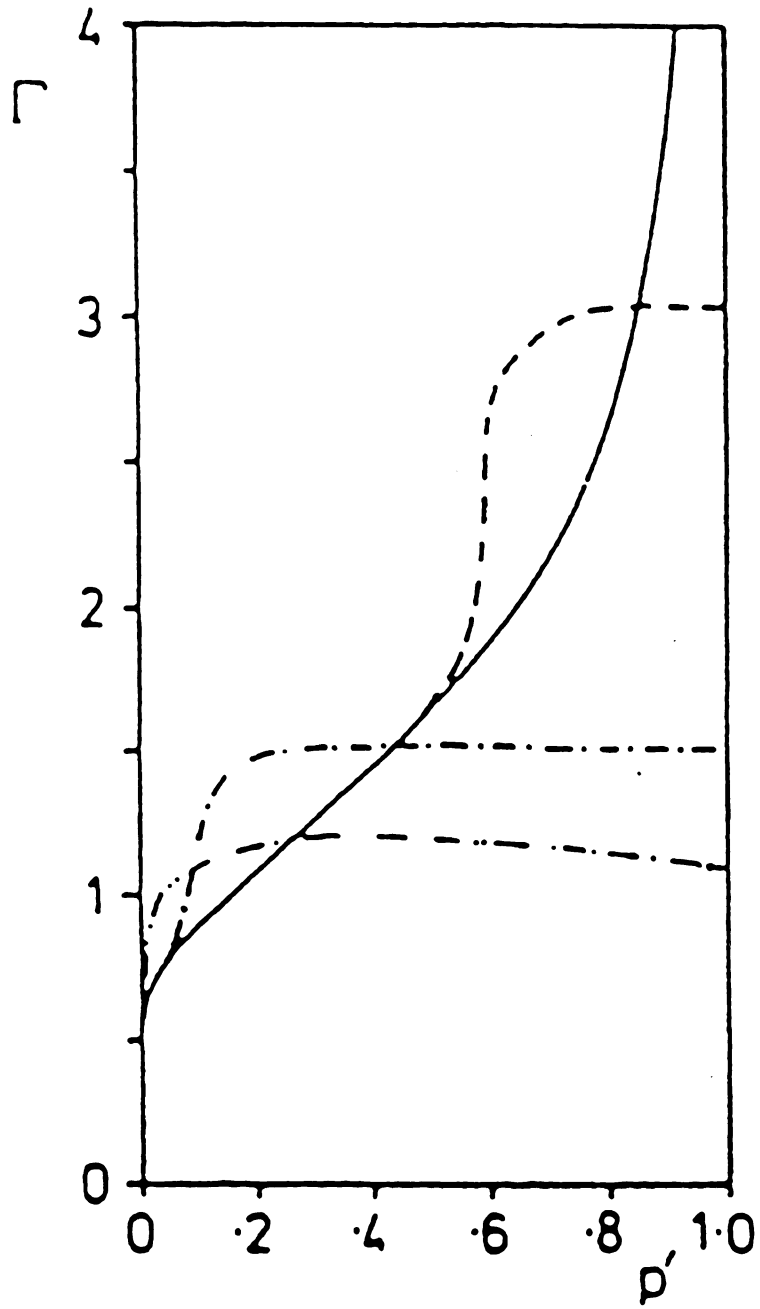

Figure 4-3: Grand Canonical Ensemble Monte Carlo Simulation of Ethylene in a Slit (T/T_c=0.85)

—h = ∞, - - - h = 10.0, -·-· h = 5.0, -···- h = 3.5

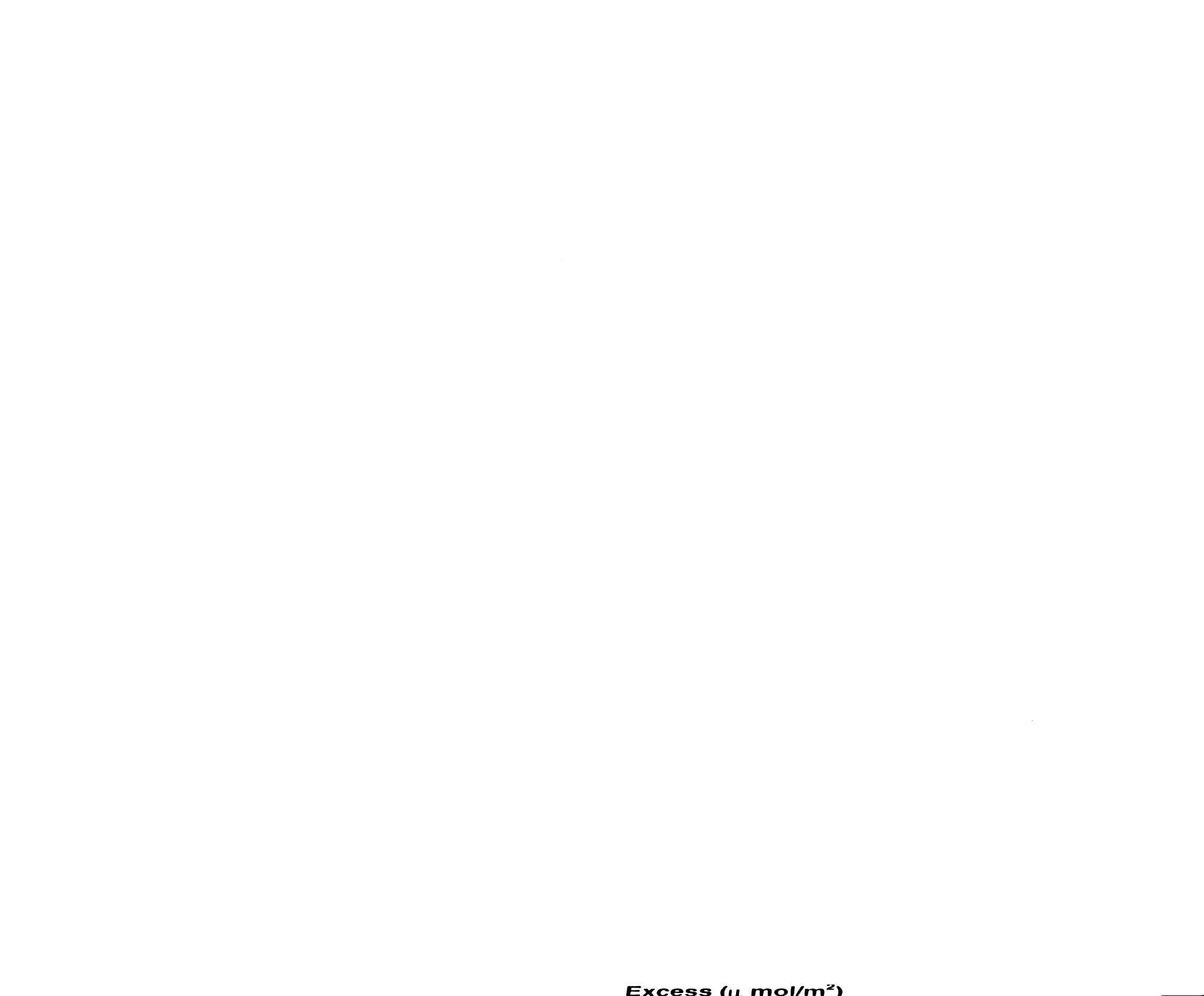
Excess (μ mol/m²)

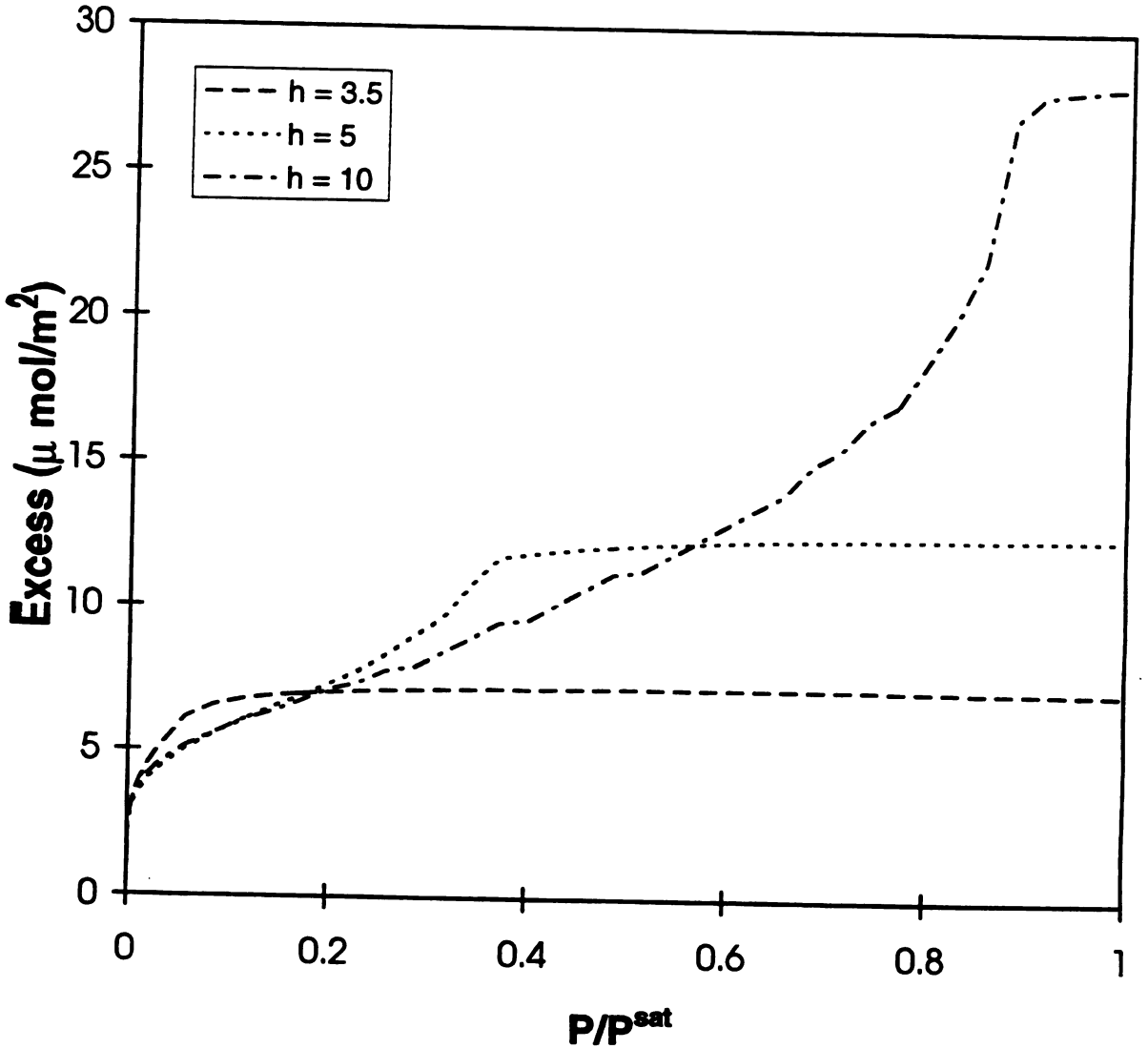

Figure 4-4: Ethylene on Carbon Slits at T/T_c of 0.85

predictions for adsorption of ethylene on a slit. Their calculations were done at T/T* of 0.95 (where T* = 202 K), yielding a ratio of $T/T_{c,sim}$ of 0.85. We used the same ratio of T/T_c (resulting temperature was 239 K) for our calculations. To convert the excess in $\mu mol/m^2$ to the units used by van Megen and Snook, divide by 9.323. 'h' is the separation between the carbon atoms in terms of ethylene molecular diameters. Qualitatively, the SLD model shows all the trends seen in the Monte-Carlo simulations. At low slit widths the pore fills quickly, resulting in Type I isotherms. There is also a slight decrease in the excess as the pressure increases, as reported by van Megen and Snook. As the slit width is increased Type IV isotherms are seen.

Figure 4-5 shows the adsorption of ethylene in pores of different diameters at low pressures. These results are compared to the data of Reich et. al. [1982], who have studied the adsorption of ethylene on BPL activated carbon with a surface area of 988 m^2/g. The value of the ε_{fs}/k that was used in Figures 3-1 and 4-4 has been retained in this case. The model predictions with a pore diameter of 2.45 nm match the experimental data rather well. However, activated carbon has a pore size distribution with pores ranging from micro to macropore range, with an average pore size of 3.2 nm, with largest portion of pores in the 1.5 - 2 nm region. As seen in Figures 4-6 and 4-7, at temperatures of 260.2 and 301.4 K, the model predictions at 2.45 nm are not as accurate. A factor in this temperature dependency may be due to the fact that in order to truly represent the experimental data, we need to sum the amount adsorbed over this pore size distribution. At small pore widths type I isotherms are seen while type IV isotherms are seen at large pore widths. The amount adsorbed for a pore width of 4.56 nm is actually smaller than the amount adsorbed in a 3.29 nm pore for pressures up to 6 bar at 212. 7 K and for the entire pressure

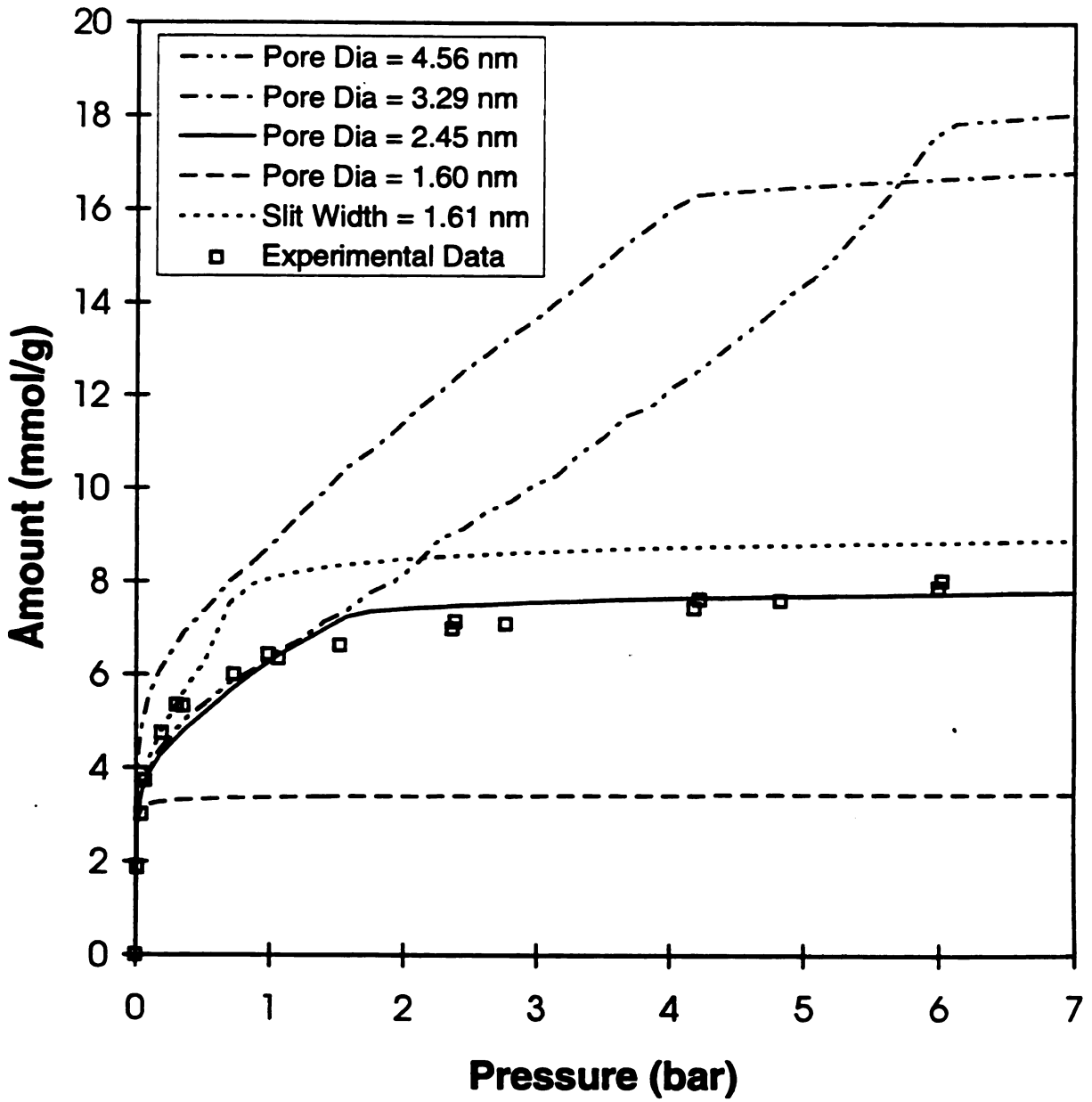

Figure 4-5: Ethylene on BPL Carbon at 212.7 K

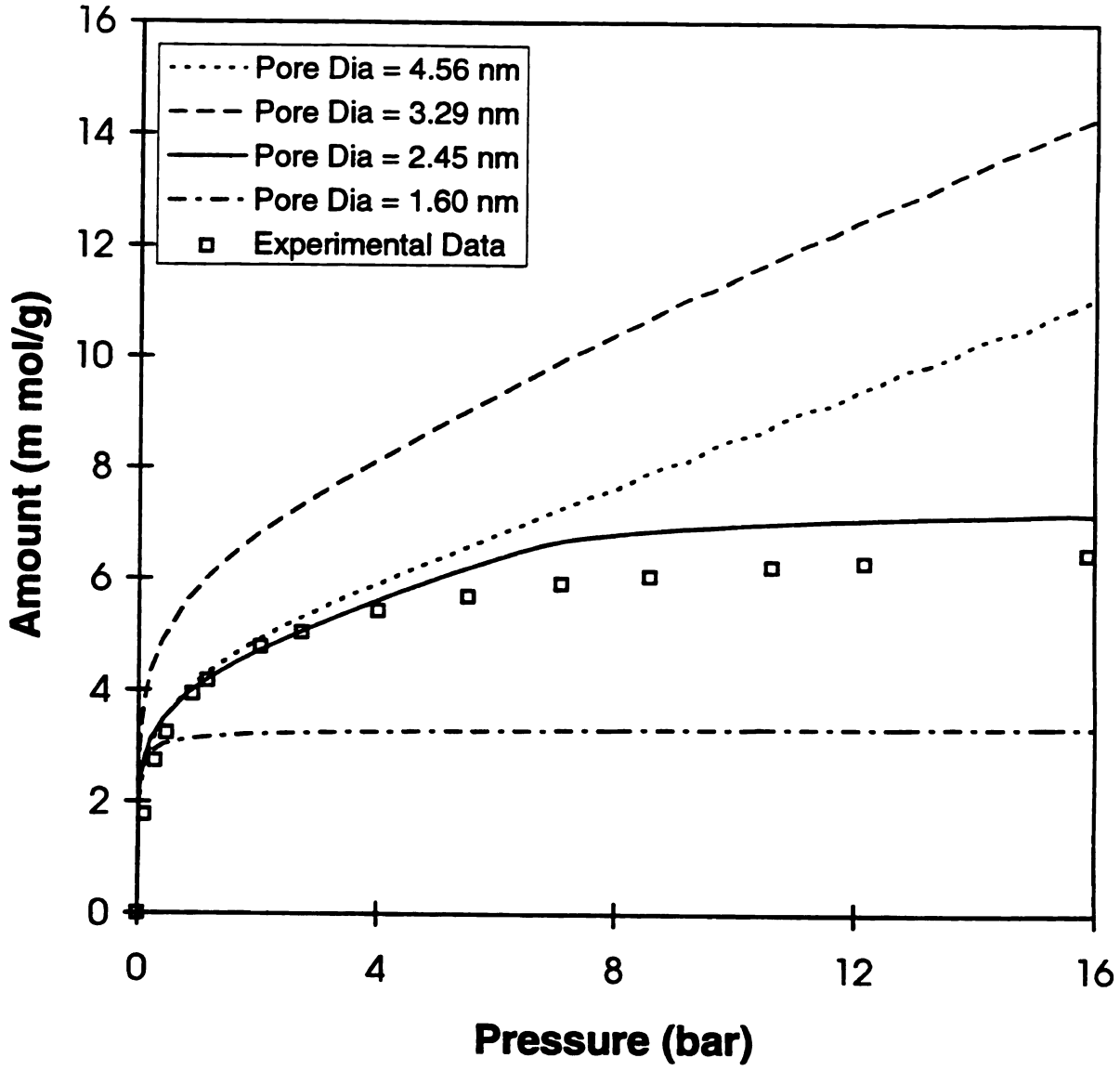

Figure 4-6: Ethylene on BPL Carbon at 260.2 K

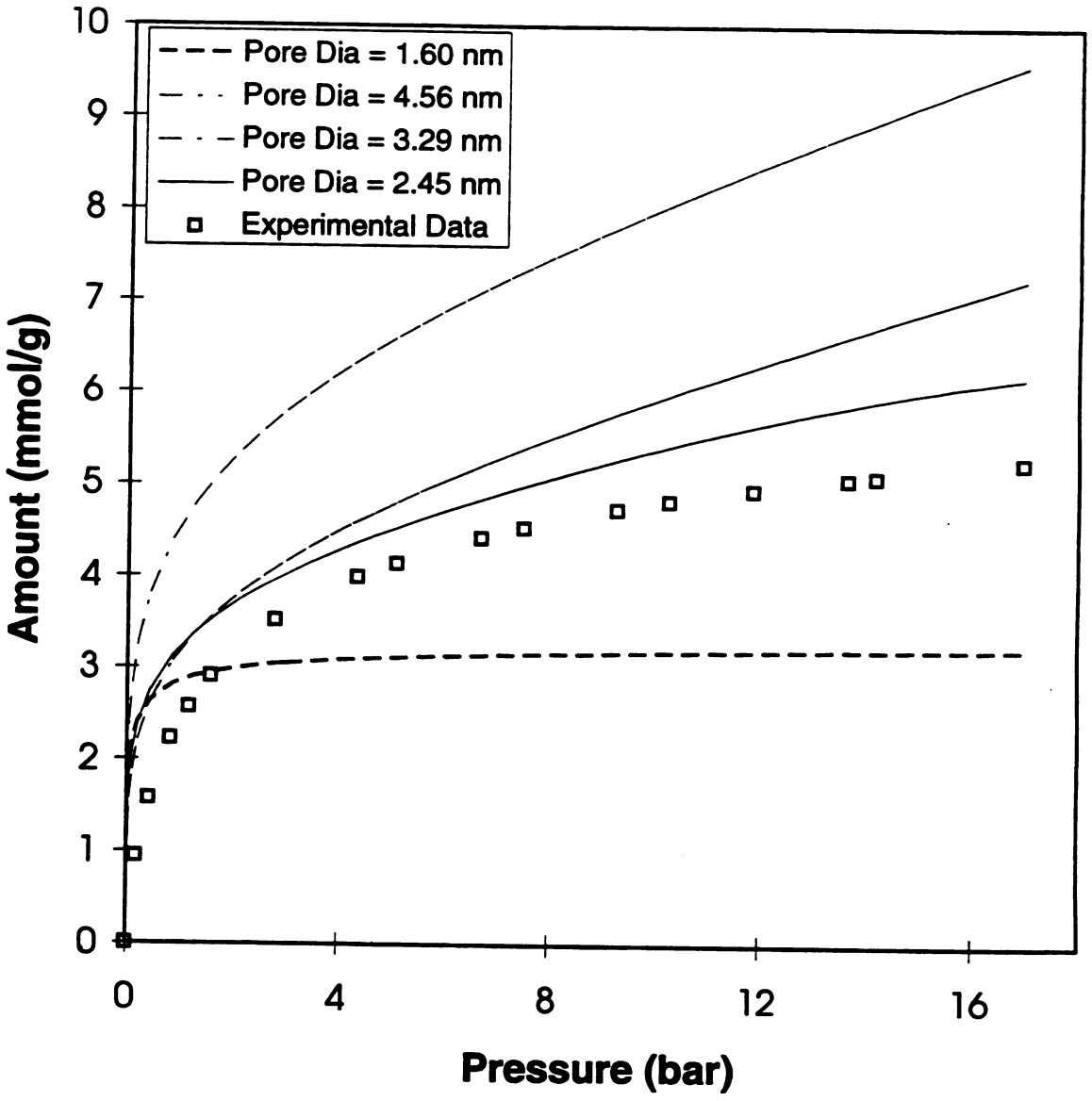

Figure 4-7: Ethylene on BPL Carbon at 301.4 K

range at 260.2 K. Model predictions of adsorption of methane at high pressure were also conducted. The results obtained were qualitatitively similar to the data of Barton et. al [1984] (Figure 4-8).

In Figures 4-9 and 4-10, the model predictions of adsorption of a binary mixture of ethylene and methane are shown. In this case the diameters of both ethylene and methane are assumed to be 0.4 nm to simplify calculations near the surface of the pore. The fluid-wall parameter for ethylene is retained as 140 K, while for methane it is taken as 107 K, which was calculated by fitting it to the pure gas adsorption data. A binary ethylene-methane interaction parameter of 0.022 was used [Sandler, 1989]. The composition of ethylene in the adsorbed phase is plotted as a function of pressure at 212.7 K with a bulk ethylene composition of 74%. The model predictions for the selectivity shows that the composition in the adsorbed phase is inversely proportional to the pressure, as seen by the experimental results of Reich et al. [1982]. Note that the model assumes a slit-like geometry to model the system. In Figure 4-5, we showed that a 1.6 nm slit shows trends similar to that of a 2.45 nm pore for ethylene adsorbing on activated carbon at 212.7 K. We used the slit-like geometry to represent this binary system to show that the SLD model is capable of showing the right trends with respect to composition and amount adsorbed in binary mixtures, and as seen by the figure, the SLD model shows great promise for mixture modeling. Figure 4-10 shows the model prediction for the amount adsorbed as a function of pressure. As seen by the figure the SLD model qualitatively predicts the amount adsorbed, and shows all the right trends seen in the figure.

Figure 4-11 shows the composition of ethylene in an ethylene-methane mixture at 260.2 K mixture. At this temperature, too, the SLD model predicts the selectivity of eth-

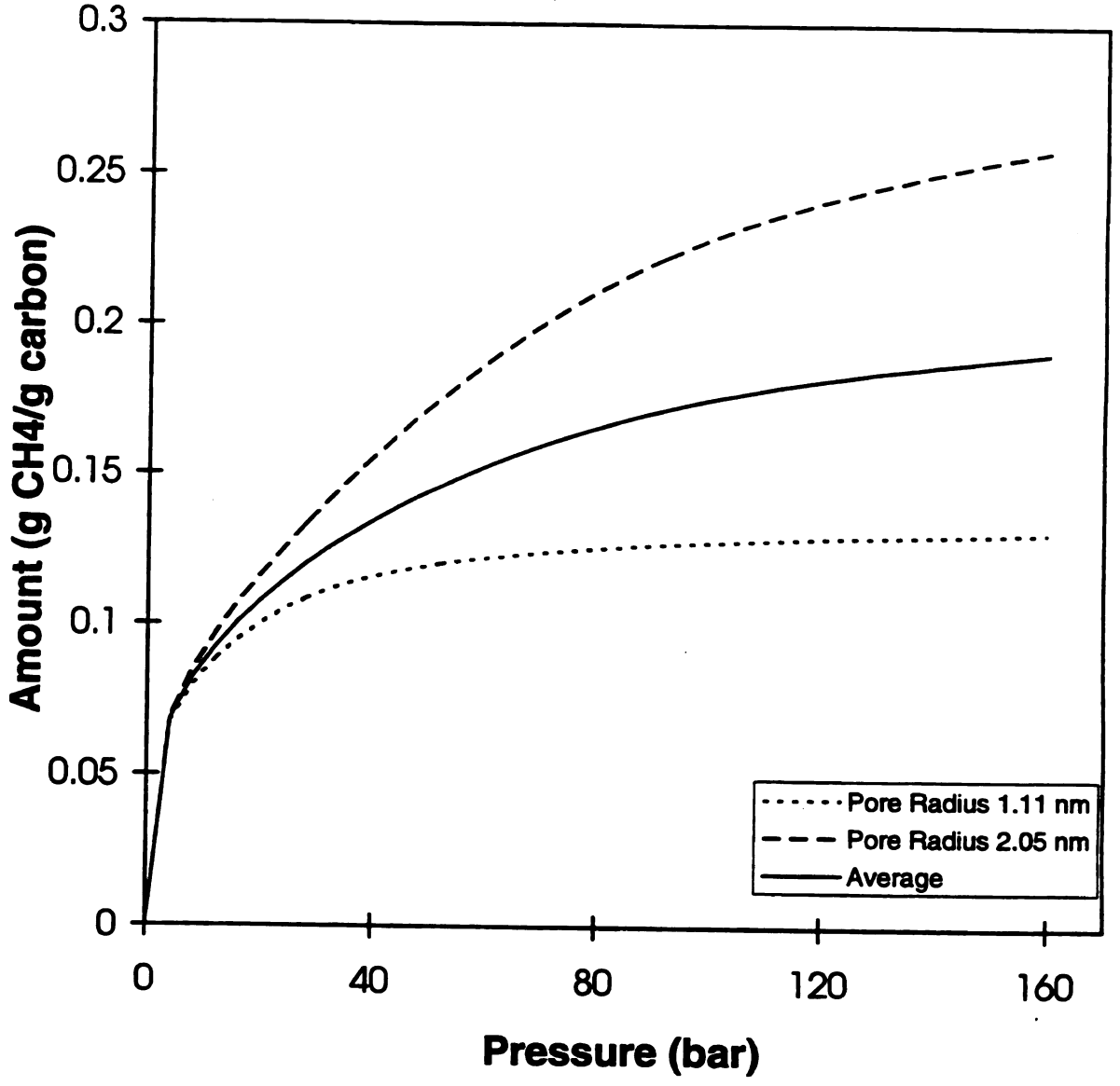

Figure 4-8: Methane on Activated Carbon at 243.15 K

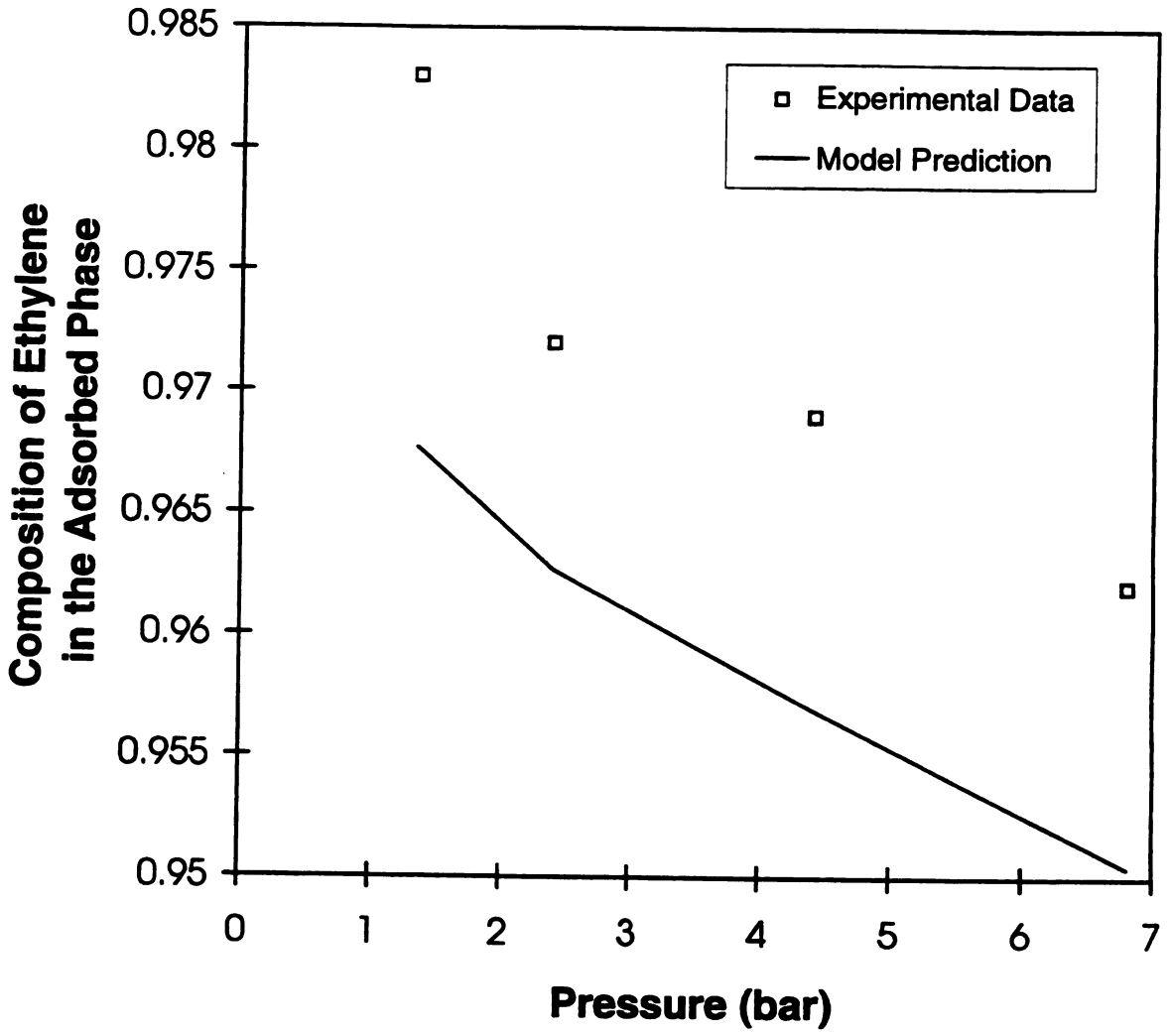

Figure 4-9: Adsorption of Ethylene - Methane mixture on BPL carbon at 212.7 K and Initial Bulk Ethylene Concentration of 0.74

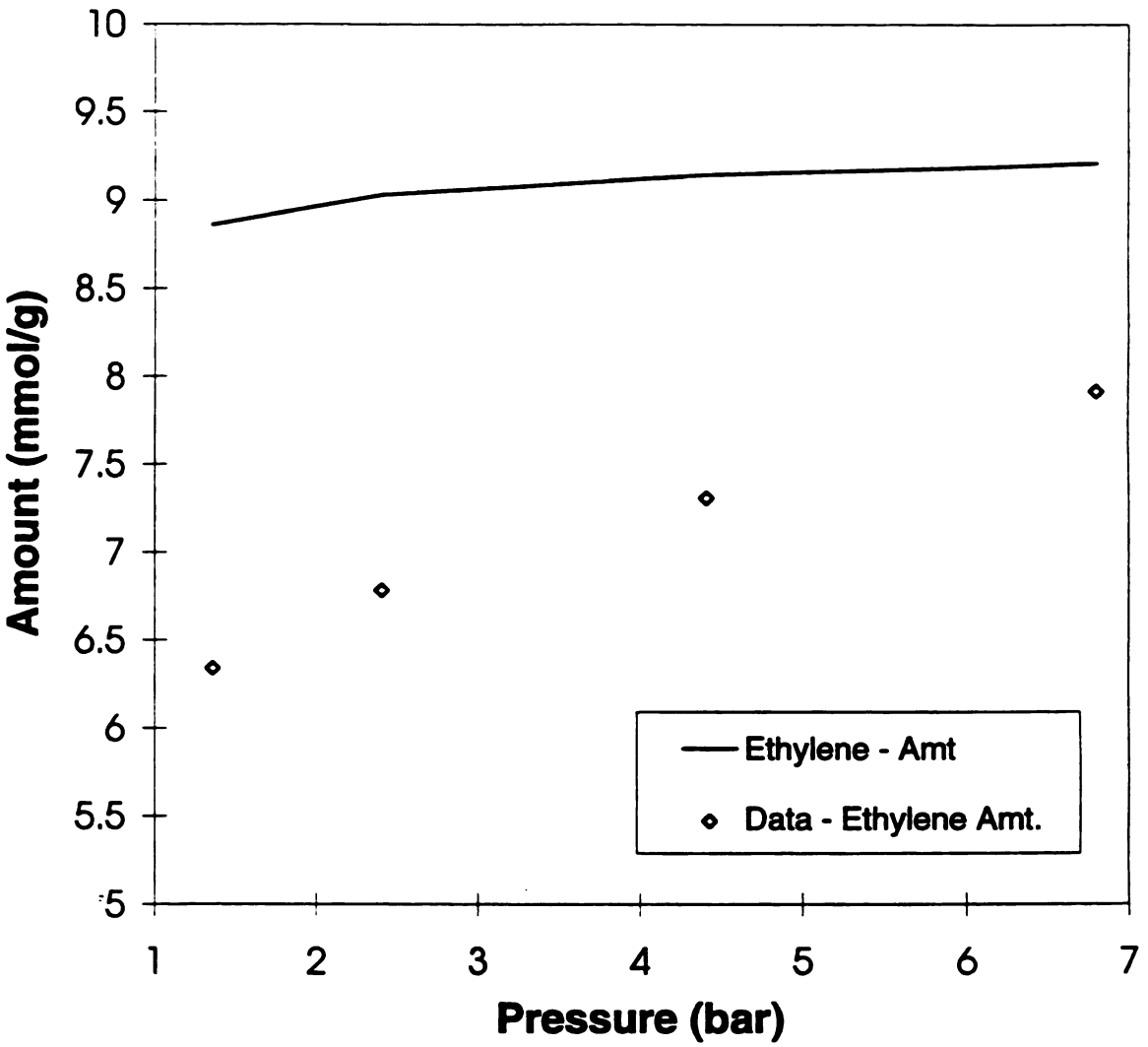

Figure 4-10: Adsorption of Ethylene - Methane mixture on BPL carbon at 212.7 K and Initial Bulk Ethylene Concentration of 0.74

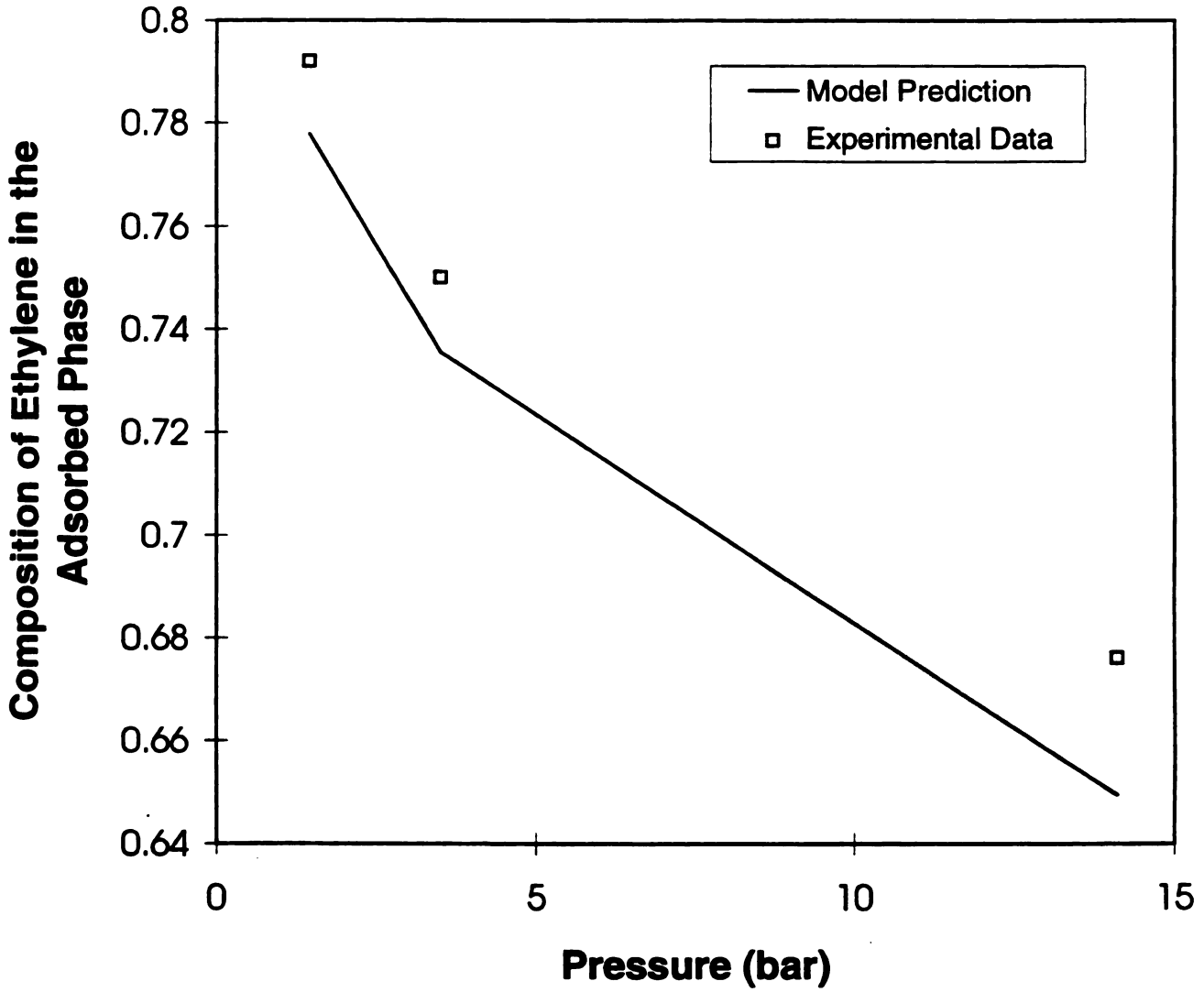

Figure 4-11: Adsorption of Ethylene - Methane mixture on BPL Carbon at 260.2 K, and Initial Bulk Ethylene Concentration of 0.235

ylene very well. Figure 4-12 shows the adsorption of two members of a homologous series propylene and ethylene adsorbing on activated carbon. This activated carbon is called Nuxit-AL, which is made by a Hungarian manufacturer and its characteristics could not be obtained readily, it was approximated to have the same physical properties as BPL carbon. Since ethylene and propylene are similar molecules, the binary interaction parameter was assumed to be zero. The experiments conducted by Szepesy and Illes [1963] were done by maintaining the pressure constant and varying the concentration of the bulk propylene. Here we wanted to see the model predictions over a wide range of concentrations. As seen in Figure 4-12, the model can predict the concentration in the adsorbed phase to a very high degree of accuracy. Once again, modeling the carbon as a pore, and incorporating the pore-size distribution data into the model will enhance the model predictions.

DISCUSSION

As discussed in the two previous chapters, the limitations of the SLD model can be attributed to: 1) the local density approximation; 2) lack of structure in the model; 3) choice of the fluid equation-of-state to describe the fluid properties. In the previous chapter, we showed how modifying the fluid equation to incorporate the Peng-Robinson equation dramatically improved the model predictions for adsorption in flat surfaces. Here, we modify the SLD approach to predict adsorption in slits and pores. Model predictions are compared to both molecular simulations and experimental data, and as seen by the results the SLD approach can quantitatively predict adsorption in activated carbon by approximating the BPL activated carbon to be a 2.45 nm pore at 212.7 K. However, as

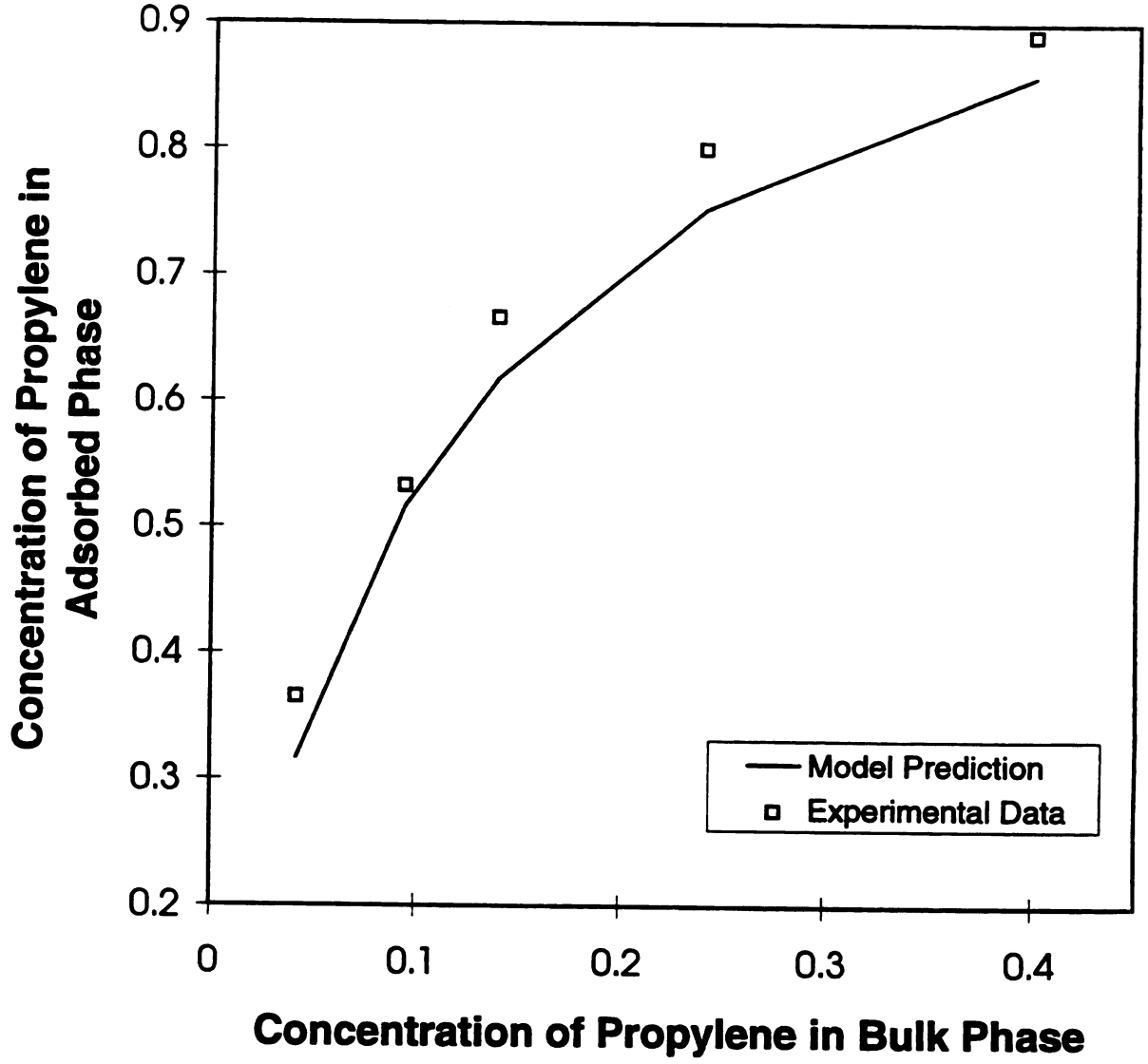

Figure 4-12 : Adsorption of Propylene-Ethylene mixture on BPL Carbon at 293.15 K and 1.013 bar

the temperature is increased the model predictions get worse. It is hoped that by suitably incorporating the pore-size distribution in the model i.e. by calculating the total amount adsorbed as the sum of the amount adsorbed over different pore sizes, the model predictions will be quantitative. Another important feature is the fact that the fluid-solid interaction parameter for pores was the same as that of flat walls. This suggests that the fluid-solid interaction parameter, while not a theoretically determined parameter, can be found by fitting the data at one temperature and for one surface. Once such a table can be written for a number of fluids, this model can be used as a predictive model over different surfaces. It also strengthens the universality of the SLD approach.

Another limitation of the SLD model is the lack of structure in the model. However, at pore sizes smaller than 3 molecular diameters, Figure 4-13 shows that the ratio $a(r):a_b$ is symmetric about the center of the pore but the maximum is off center. As a result, the calculated maximum density would be where $a(r)/a_b$ is maximum. The trends can be attributed to the fact that at pores smaller than 3 σ_f, there is a packing effect of the molecules such that if the particle is at the center of the pore then in the horizontal plane no other particles can be present, while if the particle is off-center, then another particle can exist in the same horizontal plane. This suggests that there is some inherent structure built in this model due to the sizes of the molecules which may lead to exclusion of particles. This 'structure' is not seen in slit-like pores. Slits are infinitely long in two-dimensions, while pores are infinitely long only in one-dimension. Hence, more molecules are in the vicinity of a given molecule in a slit, and the packing effect is less important.

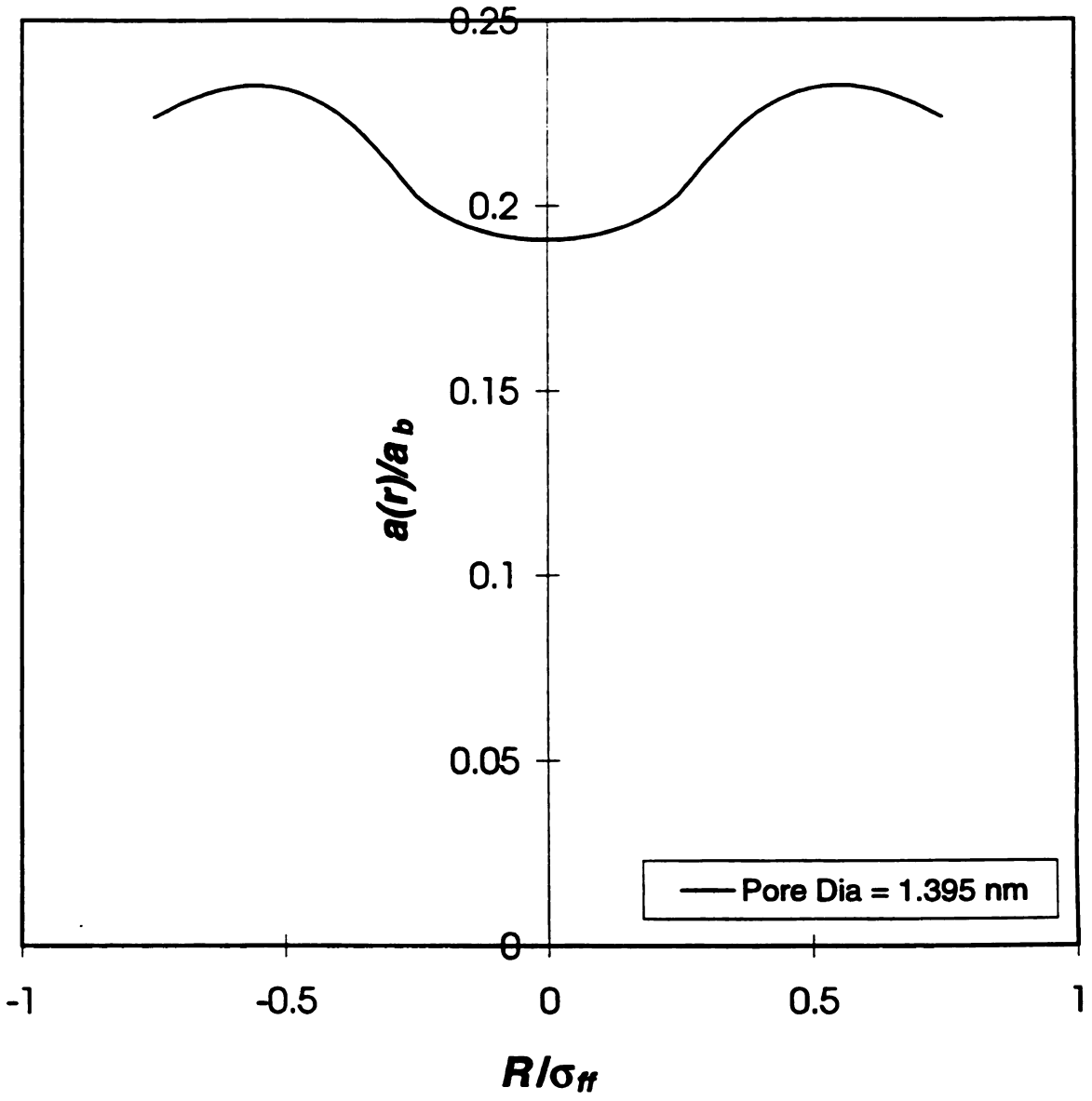

Figure 4-13: $a(r)/a_b$ for a Pore that can hold 2.5 ethylene molecules in the horizontal plane

The final limitation of the SLD model may be attributed to the local density approximation. Figures 4-14 and 4-15 show the adsorption of ethylene on graphon and on activated carbon at 212.7 K, by treating ethylene as a homogeneous fluid ($a(z)=a_b$.), similar to the Barrer and Robins van der Waals model. By comparing these figures with Figures 3-1 and 4-5, it is obvious that the volume occupied by the adsorbent must be excluded. The local density approximation makes the SLD model tractable for routine calculations. It can also solve the entire density profile over wide pressure ranges within a few seconds, and can give quantitative predictions for the surface excess and amount adsorbed. Hence, the local density approximation, while a limitation, significantly improves the model predictions over homogenous models.

There is also an incorrect limit in a/a_b in the model for slits and pores as a slit/pore width of one molecular diameter is approached. To discuss this inconsistency let us discuss slits. In such cases, for slits, the SLD model predicts that

$$\frac{a}{a_b} = \frac{3}{8}\left(\frac{L}{\sigma_{ff}} - 1\right) = 0 \quad \text{at} \quad \frac{L}{\sigma_{ff}} = 1 \qquad [4\text{-}23]$$

This requires that as the wall separation of the slit approaches σ_{ff}, a/a_b approaches zero. The physical inference of this result is that either the force of attraction between the particles is zero or that particles are not present. However, particles *can* be present in a single plane when the slit is one molecular diameter in width and they certainly attract each other. This suggests that this SLD methodology will not work in its present form for slit sizes approaching σ_{ff}. The problem arises due to the application of mean field theory that

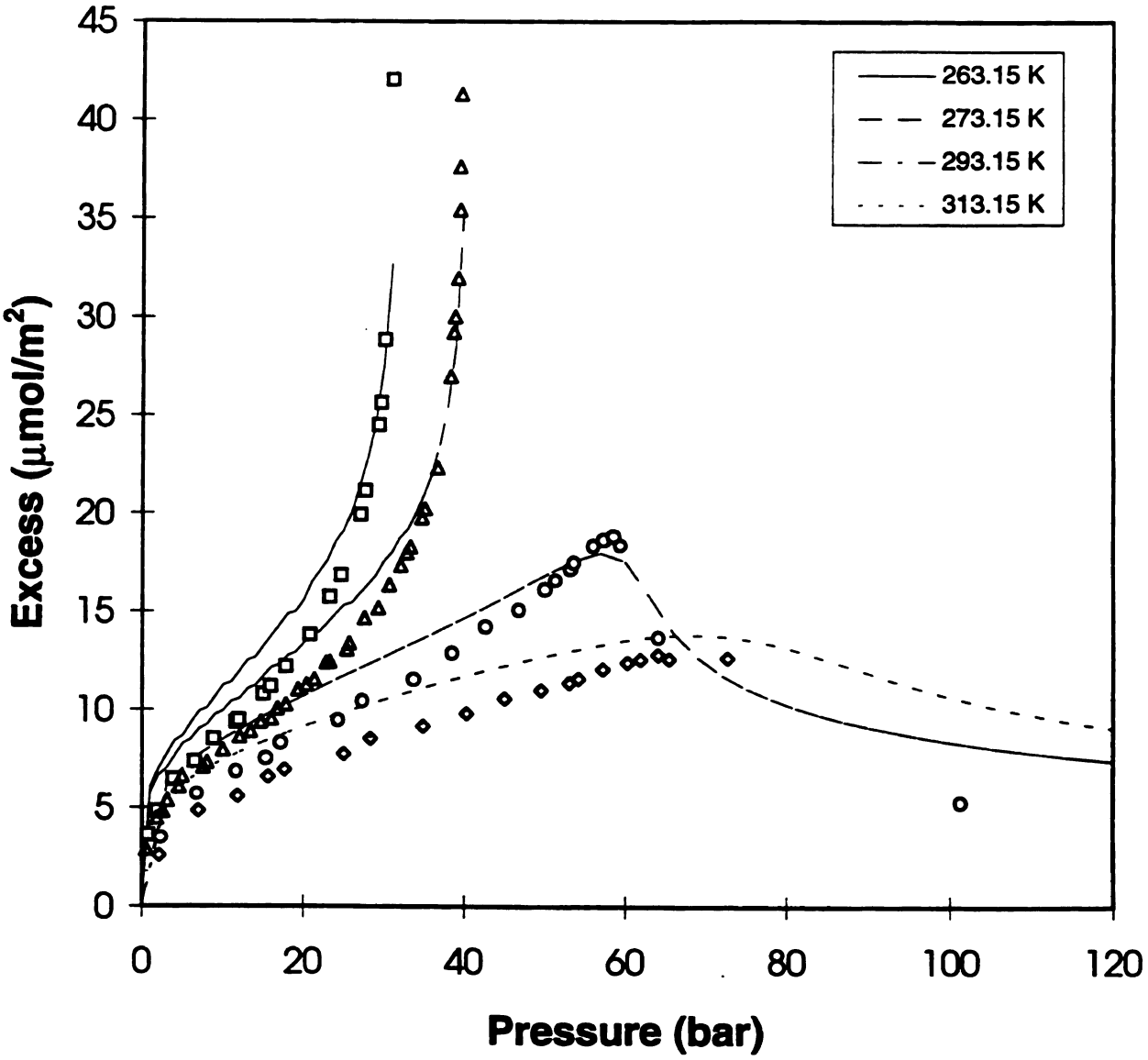

Figure 4-14: Adsorption of Homogeneous Ethylene on Graphon

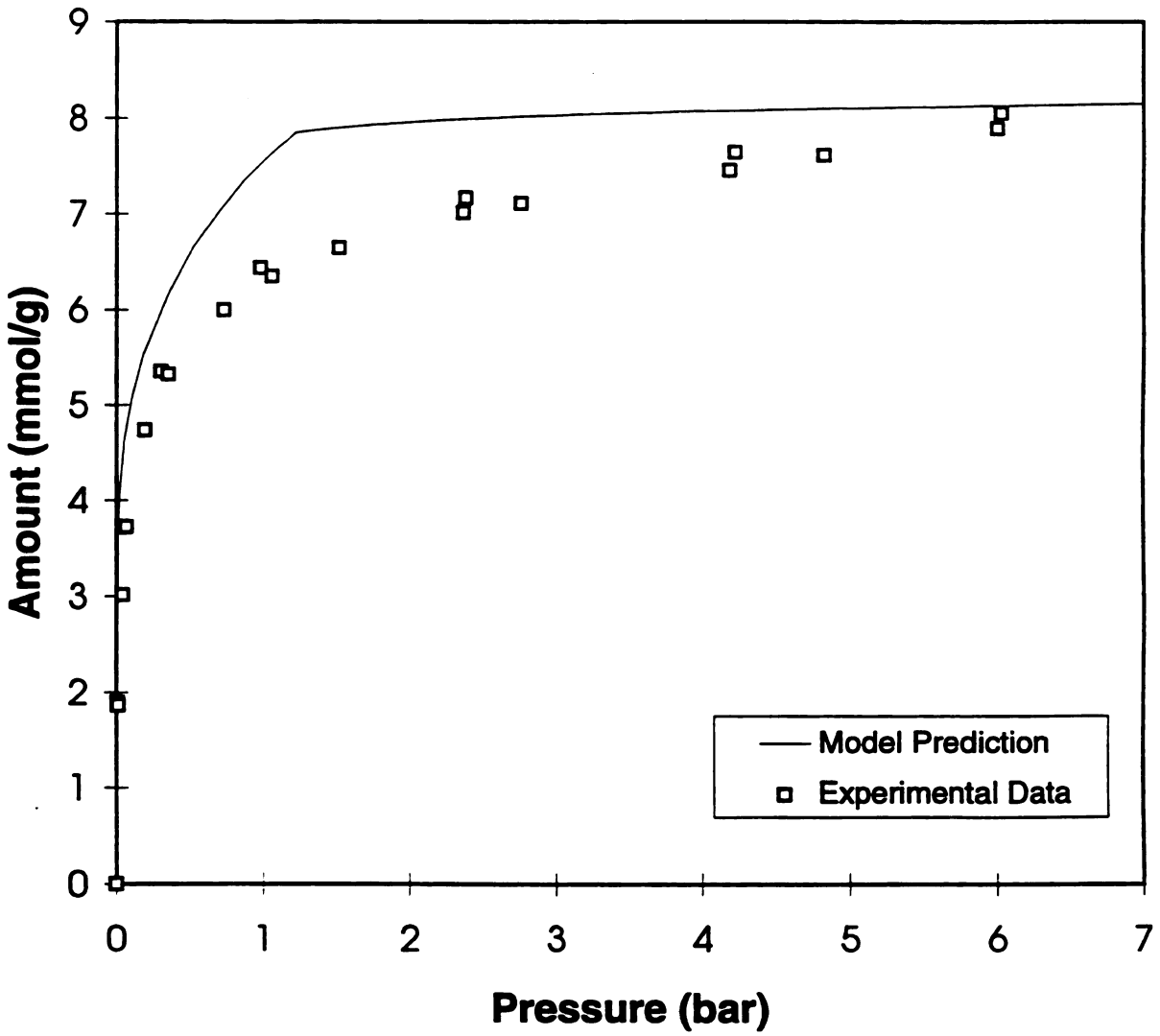

Figure 4-15: Adsorption of Homogeneous Ethylene on BPL Carbon at 212.7 K

neglects particle size, at an interface where particle size is most important. Mean field theory usually assumes that fluid particles are present in all space between the walls of a slit. At an interface this is incorrect; the reason can be visualized by considering a flat wall. In flat walls, we begin integrating from z=0.5 σ_{ff} because half the volume of this particle will not be in contact with any fluid particles. This means that no fluid centers can exist between 0 and 0.5 σ_{ff}, which is consistent with particles having finite size. As we move the fixed particle away from the wall more and more of the particle surface will be in contact with other particles, and it can be surrounded by other particles at $z \geq 2\sigma_{ff}$. In a confined slit the SLD approach is applied for each wall, excluding particles inside 0.5 σ_{ff} from each wall. When the width is just one molecular diameter, the limits overlap, thus the entire volume is excluded.

One way to correct this inconsistency is to refit a/a_b such that the integration begins from z=0 σ_{ff}, as opposed to z=0.5 σ_{ff}. This would neglect particle sizes for all but the fixed particle. The problem with this solution is that Ψ_{fs} includes particle size, and at z<0.5 σ_{ff} Ψ_{fs} becomes large and positive, and hence excludes particles, thus introducing a mathematical inconsistency.

Another approach would be to calculate the configurational integral for a slit of one molecular width as a base reference, and add to this integral as slit widths are increased. Presently, however, no clear and simple solution to this problem exists, because the problem of finite particle size is simply transferred from the first layer to each subsequent layer.

In order to investigate the behavior of a/a_b in confined spaces approaching σ_{ff}, we can easily consider packing of disks in a two-dimensional channel. Solving for the configurational energy of closest packing in a two-dimensional channel for disks of a finite size by summing a $1/r^6$ potential, the configurational energy for a channel of one molecular diameter width is approximately 2% lower than the configurational energy of a channel 1.5 molecular diameters wide. Based on this two-dimensional result, it seems reasonable to assume that a/ab is constant for slit widths below 1.5 σ_{ff}. We chose 1.5 molecular diameters because 1 molecular diameter represents total constraint in packing, while 2 molecular diameters represents total freedom in packing. Extension of the two-dimensional summation technique to three-dimensions is most easily and realistically achieved by conducting molecular simulations in small slits, and determining dependence of configurational energy on slit size to further refine a/a_b. Molecular simulations can be conducted also for pores to see if the approximation $a/a_b \approx$ constant is followed for pore widths $< 1.5\ \sigma_{ff}$.

CHAPTER 5. CONCLUSIONS

There are many different models that describe adsorption ranging from the simple empirical fits to the theoretically sound molecular simulations. The simple are widely used because of their simplicity. Models based on statistical mechanics and molecular simulations are theoretically sound but significant calculation time. A model that can retain the simplicity associated with the empirical models and contains the basic physics of the adsorption problem can be very useful. This is the basis for the development of the SLD model.

The SLD model is a simple model based on spatial invariance of the chemical potential, along with a cubic equation of state to describe the fluid properties. The SLD approach can model a variety of adsorption isotherms - from the low pressure region to the supercritical region. The model provides information about the density profile of the adsorbed fluid. In the subcritical region the SLD model predicts Type II and Type III isotherms on flat walls. It also predicts phase transitions at the surface (under certain conditions), as well as an abrupt transition between an adsorbed gas layer and fluid layer (again under certain conditions). Negative adsorption is sometimes predicted, similar to the predictions of Sullivan [1979]. In the supercritical region the model shows the experimentally observed cusp-like behavior near the critical point as well as the crossovers seen at higher pressures.

Quantitative modeling, extension to Types I, IV and V isotherms, prediction of clustering in supercritical fluids, and adsorption of multicomponent mixtures are discussed in chapters 3 and 4. By using the Peng-Robinson equation, the SLD model can quantitatively predict the adsorption of pure gases on flat walls. By modifying the solid-fluid potential to be two body fluid-fluid potential, the SLD model can predict clustering in supercritical fluids. The local density approximation calculations were modified to account for this change in geometry. Comparisons to experimental fluorescence spectra showed that the SLD model can predict the phenomenon of clustering. In slits and pores, the SLD model predicts types I, IV and V isotherms, and can also quantitatively model adsorption. Using the pore-size distributions will improve the model predictions.

By approximating activated carbon to be a slit, adsorption of binary mixtures were carried out. Calculations were done for two mixtures - ethylene & methane and propylene & ethylene. The ethylene-methane mixture calculations were done at two different temperatures - 212.7 and 260.2 K. These calculations show that the SLD model can qualitiatively predict the selectivity of a binary mixture. The SLD model qualitatively predicted the amount adsorbed. By modeling the activated carbon as a pore and suitably incorporating the pore-size distributions, the model predictions can be enhanced.

The SLD model serves as a good approximation and can provide rapid surveys of adsorption behavior to guide more detailed and time-consuming simulations. This model is not intended to replace any of the more complete theories such as Monte-Carlo simulations, molecular dynamics, or density functional theory, but instead provides a simple and approximate solution to the adsorption problem, The model may be viewed

as a compromise or a bridge between the two-dimensional equations-of-state models, Frenkel-Halsey-Hill theory, and the more rigorous density functional or integral equation approaches.

APPENDICES

APPENDIX 1

The van der Waals equation and configurational energy calculations - Flat Walls

If we consider a canonical ensemble, the partition function Q is given by [Vera and Prausnitz, 1972]

$$Q = \frac{1}{N!} V_f^N \left(\exp - \frac{\Phi}{2kT} \right)^N \left(\frac{q_{r,v,e}}{\Lambda^3} \right)^N$$

where $\Lambda = h/(2\pi mkT)^{1/2}$. The Helmholtz energy A and the pressure are related to the partition function:

$$P = -\left(\frac{\partial A}{\partial V}\right)_{T,N} = kT \left(\frac{\partial \ln Q}{\partial V}\right)_{T,N}$$

$$= kTN \frac{\partial \ln V_f}{\partial V} - \frac{N \partial \Phi/2}{\partial V}$$

$$= P_{rep} + P_{att}$$

where the molecular rotational, vibrational, electronic partition function, $q_{r,v,e}$, is assumed to have no volume dependence. The van der Waals free volume V_f, for a system with N molecules, is given by

$$V_f = V - \frac{N}{N_A} b$$

The repulsive part of the pressure is

$$P_{rep} = kTN \frac{1}{V - \frac{N}{N_A} b} = \frac{RT}{v - b}$$

$$P_{rep} = kTN \frac{1}{V - \frac{N}{N_A} b} = \frac{RT}{v - b}$$

If Φ is the sum of two-body interactions between an arbitrarily selected central molecule and all other molecules around it, and $\phi(r)$ is the two-body interaction potential, and $g(r)$ the radial distribution function, then,

$$\Phi = \int_0^\infty \frac{N}{V} \phi(r)\, g(r)\, 4\pi r^2 dr$$

For a van der Waals fluid, following McQuarrie [1976], $g(r) = 0$, for $r \leq \sigma$, and $g(r) =$ constant, for $r > \sigma$, where σ is the hard-core radius of the fluid molecule. To simplify notation, the subscript *ff* is omitted from σ throughout the appendix.

If we assume that the molecules interact with an infinite hard-core repulsive potential and an inverse-sixth attractive potential, then for $r > \sigma$,

$$\phi(r) = -\epsilon_{ff} \frac{\sigma^6}{r^6}$$

where ϵ_{ff} is the maximum energy of attraction between a pair of fluid molecules. In the bulk fluid, this leads to

$$\Phi_{bulk} = \frac{-4\pi \epsilon_{ff} \sigma^3 N_A}{3} \rho$$

$$a_{bulk} = 2\pi \epsilon_{ff} \sigma^3 N_A^2/3$$

$$P_{att} = -N \frac{\partial \Phi/2}{\partial V} = -\frac{2\pi \epsilon_{ff} \sigma^3 N_A^2}{3 v^2} = -\frac{a}{v^2}$$

Nonhomogeneous Systems. Consider a fluid molecule of diameter σ at location z in the vicinity of a wall, where $0.5\sigma \le z \le 1.5\sigma$. For convenience of integration we define a cylindrical coordinate system with the origin at an arbitrary molecular center at z, and let y be a dummy variable to denote axial distance and let r denote radial distance. The configurational energy can be calculated from the two integrals:

$$\Phi_1 = -\epsilon_{ff}\,\sigma^6\,N_A \int_{\frac{\sigma}{2}-z}^{\sigma} \int_{\sqrt{\sigma^2-y^2}}^{\infty} \rho(y)\,\frac{2\pi r}{(y^2+r^2)^3}\,dr\,dy$$

$$\Phi_2 = -\epsilon_{ff}\,\sigma^6\,N_A \int_{\sigma}^{\infty} \int_{0}^{\infty} \frac{\rho(y)\,2\pi r}{(y^2+r^2)^3}\,dr\,dy$$

$$\Phi = \Phi_1 + \Phi_2$$

With the local density approximation: $\rho(y) \approx \rho(z)$

$$\Phi = -1/2\epsilon_{ff}\,\sigma^3\,N_A\,\pi\,\rho(z)\left(\frac{z}{\sigma}+\frac{5}{6}\right)$$

Since a is proportional to Φ, for $0.5\sigma \le z \le 1.5\sigma$, we find

$$\frac{a(z)}{a_{bulk}} = \frac{\Phi(z)}{\Phi_{bulk}(\rho(z))} = \left(\frac{5}{16}+\frac{6}{16}\,\frac{z}{\sigma}\right)$$

For $1.5\sigma \le z < \infty$, the integration is performed in three parts:

$$\Phi_2 = -\epsilon_{ff}\,\sigma^6\,N_A \int_{-\sigma}^{\sigma} \int_{\sqrt{\sigma^2-y^2}}^{\infty} \frac{\rho\,(y)\,2\pi r}{(y^2+r^2)^3}\,dr\,dy$$

With the

$$\Phi_1 = -\epsilon_{ff}\,\sigma^6\,N_A \int_{\frac{\sigma}{2}-z}^{\infty} \int_0^{\infty} \frac{\rho(y)\,2\pi r}{(y^2+r^2)^3}\,dr\,dy$$

$$\Phi_3 = -\epsilon_{ff}\,\sigma^6\,N_A \int_{\sigma}^{\infty} \int_0^{\infty} \frac{\rho(y)\,2\pi r}{(y^2+r^2)^3}\,dr\,dy$$

With the local density approximation $\rho(y) \approx \rho(z)$ these can be integrated to give:

$$\Phi = -\epsilon_{ff}\,\sigma^3\,N_A\,\pi\,\rho(z)\left(\frac{4}{3} - \frac{1}{6\left(\frac{z}{\sigma}-\frac{1}{2}\right)^3}\right)$$

$$\frac{a}{a_{bulk}} = \frac{\Phi}{\Phi_{bulk}} = \left(1 - \frac{1}{8\left(\frac{z}{\sigma}-\frac{1}{2}\right)^3}\right)$$

and

$$a_{bulk} = \frac{27}{64}\frac{R^2T_c^2}{P_c} \rightarrow \frac{T_c}{T_{c_{bulk}}} = \frac{1}{2}$$

Note that at $z = \sigma/2$, $a = a_{bulk}/2$, and at $z \to \infty$, $a \to a_{bulk}$

Note that a and its derivative with respect to z are continuous functions at $z = 1.5\sigma$.

Calculation of Configurational Integral for Clustering

This calculation is similar to the configurational integral calculation for adsorption on a flat wall and further details are given in the appendix of a previous publication [Rangarajan et. al., 1995].

If Φ is the sum of two-body interactions between an arbitrarily selected central molecule and all other molecules around it and $\phi(r)$ is the two-body interaction potential, and $g(r)$ is the radial distribution function, then

$$\Phi = \int_0^\infty \frac{N}{V} \phi(r) g(r) 4\pi r^2 dr$$

For a van der Waals type fluid, following McQuarrie [1976], $g(r) = 0$ for $r \leq \sigma$, and $g(r) =$ constant, for $r > \sigma$, where σ is the hard-core radius of the fluid molecule. Note that the subscript f has been dropped from σ for the appendix to simplify the equations.

If we assume that the molecules interact with an infinite hard-core repulsive potential and an inverse sixth attractive potential, then for $r > \sigma$,

$$\phi(r) = -\epsilon_{ff} \frac{\sigma^6}{r^6}$$

where ϵ_{ff} is the maximum energy of attraction between a pair of fluid molecules. In the bulk fluid, this leads to

$$\Phi_b = \frac{-4\pi \epsilon_{ff} \sigma^3 N_A}{3} \rho$$

$$a_b = \frac{2\pi \in_{ff} \sigma^3 N_A^2}{3}$$

The relation between the partition function, the attractive and repulsive part of the pressure, a and Φ are given in previously [Rangarajan et. al., 1995; Vera and Prausnitz, 1972]].

Nonhomogeneous Systems. Consider a fluid (solvent)molecule of diameter σ at location r in the vicinity of a solute molecule of diameter σ_s (typically larger than σ), where $0.5\sigma \le r - \frac{\sigma_s}{2} \le 1.5\sigma$.

Using cylindrical coordinates with the origin at the center of the solute molecule, we integrate across all space with r denoting radial distance from the center of the solute molecule, x be the radial distance from the center of an arbitrary molecule (parallel to the intermolecular vector) and y be a dummy variable denoting axial distance (perpendicular to the intermolecular vector). The configurational integral can be calculated from five integrals:

$$\Phi_1 = -\in_{ff} \sigma^6 N_A \int_{\sigma}^{\infty}\int_{0}^{\infty} \rho(x,y)\frac{2\pi y dy dx}{(x^2+y^2)^3}$$

$$\Phi_2 = -\in_{ff} \sigma^6 N_A \int_{\sigma}^{\infty}\int_{0}^{\infty} \rho(r,y)\frac{2\pi y dy dr}{(r^2+y^2)^3}$$

$$\Phi_3 = -\in_{ff} \sigma^6 N_A \int_{0}^{r-r''}\int_{\sqrt{\sigma^2-x^2}}^{\infty} \rho(x,y)\frac{2\pi y dy dx}{(x^2+y^2)^3}$$

$$\Phi_4 = -\in_{ff} \sigma^6 N_A \int_{r-r''}^{r+r'}\int_{\sqrt{r'^2-(r-x)^2}}^{\infty} \rho(x,y)\frac{2\pi y dy dx}{(x^2+y^2)^3}$$

$$\Phi_5 = -\in_{ff} \sigma^6 N_A \int_{r+r'}^{\infty}\int_{0}^{\infty} \rho(x,y)\frac{2\pi y dy dx}{(x^2+y^2)^3}$$

where

$$r' = \frac{(\sigma+\sigma_s)}{2}$$

$$r'' = \frac{r'^2 + r^2 - \sigma^2}{2r'}$$

$$\Phi = \Phi_1 + \Phi_2 + \Phi_3 + \Phi_4 + \Phi_5$$

With the local density approximation: $\rho(x,y) = \rho(r)$ and since a is proportional to Φ, we find that

$$\frac{a(r)}{a_b} = \frac{\Phi(r)}{\Phi_b}$$

and leads to

$$a(r) = \frac{3}{16} a_b \left(\frac{8}{3} + \frac{2}{\sigma}(r - r') + \frac{\sigma^3}{r}\left(\frac{1}{r'^2 + r^2 - 2rr''} - \frac{1}{r'^2 + r^2 + 2rr'}\right) + \frac{2}{3}\sigma^3 \left(\frac{1}{(r + r')^3}\right)\right)$$

Similarly, for $1.5\sigma \le r - \frac{\sigma_s}{2} < \infty$, the integration is performed as before with an additional integral. As the fluid molecule under consideration is moved to a distance greater than 1.5σ the additional integral accounts for the cohesive energy in the region between $\sigma_{fs} \le x \le r - \sigma$. This leads to a six-part integral resulting in

$$a(r) = \frac{3}{16} a_b \left(\frac{16}{3} - \frac{2\sigma^3}{3}\frac{1}{(r - r')^3} + \frac{\sigma^3}{r}\left(\frac{1}{r'^2 + r^2 - 2rr'} - \frac{1}{r'^2 + r^2 + 2rr'}\right) + \frac{2\sigma^3}{3}\frac{1}{(r + r')^3}\right)$$

These modified $a(r)$ are then used in the calculation of the fluid fugacity.

Calculation of Configurational Integral for Slits

Definitions: z is the distance from the surface of one of the walls. L is the distance between the two wall surfaces. r is the radial distance. x is a dummy variable that denotes axial diatance.

Case I. Particle is near the wall: $\frac{\sigma}{2} \le z \le 3\frac{\sigma}{2}$

The integral is carried out by splitting the regions as follows:

Region 1. x ranges from 0 to z-$\sigma/2$

$$\Phi_1 = -4\varepsilon_{ff}\sigma^6 N_A \int_0^{z-\frac{\sigma}{2}} \int_{\sqrt{\sigma^2-x^2}}^{\infty} \rho(x) \frac{2\pi r}{(x^2+r^2)^3} dr dx$$

$$\Phi_1 = -2\varepsilon_{ff}\sigma^3 N_A \pi \rho(z) \left[\frac{z}{\sigma} - \frac{1}{2}\right]$$

Note that the steps needed to carry out the integration are given in detail in the integral for flat walls.

Region 2. x ranges from 0 to σ

$$\Phi_2 = -4\varepsilon_{ff}\sigma^6 N_A \int_0^{\sigma}\int_{\sqrt{\sigma^2-x^2}}^{\infty} \rho(x)\frac{2\pi r}{(x^2+r^2)^3}drdx$$

$$\Phi_2 = -2\varepsilon_{ff}\sigma^3 N_A \pi\rho(z)$$

Region 3. x ranges from σ to L-σ/2-z

$$\Phi_3 = -4\varepsilon_{ff}\sigma^6 N_A \int_{\sigma}^{L-\sigma/2-z}\int_0^{\infty} \rho(x)\frac{2\pi r}{(x^2+r^2)^3}drdx$$

$$\Phi_3 = -4\varepsilon_{ff}\sigma^6 N_A \pi\int_{\sigma}^{L-\sigma/2-z}\frac{\rho(x)}{x^4}dx$$

$$\Phi_3 = -\frac{2}{3}\varepsilon_{ff}\sigma^3 N_A \pi\rho(z)\left[1-\frac{1}{\left(\frac{L}{\sigma}-\frac{1}{2}-\frac{z}{\sigma}\right)^3}\right]$$

$$\Phi = \Phi_1 + \Phi_2 + \Phi_3$$

$$\Phi = -2\varepsilon_{ff}\sigma^3 N_A \pi\rho(z)\left[\frac{z}{\sigma}+\frac{5}{6}-\frac{1}{3\left(\frac{L}{\sigma}-\frac{1}{2}-\frac{z}{\sigma}\right)^3}\right]$$

Note that for particle near the other wall, the result is a mirror image of the above result

i.e. replace z with L - z.

Case II. For Large Slits, there is also a region $1.5 \le \frac{z}{\sigma} \le \frac{L}{\sigma} - 1.5$

In this case, the axial distance is split into 4 parts

Region 1. x going from σ to z-$\sigma/2$

$$\Phi_1 = -4\varepsilon_{ff}\sigma^6 N_A \int_{\sigma}^{z-\sigma/2}\int_0^{\infty} \rho(x)\frac{2\pi r}{(x^2+r^2)^3}drdx$$

$$\Phi_1 = -\frac{2}{3}\varepsilon_{ff}\sigma^3 N_A \pi\rho(z)\left[1-\frac{1}{\left(\frac{z}{\sigma}-\frac{1}{2}\right)^3}\right]$$

Region 2. x going from 0 to σ - the result is same as case I - region 2.

Region 3. x going from 0 to σ - the result is same as case I - region 2.

Region 4. x going from σ to L-$\sigma/2$-z - the result is same as case I - region 3.

$$\Phi = \Phi_1 + \Phi_2 + \Phi_3 + \Phi_4$$

$$\Phi = -2\varepsilon_{ff}\sigma^3 N_A \pi\rho(z)\left[\frac{z}{\sigma}+\frac{5}{6}-\frac{1}{3\left(\frac{L}{\sigma}-\frac{1}{2}-\frac{z}{\sigma}\right)^3}\right]$$

Case III. In small slits i.e less than three fluid molecular diameters big, all three regions may not be present. In such cases, case I - region 2's upper limt will become the same as case I - region 3's upper limit i.e. region 2's upper limit will become L-σ/2-z. Region 1 will be the same as case I - region 1.

$$\therefore \Phi_2' = -4\varepsilon_{ff}\sigma^6 N_A \int_0^{L-\sigma/2-z}\int_{\sqrt{\sigma^2-x^2}}^{\infty}\rho(x)\frac{2\pi r}{(x^2+r^2)^3}drdx$$

$$\Phi_2' = -2\varepsilon_{ff}\sigma^3 N_A \pi\rho(z)\left[\frac{L}{\sigma}-\frac{1}{2}-\frac{z}{\sigma}\right]$$

$$\Phi = \Phi_1 + \Phi_2'$$

$$\Phi = -2\varepsilon_{ff}\sigma^3 N_A \pi\rho(z)\left[\frac{L}{\sigma}-1\right]$$

In the limit that $L = \sigma$, the integral reduces to a two-dimensional integral. Here the solution is given by

$$\Phi_{2D} = -4\varepsilon_{ff}\sigma^6 N_A \int_\sigma^\infty \rho' \frac{2\pi r dr}{r^6}$$

where ρ' is given by mol/area.

$$\Phi_{2D} = -2\varepsilon_{ff}\sigma^2 N_A \rho'$$

$$\frac{\Phi_{2D}}{\Phi_b} = \frac{3}{8}\frac{\rho'}{\rho_b \sigma}$$

For slits smaller than 2 σ in width the density is a constant. To convert density in moles/volume to moles/area multiply by the slit width L. i.e.

$$\rho' = \rho_b L$$

However, noting that in a slit there are two walls, i.e. the surface area is twice that of a flat wall, the equation has to be modified to become

$$\rho' = \rho_b \frac{L}{2}$$

Using this equation we get

$$\frac{a}{a_b} = \frac{\Phi_{2D}}{\Phi_b} = \frac{3}{16}\frac{L}{\sigma}$$

Note that at the limit $L = 2\sigma$

$$\frac{a}{a_b} = \frac{3}{16}\frac{L}{\sigma} = \frac{3}{8}, \text{ and } \frac{a}{a_b} = \frac{3}{8}\left(\frac{L}{\sigma} - 1\right) = \frac{3}{8}$$

However, the derivative is not constant at $L = 2\sigma$.

Calculation of Configurational Integral for Cylindrical Pores

Definitions: The distance between the fixed particle and any particle is given by a. R is the distance from the center to the pore surface. r is the radial distance, and r_1 is the distance from the center of the pore and the fixed particle. θ is the angle formed between the center of the pore, the fixed particle and the projection of any particle on the horizontal plane. z is the distance between any particle and the horizontal plane in which the fixed particle is located.

$$a = \sqrt{r^2 + z^2}$$

The cylinder makes a circle in the horizontal plane. The locus of the circle is given by the equation

$$x^2 + y^2 = r^2$$

where x and y are the x and y coordinates from the center of the circle (r is the radius of this circle).

$$x = r_1 - r\cos(\theta), \quad y = r\sin(\theta)$$

Solving the above two equations we get

$$r = r_1 \cos(\theta) + \sqrt{(R - \frac{\sigma}{2})^2 - r_1^2 \sin^2(\theta)}$$

where σ is the fluid diameter. Note that the subscript *ff* has been dropped from σ to simplify notation.

Now, the configurational energy is given as

$$\Phi = -4\varepsilon_{ff} N_A \sigma^6 \int_\theta \int_z \int_r \frac{r}{a^6} dr\, d\theta\, dz \quad = \beta \int_\theta \int_z \int_r \frac{r}{a^6} dr\, d\theta\, dz$$

where $\beta = -4\varepsilon_{ff} N_A \sigma^6$.

I. Particle away from the wall

Region 1. z varies from σ to ∞

$$\frac{\Phi}{\beta} = \int_\sigma^\infty \int_0^\pi \int_0^{r_1 \cos\theta + \sqrt{(R-\frac{\sigma}{2})^2 - r_1^2 \sin^2\theta}} \frac{r dr d\theta dz}{(r^2 + z^2)^3}$$

$$\frac{\Phi}{\beta}=\int_{\sigma}^{\infty}\int_{0}^{\pi}\left\{\frac{1}{4z^4}-\frac{1}{4\left[r_1\cos\theta+\sqrt{\left(R-\frac{\sigma}{2}\right)^2-r_1^2\sin^2\theta}\right]^2+z^2}\right\}d\theta\,dz$$

Let $b=r_1\cos\theta+\sqrt{\left(R-\frac{\sigma}{2}\right)^2-r_1^2\sin^2\theta}$

Solving this equations yields

$$\frac{\Phi}{\beta}=\frac{\pi}{12\sigma^3}-\frac{1}{4}\int_0^{\pi}\left(\frac{\pi}{4b^3}-\frac{\sigma}{2b^2(b^2+\sigma^2)}-\frac{\tan^{-1}(\sigma/b)}{2b^3}\right)d\theta$$

Region 2. z = 0 to σ

$$\frac{\Phi}{\beta}=\int_0^{\sigma}\int_0^{\pi}\int_0^{r_1\cos\theta+\sqrt{(R-\frac{\sigma}{2})^2-r_1^2\sin^2\theta}}\frac{r\,dr\,d\theta\,dz}{(r^2+z^2)^3}$$

Just as before solving the above equation yields

$$\frac{\Phi}{\beta}=\frac{\pi}{4\sigma^3}-\frac{1}{4}\int_0^{\pi}\left[\frac{\sigma}{2b^2(b^2+\sigma^2)}+\frac{\tan^{-1}(\sigma/b)}{2b^3}\right]d\theta$$

Hence, for particle away from the wall i.e. $0 \le r_1 \le R - 3\sigma / 2$, Φ is the sum of the two.

II. Particle near the wall i.e. $R - 3\sigma / 2 \le r_1 \le R - \sigma / 2$

Region 1. For $z = \sigma$ to $\propto$, the integral remains the same as in I.

Region 2. For z = o to σ

In this case, θ cannot go from 0 to π, but can only go from 0 to

$\cos^{-1}\left[\dfrac{r_1^2 + \sigma^2 - z^2 - (R - \frac{\sigma}{2})^2}{2r_1\sqrt{\sigma^2 - z^2}}\right]$, because of exclusion due to the presence of the fixed particle.

Note that at $z = \sqrt{\sigma^2 - (R - \frac{\sigma}{2} - r_1)^2}$, $\cos\theta = -1$, $\theta = \pi$

The integral in the r direction is the same as before. This yields

$$\frac{\Phi}{\beta} = \frac{1}{4\sigma^4}\int_0^w \cos^{-1}(w)dz - \frac{1}{4}\int_0^\sigma \int_0^{\cos^{-1}w} \frac{1}{(b^2 + z^2)^2} d\theta dz$$

where $w = \dfrac{r_1^2 + \sigma^2 - z^2 - (R - \frac{\sigma}{2})^2}{2r_1\sqrt{\sigma^2 - z^2}}$

Hence for particles near the wall i.e. $R - 3\sigma/2 \le r_1 \le R - \sigma/2$

$$\frac{\Phi}{\beta} = \frac{\pi}{12\sigma^3} - \frac{1}{4}\int_0^{\pi}\left(\frac{\pi}{4b^3} - \frac{\sigma}{2b^2(b^2+\sigma^2)} - \frac{\tan^{-1}(\sigma/b)}{2b^3}\right)d\theta + \frac{1}{4\sigma^4}\int_0^{w}\cos^{-1}(w)dz - \frac{1}{4}\int_0^{\sigma}\int_0^{\cos^{-1}w}\frac{1}{(b^2+z^2)^2}d\theta dz$$

III. Particle at the wall

In this case θ varies only from 0 to π.

Region 1. z varies from σ to $\propto$

Here,

$$r_1 = R - \frac{\sigma}{2}$$

$$r_1\cos\theta + \sqrt{(R-\frac{\sigma}{2})^2 - r_1^2\sin^2\theta} = 2r_1\cos\theta$$

Hence, the integral becomes

$$\frac{\Phi}{\beta} = \int_{\sigma}^{\infty}\int_{0}^{\pi/2}\int_{0}^{2r_1\cos\theta} \frac{r dr d\theta dz}{(r^2+z^2)^3}$$

$$\frac{\Phi}{\beta} = \int_{\sigma}^{\infty}\int_{0}^{\pi/2} \frac{1}{4z^4} d\theta dz - \int_{\sigma}^{\infty}\int_{0}^{\pi/2} \frac{1}{4[4r_1^2\cos^2\theta + z^2]^2} d\theta dz$$

$$\frac{\Phi}{\beta} = \frac{\pi}{24\sigma^3} - \int_{\sigma}^{\infty} \frac{\pi(2r_1^2+z^2)}{2z^3(4r_1^2+z^2)^{3/2}} dz$$

Region 2. For $z = 0$ to σ

Once again θ cannot go from 0 to π, but can only go from 0 to

$\cos^{-1}\left[\dfrac{r_1^2+\sigma^2-z^2-(R-\frac{\sigma}{2})^2}{2r_1\sqrt{\sigma^2-z^2}}\right]$, because of exclusion due to the presence of the fixed particle.

$$w = \frac{r_1^2+\sigma^2-z^2-(R-\frac{\sigma}{2})^2}{2r_1\sqrt{\sigma^2-z^2}} = \frac{\sqrt{\sigma^2-z^2}}{2r_1}$$

Doing the calculations as before,

$$\frac{\Phi}{\beta} = \int_{\sigma}^{\infty} \frac{1}{4\sigma^4}\cos^{-1}\left(\frac{\sqrt{\sigma^2-z^2}}{2r_1}\right) dz - \frac{1}{4}\int_{\sigma}^{\infty}\int_{0}^{\cos^{-1}w} \frac{1}{[4r_1^2\cos^2\theta + z^2]^2} d\theta dz$$

$$\frac{\Phi}{\beta} = \frac{\pi}{24\sigma^3} - \int_{\sigma}^{\infty} \frac{\pi(2r_1^2 + z^2)}{2z^3(4r_1^2 + z^2)^{3/2}} dz + \int_{\sigma}^{\infty} \frac{1}{4\sigma^4} \cos^{-1}\left(\frac{\sqrt{\sigma^2 - z^2}}{2r_1}\right) dz - \frac{1}{4} \int_{\sigma}^{\infty} \int_{0}^{\cos^{-1} w} \frac{1}{[4r_1^2 \cos^2\theta + z^2]^2} d\theta dz$$

Note that in all cases $\frac{\Phi}{\Phi_b} = \frac{a}{a_b} = \frac{\Phi}{-16\varepsilon_{ff}\sigma^3 N_A \pi \rho / 3}$

Appendix 2 - Programs

```
C       FLAT WALL - Pure Gas
C   Program to calculate surface excess or adsorption isotherms
C    The program uses Peng-Robinson equation of state, with a modified
C    a to account for exclusion. The strength of the adsorption
C    potential and its dependence on position is given by Psi.
C    The fluid-fluid potential uff = u total - u ads.
C    From this potential the various fluid properties are calculated.
C
C    The variables used are defined below.
C    All units used are SI unless otherwise stated.
C
     COMMON R,TC,PC,OMEGA
C
C    Define Psi as a statement function
C    Use a 10-4 potential where PSI is the negative of the
C    intermolecular potential.
C    SIGFW is  sigma fluid-wall, in Angstroms.
C    EPSFW is the fluid-wall potential in K
C    ALPHA is the ratio of the spacing of the graphite basal planes
C    (3.35 A) to SIGFW.
C    The number density of C atoms in graphite is 0.382 atoms/A^2.
C    The equation used is that suggested by Lee (1.5).

     PSI(ETA)=4.0*3.1415926*0.382*SIGFW*SIGFW*EPSFW*(-0.2
    1/ETA**10+0.5/ETA**4+0.5/(ETA+ALPHA)**4+0.5/(ETA+2.0*
    *ALPHA)**4+0.5/(ETA+3.0*ALPHA)**4+0.5/(ETA+4.0*ALPHA)
    ***4)

C    WRITE(*,*)'Temp Plim Epsilon Sigff Sigww Tc Pc omega'
C     READ(*,*) T,PLIM,EPSFW,SIGFF,SIGWW,TC,PC,OMEGA
     WRITE(*,*) 'EPSILON'
     READ(*,*) EPSFW
     T=212.7
     PLIM=7.E5
     SIGFF=4.22
     SIGWW=3.4
     TC=282.4
     PC=50.4e5
     OMEGA=0.089

     OPEN(UNIT=7,FILE='denpro.dat',STATUS='UNKNOWN')
     OPEN(UNIT=8,FILE='adsorp.dat',STATUS='UNKNOWN')

C    R = Gas constant J/K/mol
C    Tc = Critical Temperature K
C    Pc = Critical Pressure   N/m2
C       OMEGA = Acentric Factor
C    SIGMA = Sigma fluid-wall in m.
C    T = Temperature K
C    FLIM = Bulk fugacity limit.
```

```
C     EPSFW = Fluid-wall potential well depth in K
C     SIGFW = Sigma fluid-wall in Angstroms
C     ALPHA = Spacing of graphite planes / Sigfw
C        SIGFF = Sigma fluid-fluid in Angstroms
C        SIGWW = Sigma wall-wall in Angstroms
C     AB = Bulk Peng-Robinson 'a'
C     BB = Bulk Peng-Robinson 'b'



      R=8.314
         FOMEG=0.37464+1.54226*OMEGA-0.26992*(OMEGA**2)

      TR = T/TC
         SIGFW=(SIGWW+SIGFF)/2.
         SIGMA=SIGFW*1E-10
         ALPHA=3.35/SIGFW
C        ALPHA = Spacing of graphite planes / Sigfw
C     SIGFF = Sigma fluid-fluid in Angstroms



C     Calculate a bulk and b
      AB=0.45724*(R*TC*(1+FOMEG*(1-SQRT(TR))))**2/PC
      BB=0.07780*R*TC/PC


C     Write parameters to files


      PCB=PC/1.0E5
      IF(TR.GE.1) GO TO 2
      CALL FSAT(AB,BB,T,FUGS,PS,VV,VL)

 2    DELP=PLIM/40.
C          Loop for bulk fugacity
           PB=0.0E5
           J=0

C     FOR EACH BULK FUGACITY VALUE
 5         PB=PB+DELP

C               PB=PLIM
                B=BB
                A=AB



C     First calculate bulk density (DENB) and bulk pressure (BP)
                CALL BVCAL(A,B,T,PB,PS,V,FB)
                CALL PV(A,B,T,V,P)

                DENB=1.0/V
                BP=P
```

```
C       WRITE(7,*) 'PRESSURE', P
C       WRITE(7,*)'BULK DENSITY', DENB

              DELETA=0.1
              ETA=.9
              EXCESS=0.0

              K=0


6             ETA=ETA+DELETA

C                       Calculate local fugacity
C     Use the following formula to get the local
C     fugacity (F), for a given position ETA.
C                       F=FB*EXP(PSI(ETA)/T)

                       ALNFB=ALOG(FB)
                       ALNF=ALNFB+PSI(ETA)/T
                       PSIV=PSI(ETA)/T



C                       Calculate local a
             CALL ACALC(ETA,AB,A,SIGWW,SIGFW,SIGFF)

C     Using local parameters calculate V and local density DENL

                   CALL VCALC(A,B,T,ALNF,BP,V)
                      DENL=1.0/V
            EXCESS=SIGMA*(DENL-DENB)*DELETA*1.E6+EXCESS

C     DENLG is the density in gmoles/cc

              DENLG=DENL/1.0E6
              WRITE (7,102)ETA,DENLG
              WRITE(8,*) 'A',',',A,',','B',',',B,',',ETA

              K=K+1

              IF(K.LT.200) GOTO 6


90                 CONTINUE
           BP=P/1.0E5
           DENBG=DENB/1.E6

           WRITE(6,*) BP, ',', EXCESS, ',', DENBG
           WRITE(8,*) BP, ',', EXCESS, ',', DENBG

            J=J+1
            IF (J.LT.40) GOTO 5
```

```
100         CONTINUE

C           WRITE(*,*)'Press 1 to continue'
C           READ(*,*) INT
C           IF (INT.EQ.1) GOTO 566
          CONTINUE


102      FORMAT(1X,F8.2,2X,F12.5)


      END



C*********************************************************************
C234567
C   SUBROUTINES
C*********************************************************************


    SUBROUTINE VCALC(A,B,T,ALNF,BP,V)

    COMMON R,TC,PC,OMEGA

    IV1=1
    IV3=1
    DPDV1=1
    DPDV3=1

    P1=0
    P3=0

    V=0

C     IF(BP.GT.PS) GOTO 16

    CALL V1CALC(A,B,T,ALNF,V1,IV1)

    IF(IV1.EQ.1) GOTO 10

    CALL DPDV(A,B,T,V1,IDPDV1)

    IF(IDPDV1.EQ.1) GOTO 10

     CALL PV(A,B,T,V1,P1)


10   CONTINUE

    CALL V3CALC(A,B,T,ALNF,V3,IV3)

    IF (IV3.EQ.1) GOTO 14
```

```
      CALL DPDV(A,B,T,V3,IDPDV3)
      IF(IDPDV3.EQ.0) THEN
        CALL PV(A,B,T,V3,P3)
      ELSE
        CONTINUE
      ENDIF

   14 CONTINUE
      IF (P1.GT.P3) THEN
        V=V1
      ELSE
        V=V3
      ENDIF
      CONTINUE
C     WRITE(2,*)P1,P3
      GOTO 15

C 16  CALL V3CALC(A,B,T,ALNF,V3,IV3)
C     IF(IV3.EQ.0) GOTO 21

C 16  CALL V1CALC(A,B,T,ALNF,V1,IV1)
C     V=V1

C     GOTO 15

C 21  CALL PV(A,B,T,V3,P3)

C     V=V3

   15 RETURN
      END

C*********************************************************************

C234567
```

```
      SUBROUTINE DPDV(A,B,T,V,IDPDV)
      COMMON R

C     Input A,B,T,V and Output = IDPDV

C     THIS SUBROUTINE EVALUATES THE DERIVATIVE dP/dv
C     AND RETURNS A VALUE OF 1 FOR IDPDV IF THE SLOPE
C     IS POSITIVE, i.e. THE ROOT IS UNSTABLE.

      IDPDV=0
      DP=-R*T/(V-B)/(V-B)+2.0*A*(V+B)/((V*V+2*B*V-B*B)**2)
      IF (DP.GT.0) IDPDV=1

      RETURN
      END



C*********************************************************************

      SUBROUTINE V1CALC(A,B,T,ALNF,V1,IV1)
      COMMON R,TC,PC,OMEGA

      IV1=0

C     This subroutine uses a successive substituion method
C     to get the small root V1.
C     Inputs A,B,T,ALNF and Output V1, IV1


C     Starting guess for calculating v
      V1=1.05*B
C      Iterate 60 times

      DO 20 I = 1,60

          ARG=(V1-B)/R/T

        IF((V1.LE.B).OR.(ARG.LE.0.0)) THEN
              IV1=1
C     WRITE(9,*)'INV1CAL V1= ',V1,' B = ',B,'ARG = ',ARG
C     1,'I =',I,' ALNF',ALNF
              GOTO 30
          ELSE
      DENO=ALNF+ALOG(ARG)+A*V1/R/T/(V1**2+2*B*V1-B**2)
      DENO=DENO+A/2.82/R/T/B*ALOG((V1+2.414*B)/(V1-0.414*B))


      V1=B+B/DENO


          ENDIF
C     WRITE(6,*)'V1,B',V1,B
C     STOP
```

```
 20  CONTINUE

     ALNFC=B/(V1-B)-A*V1/R/T/(V1*V1+2*B*V1-B*B)

     ALNFC=ALNFC+ALOG(R*T/(V1-B))

     ALNFC=ALNFC+A/2.82/B/R/T*ALOG((V1-0.414*B)/(V1+2.414*B))


     ERROR=EXP(ALNFC-ALNF)-1.0
     IF (ABS(ERROR).GE.0.001) IV1=1
 30  CONTINUE
C    WRITE(9,*)'v1',ALNFC,ALNF,V1
     RETURN
     END

C*********************************************************************
C234567
     SUBROUTINE V3CALC(A,B,T,ALNF,V3,IV3)

     COMMON R,TC,PC,OMEGA

     IV3=0

C    STARTING GUESS FOR V3 = RT/F

     ALNV3=ALOG(R*T)-ALNF
     V3=EXP(ALNV3)
C    ITERATE TILL DONE OR 40 TIMES

     DO 20 I=1,40

      IF (V3.LE.B) THEN
C      WRITE(9,*)'V3 LE B', V3,' B ',B
      IV3=1
      GOTO 30
      ENDIF
     ARG=B/(V3-B)-A*V3/R/T/(V3**2+2*B*V3-B**2)
     IF(ARG.GT.40.) THEN
C       D3=1./V3
C       WRITE(9,*)'V3 = ',V3,' ARG LARGE = ',ARG,'D3 =',D3
        IV3=1
        GOTO 30
     ELSE
     DENO=A/2.824/R/T/B*ALOG((V3-0.414*B)/(V3+2.414*B))
     ALNV3B=ALOG(R*T)-ALNF+ARG+DENO
       V3=B+EXP(ALNV3B)
      ENDIF

 20  CONTINUE
     ALNFC=B/(V3-B)-A*V3/R/T/(V3*V3+2*B*V3-B*B)

     ALNFC=ALNFC+ALOG(R*T/(V3-B))
```

```
      ALNFC=ALNFC+A/2.824*ALOG((V3-0.414*B)/(V3+2.414*B))/B/R/T

C     WRITE(9,*)' IN V3. ln fc, V3 ',ALNFC,V3
      ERROR=EXP(ALNFC-ALNF)-1.0
      IF(ABS(ERROR).GE.0.001) IV3=1
 30   CONTINUE
C     WRITE(4,*)'V3',ALNFC,ALNF,V3
      RETURN
      END

C*********************************************************************
C234567
      SUBROUTINE PV(A,B,T,V,P)
      COMMON R
C     This subroutine returns the value of P given a,b,T,v
C     using the van der Waals equation of state.

      P=R*T/(V-B)-A/(V*V+2*B*V-B*B)

      RETURN
      END

C*************************************************************
C234567
      SUBROUTINE ARANGE(R1,R2,R3)

C     PROGRAM TO PUT 3 NUMBERS IN DESCENDING ORDER

      DO 20 J=1,3

      IF(R2.GT.R1) THEN
        TEMP=R1
        R1=R2
        R2=TEMP
      ENDIF

      IF(R3.GT.R2) THEN
        TEMP=R2
        R2=R3
        R3=TEMP
      ENDIF

 20   CONTINUE

      RETURN
      END

C*************************************************************************************
C234567
      SUBROUTINE ACALC(ETA,AB,A,SIGWW,SIGFW,SIGFF)

C     This subroutine calculates the van der Waals a term
C     after taking into account the effect of exclusion.
```

```
C     AB = Value of a in the bulk
C     ETA = reduced distance from the center of wall
C     The main program sends a reduced distance ETA from the
C     center of the wall molecule, which is the basis for
C     the integrated 9-3 potential.
C     However the integrations for configurational energy have
C     been done from the edge of the wall molecule.
C     Therefore it is necessary to translate the coordinate.
C     BETA is the distance from the edge of the wall
C     in reduced units

      BETA =( ETA - (0.5*SIGWW/SIGFW))*(SIGFW/SIGFF)

      IF (BETA.LE.1.5) THEN
          A=AB*(5.0+6.0*BETA)/16.0
      ELSE
          A=AB*(1.0-1.0/8.0/(BETA-0.5)**3)
      ENDIF

      RETURN
      END



C*************************************************************

C  &7 1      2      3      4      5      6      7 2
C     ********************************************************************
C     * SUBROUTINE CUBIC                                                 *
C     ********************************************************************
C     * THIS SUBROUTINE FINDS THE ROOTS OF A CUBIC EQUATION OF THE       *
C     * FORM     X**3 + A2*X**2 + A1*X + A0 = 0     ANALYTICALLY.        *
C     ********************************************************************
C     * VARIABLES
      SUBROUTINE CUBIC(A2,A1,A0,R1,R2,R3,C1,C2,C3,IFLAG)
      DOUBLE PRECISION CHECK,DA0,DA1,DA2,P1,P2,Q,R,SS1,SS2
      COMPLEX ES1,ES2,S1,S2,Z1,Z2,Z3,CCHECK
      DA0 = DBLE(A0)
      DA1 = DBLE(A1)
      DA2 = DBLE(A2)
      Q = DA1/3.D00 - DA2*DA2/9.D00
      R = (DA1*DA2-3.D00*DA0)/6.D00 - (DA2/3.D00)**3
      CHECK = Q**3 + R*R
      IF(CHECK.GT.0.0) THEN
        IFLAG = 1
        P1 = R+DSQRT(CHECK)
        P2 = R-DSQRT(CHECK)
        IF(P1.LT.0.0) THEN
          SS1 = -DEXP((DLOG(-1.D00*P1))/3.D00)
        ELSE
          SS1 = DEXP((DLOG(P1))/3.D00)
        ENDIF
      IF(P2.LT.0.0) THEN
          SS2 = -DEXP((DLOG(-1.D00*P2))/3.D00)
```

```
      ELSE
       SS2 = DEXP((DLOG(P2))/3.D00)
       ENDIF
     R1 = SS1 + SS2 -DA2/3.D00
     R2 = -(SS1+SS2)-DA2/3.D00
     R3 = R2
     C1 = 0.0
     C2 = (SQRT(3.))*(SS1-SS2)/2.D00
     C3 = - C2
    ELSE IF (CHECK.LT.0.0) THEN
      IFLAG = 3
      RR = 1.*R
      RECK =1.*CHECK
    CCHECK = CMPLX(RECK,0.0)
    ES1 = CLOG(RR+CSQRT(CCHECK))/3.
    ES2 = CLOG(RR-CSQRT(CCHECK))/3.
    S1 = CEXP(ES1)
    S2 = CEXP(ES2)
    Z1 = (S1+S2) - A2/3
    Z2 = -(S1+S2)/2 - A2/3 +(CMPLX(0.0,3**.5))*(S1-S2)/2
    Z3 = -(S1+S2)/2 - A2/3 - (CMPLX(0.0,3**.5))*(S1-S2)/2
    R1 = REAL(Z1)
    R2 = REAL(Z2)
    R3 = REAL(Z3)
    C1 = 0.0
    C2 = C1
    C3 = C1
   ELSE
    IFLAG = 2
    IF(R.LT.0.0) THEN
      SS1 = -DEXP((DLOG(-1.D00*R))/3.D00)
     ELSE IF(R.EQ.0.0) THEN
      SS1 = 0.0
     ELSE
      SS1 = DEXP((DLOG(R))/3.D00)
     ENDIF
   SS2 = SS1
   R1=SS1+SS2-DA2/3.D00
   R2 = -(SS1+SS2)/2-DA2/3.D00
   R3 = R2
   C1 = 0.0
   C2 = C1
   C3 = C2
 ENDIF
RETURN
END
```

```
C   PROGRAM FOR CLUSTERING
C   ***********************************************************************
C234567
C   Program to calculate surface excess or adsorption isotherms
C
C
C   The program uses Peng-Robinson equation of state, with a modified
C   a to account for exclusion. The strength of the adsorption
C   potential and its dependence on position is given by Psi.
C   The fluid-fluid potential uff = u total - u ads.
C   From this potential the various fluid properties are calculated.
C
C
C   The variables used are defined below.
C   All units used are SI unless otherwise stated.
C
      COMMON R,TC,PC,OMEGA
C
C   Define Psi as a statement function
C   Use a 10-4 potential where PSI is the negative of the
C   intermolecular potential.
C   SIGFW is  sigma fluid-wall, in Angstroms.
C   EPSFW is the fluid-wall potential in K
C   ALPHA is the ratio of the spacing of the graphite basal planes
C   (3.35 A) to SIGFW.
C   The number density of C atoms in graphite is 0.382 atoms/A^2.
C   The equation used is that suggested by Lee (1.5).

      PSI(ETA)=4.*EPSGS*(1./ETA**6-1./ETA**12)

C   R = Gas constant J/K/mol
C   Tc = Critical Temperature K
C   Pc = Critical Pressure   N/m2
C   OMEGA = Acentric Factor
C   SIGMA = Sigma fluid-wall in m.
C   T = Temperature K
C   FLIM = Bulk fugacity limit.
C   EPSGS = Fluid-wall potential well depth in K
C   SIGFW = Sigma fluid-wall in Angstroms
C   ALPHA = Spacing of graphite planes / Sigfw
C   SIGFF = Sigma fluid-fluid in Angstroms
C   SIGWW = Sigma wall-wall in Angstroms
C   AB = Bulk Peng-Robinson 'a'
C   BB = Bulk Peng-Robinson 'b'

      WRITE(*,*)' Plim ,T,EPSILON'
      READ(*,*) PLIM,T,EPSGS

      R=8.314
      TC=282.4
      PC=50.4E5
      OMEGA=0.089
      SIGFF=4.22
```

```
      SIGWW=7.14
      SIGFW=(SIGWW+SIGFF)/2.
      SIGMA=SIGFW*1E-10

C     Write parameters to files
      OPEN(UNIT=7,FILE='denpro.dat',STATUS='UNKNOWN')
      OPEN(UNIT=8,FILE='adsorp.dat',STATUS='UNKNOWN')

      WRITE(7,*) ' Ethylene at ',T,' K with an epsilon of ',EPSGS
      WRITE(8,*) ' Ethylene at ',T,' K with an epsilon of ',EPSGS
      WRITE(8,*) 'P (Pa) Excess (micro mol/m^2) Den (mol/cc)'
      WRITE(8,*) 'Clus (# molecules solvent/molecule solute)'
      WRITE(8,997)
      WRITE(8,*)
      WRITE(8,998)
  997 FORMAT(7X,'P',9X,'EXCESS',8X,'CLUS',9X,'DEN')
  998 FORMAT(7X,'0,',10X,'0,',13X,'0,',13X,'0')

      TR=T/TC
      FOMEG=0.37464+1.54226*OMEGA-0.26992*(OMEGA**2)

C     Calculate a bulk and b
      AB=0.45724*(R*TC*(1+FOMEG*(1-SQRT(TR))))**2/PC
      BB=0.07780*R*TC/PC

      PCB=PC/1.0E5
      IF(TR.GE.1) GOTO 2
      CALL FSAT(AB,BB,T,FUGS,PS,VV,VL)

    2 DELP=PLIM/40.

C     Loop for bulk fugacity
      PB=0.0E5
      J=0

C     FOR EACH BULK FUGACITY VALUE
    5 PB=PB+DELP
      PB=PLIM
      B=BB
      A=AB

C     First calculate bulk density (DENB) and bulk pressure (BP)
      CALL BVCAL(A,B,T,PB,PS,V,FB)
      CALL PV(A,B,T,V,P)
      DENBN=1.0/V
C     In this method, we calc. the bulk density from the program
C     in which eta starts at 20.9 and comes inward. Sometimes do check
C     DENBN and DENB and make sure
      WRITE(*,*) 'BULK DENSITY = ?'
      READ(*,*) DENB
      BP=P

      WRITE(7,*)'P = ', P,' Pa',' DEN CALC = ',DENBN,' gmol/m3'
      WRITE(7,*)'DENB = ',DENB,' gmol/m3',' FB = ',FB,' Pa'
```

```
      WRITE(7,*) 'DEN (gmol/m3) PMV (cc/gmol)'
      WRITE(7,*) 'CLUS (# excess solvent molec/molec. solute)'
      WRITE(7,*) 'AMOUNT (# total solvent molec/molec. solute)'
      WRITE(7,*)
      WRITE(7,999)
  999 FORMAT(7X,'ETA',8X,'DEN',10X,'PMV',9X,'CLUS',7X,'AMOUNT')

C     Start iterating in ETA
      DELETA=0.01
      ETA=.99
      EXCESS=0.0
      CLUS=0.0
      K=0
    6 ETA=ETA+DELETA

C     Calculate local fugacity
C     Use the following formula to get the local
C     fugacity (F), for a given position ETA.
C     F=FB*EXP(PSI(ETA)/T)

      ALNFB=ALOG(FB)
      ALNF=ALNFB+PSI(ETA)/T
      PSIV=PSI(ETA)/T

C     Calculate local a
      CALL ACALC(ETA,AB,A,SIGWW,SIGFW,SIGFF)
      IF(TR.GE.1.) GO TO 20
      CALL FSAT(A,B,T,FUGS,PS,VV,VL)

C     Using local parameters calculate V and local density DENL
   20 CALL VCALC(A,B,T,ALNF,BP,PS,V)
      DENL=1.0/V
      IF((DENL/DENB.GT.0.999).AND.(DENL/DENB.LT.1.001)) THEN
        DENL=DENB
      ENDIF
      CLUS=SIGMA**3*(DENL-DENB)*4.*3.1416*ETA*ETA*DELETA*6.023E23+CLUS
      IF(K.EQ.0) THEN
        CLUS=CLUS-DENB*4./3*3.1416*SIGMA**3*6.023E23
        write(*,*) eta,clus
      ENDIF
C     AMT is the excess amount (moles) of solvent moles in the system
C     TV is the vol of the system at any given eta
C     EV is the equivalent volume in the pure system
C     TW is the vol of the solvent molecules in the actual system
C     provided they are present at bulk density

      AMT=4.*3.1416*SIGMA**3*ETA*ETA*(DENL-DENB)*DELETA+AMT
      TW=4./3.*3.1416*SIGMA**3*(ETA**3-1.)
      TV=4./3.*3.1416*(ETA*SIGMA)**3
      EV=AMT/DENB+TW
      PMV=TV-EV
      PMV=PMV*6.023E29

C     AMOUNT is the total # of solvent molecules in the system
```

```
C   TN is the total # of molecules in the pure system at any eta
C   EXCESS is the excess # of solvent molecules in the system
    AMOUNT=4.*3.1416*SIGMA**3*ETA*ETA*DENL*DELETA*6.023E23+AMOUNT
    TN=DENB*6.023E23*TV
    EXCESS=AMOUNT-TN

C   DENLG is the density in gmoles/cc
    DENLG=DENL/1.0E6

    IF((K.EQ.114).OR.(K.EQ.190)) THEN
     WRITE(*,*) ETA,AMOUNT
    ENDIF
    WRITE (7,*)ETA,',',DENL,',',PMV,',',CLUS,',',AMOUNT

    K=K+1
    IF(K.LT.2000) GOTO 6
 90 CONTINUE

    BP=P/1.0E5
    DENBG=DENB/1.E6

    WRITE(8,*)BP,',',EXCESS,',',CLUS,',',DENBG
    WRITE(6,*) BP,EXCESS,CLUS,PMV

    J=J+1
C   IF (J.LT.40) GOTO 5
100 CONTINUE

102 FORMAT(1X,F8.2,2X,F12.5,2X,F10.5)
    END

C*********************************************************************
C234567
C   SUBROUTINES
C*********************************************************************

C   Use subroutine VCALC as per flat wall program

C   Use subroutine DPDV as per flat wall program

C   Use subroutine V1CALC as per flat wall program

C   Use subroutine V3CALC as per flat wall program

C   Use subroutine PV as per flat wall program

C   Use subroutine ARANGE as per flat wall program

C   SUBROUTINE ACALC(ETA,AB,A,SIGWW,SIGFW,SIGFF)

C   This subroutine calculates the van der Waals a term
C   after taking into account the effect of exclusion.
C   AB = Value of a in the bulk
C   ETA = reduced distance from the center of wall
```

```
C   The main program sends a reduced distance ETA from the
C   center of the wall molecule, which is the basis for
C   the integrated 9-3 potential.
C   However the integrations for configurational energy have
C   been done from the edge of the wall molecule.
C   Therefore it is necessary to translate the coordinate.
C   BETA is the distance from the edge of the wall
C   in reduced units

      BETA = (ETA*(SIGFF+SIGWW)-SIGWW)/(2.*SIGFF)

      SIGMA1=SIGFF
      SIGMA2=SIGWW
      R=(SIGMA1+SIGMA2)/2.
      Z=ETA*(SIGMA1+SIGMA2)/2.
      R1=(R*R-SIGMA1*SIGMA1+Z*Z)/(2*Z)

      IF (BETA.LE.1.5) THEN
        A1=8./3.+2.*(Z-R1)/SIGMA1
        A2=SIGMA1**3/(Z*(R*R+Z*Z-2.*R1*Z))
        A3=(SIGMA1**3)/(Z*(R*R+Z*Z+2.*R*Z))
        A4=2.*SIGMA1**3/(3.*(Z+R)**3)
        A=AB*(A1+A2-A3+A4)*3./16.

      ELSE
        A1=16./3.-2.*SIGMA1**3/(3.*(Z-R)**3)
        A2=2.*SIGMA1**3/(3.*(Z+R)**3)
        A3=SIGMA1**3/(Z*(R*R+Z*Z-2.*Z*R))
        A4=SIGMA1**3/(Z*(R*R+Z*Z+2.*Z*R))
        A=AB*(A1+A2+A3-A4)*3./16.

      ENDIF

      RETURN
      END

C   Use subroutine CUBIC as per flat wall program
```

```
C       SLITS - PURE GAS
C  ***********************************************************************
C234567
C   Program to calculate surface excess or adsorption isotherms
C
C
C   The program uses Peng-Robinson equation of state, with a modified
C   a to account for exclusion.  The strength of the adsorption
C   potential and its dependence on position is given by Psi.
C   The fluid-fluid potential uff = u total - u ads.
C   From this potential the various fluid properties are calculated.
C
C
C   The variables used are defined below.
C   All units used are SI unless otherwise stated.
C
      COMMON R,TC,PC,OMEGA
C
C   Define Psi as a statement function
C   Use a 10-4 potential where PSI is the negative of the
C   intermolecular potential.
C   SIGFW is  sigma fluid-wall, in Angstroms.
C   EPSFW is the fluid-wall potential in K
C   ALPHA is the ratio of the spacing of the graphite basal planes
C   (3.35 A) to SIGFW.
C   The number density of C atoms in graphite is 0.382 atoms/A^2.
C   The equation used is that suggested by Lee (1.5).

      PSI1(ETA)=4.0*3.1415926*0.382*SIGFW*SIGFW*EPSFW*(-0.2
     1/ETA**10+0.5/ETA**4+0.5/(ETA+ALPHA)**4+0.5/(ETA+2.0*
     *ALPHA)**4+0.5/(ETA+3.0*ALPHA)**4+0.5/(ETA+4.0*ALPHA)
     ***4)

      PSI2(XI)=4.0*3.1415926*0.382*SIGFW*SIGFW*EPSFW*(-0.2
     1/XI**10+0.5/XI**4+0.5/(XI+ALPHA)**4+0.5/(XI+2.0*
     *ALPHA)**4+0.5/(XI+3.0*ALPHA)**4+0.5/(XI+4.0*ALPHA)
     ***4)

      PSI(ETA)=PSI1(ETA)+PSI2(XI)

C   R = Gas constant J/K/mol
C   Tc = Critical Temperature K
C   Pc = Critical Pressure  N/m2
C   OMEGA = Acentric Factor
C   SIGMA = Sigma fluid-wall in m.
C   T = Temperature K
C   FLIM = Bulk fugacity limit.
C   EPSFW = Fluid-wall potential well depth in K
C   SIGFW = Sigma fluid-wall in Angstroms
C   ALPHA = Spacing of graphite planes / Sigfw
C   SIGFF = Sigma fluid-fluid in Angstroms
C   SIGWW = Sigma wall-wall in Angstroms
C   AB = Bulk Peng-Robinson 'a'
```

```
C   BB = Bulk Peng-Robinson 'b'
C   ALPHA = Spacing of graphite planes / Sigfw
C   SIGFF = Sigma fluid-fluid in Angstroms

      WRITE(*,*)' Plim ,T,EPSILON, WIDTH'
      READ(*,*) PLIM,T,EPSFW,ZETA

      R=8.314
      TC=282.4
      PC=50.4E5
      OMEGA=0.089
      SIGFF=4.22
      SIGWW=3.4
      SIGFW=(SIGWW+SIGFF)/2.
      SIGMA=SIGFW*1E-10
      ALPHA=3.35/SIGFW

C   Write parameters to files
      OPEN(UNIT=7,FILE='denpro.dat',STATUS='UNKNOWN')
      OPEN(UNIT=8,FILE='adsorp.dat',STATUS='UNKNOWN')

      WRITE(7,*) ' Ethylene at ',T,' K with an epsilon of ',EPSFW
      WRITE(8,*) ' Ethylene at ',T,' K with an epsilon of ',EPSFW
      WRITE(7,*) ' with slit width of ',ZETA ,' ethylene mol dia'
      WRITE(8,*) ' with slit width of ',ZETA ,' ethylene mol dia'
      WRITE(8,*)
      WRITE(8,*)'P bar  Exc um/m2   Amt mmol/g  Amt1 mmol/g Den gmol/cc'
      WRITE(8,*)    0.',    ',   0.',    ',0.',   ',   0

      TR=T/TC
      FOMEG=0.37464+1.54226*OMEGA-0.26992*(OMEGA**2)

C   Calculate a bulk and b
      AB=0.45724*(R*TC*(1+FOMEG*(1-SQRT(TR))))**2/PC
      BB=0.07780*R*TC/PC

      PCB=PC/1.0E5
      IF(TR.GE.1) GOTO 2
      CALL FSAT(AB,BB,T,FUGS,PS,VV,VL)

2     DELP=PLIM/40.

C   Loop for bulk fugacity
      PB=0.0E5
      J=0

C   FOR EACH BULK FUGACITY VALUE
C   PB=PLIM
3     PB=PB+DELP
      B=BB
      A=AB

C   First calculate bulk density (DENB) and bulk pressure (BP)
      CALL BVCAL(A,B,T,PB,PS,V,FB)
```

```
      CALL PV(A,B,T,V,P)
      DENB=1.0/V
      BP=P
      WRITE(7,*)'P = ', P,' bar'
      WRITE(7,*)'DENB = ',DENB,' gmol/m3',' FB = ',FB,' bar'
      WRITE(7,*)
      WRITE(7,*) '   ETA',',    ',' DEN gmol/m3',',  ','Log(Fugacity)'


      BETA=0.5-(ZETA-1.)/100.
      DELETA=(ZETA-1.)/100.
      EXCESS=0.0
      AMOUNT=0.0
      AMOUNT1=0.0
      L=0
C     Start iterating in ETA

5     BETA=BETA+DELETA
      ETA=(BETA*2.*SIGFF+SIGWW)/(SIGFF+SIGWW)
      XI=(ZETA*SIGFF+SIGWW/2.-BETA*SIGFF)/SIGFW

C     Calculate local fugacity
C     Use the following formula to get the local
C     fugacity (F), for a given position ETA.
C     F=FB*EXP(PSI(ETA)/T)

      ALNFB=ALOG(FB)
      ALNF=ALNFB+PSI(ETA)/T
      PSIV=PSI(ETA)/T

C     Calculate local a
      CALL ACALC(BETA,AB,A,ZETA)

      IF(TR.GE.1.) GO TO 20
      CALL FSAT(A,B,T,FUGS,PS,VV,VL)

C     Using local parameters calculate V and local density DENL
20    CALL VCALC(A,B,T,ALNF,BP,PS,V)
      DENL=1.0/V
      EXCESS=SIGMA*(DENL-DENB)*DELETA*1.E6/2.+EXCESS
C     Amount is den(gmol/m^3)*sigma(m)*deleta*S.A.(m^2/g)
C     to convert Amount to mmol/g multiply by 1000
      AMOUNT=DENL*SIGMA*DELETA*988.*1.E3+AMOUNT

      AMOUNT1=DENL*SIGMA*DELETA*988./2.*1.E3+AMOUNT1
C     DENLG is the density in gmoles/cc
      DENLG=DENL/1.0E6
      WRITE (7,*)BETA,',',DENLG,',',ALNF

      L=L+1
      IF(L.LT.101) GOTO 5

      BP=P/1.0E5
      DENBG=DENB/1.E6
```

```
      WRITE(8,*)BP,',',EXCESS,',',AMOUNT,',',AMOUNT1,',',DENBG
      WRITE(6,*) BP,EXCESS,AMOUNT,AMOUNT1

      J=J+1
      IF(J.LT.40) GOTO 3

  102 FORMAT(1X,F8.2,2X,F12.5,2X,F10.5)
      END

C*********************************************************************
C234567
C   SUBROUTINES
C*********************************************************************

C   Use subroutine VCALC as per flat wall program

C   Use subroutine DPDV as per flat wall program

C   Use subroutine V1CALC as per flat wall program

C   Use subroutine V3CALC as per flat wall program

C   Use subroutine PV as per flat wall program

C   Use subroutine ARANGE as per flat wall program

C234567
      SUBROUTINE ACALC(BETA,AB,A,ZETA)

C     This subroutine calculates the van der Waals a term
C     after taking into account the effect of exclusion.
C     AB = Value of a in the bulk
C     ETA = reduced distance from the center of wall
C     The main program sends a reduced distance ETA from the
C     center of the wall molecule, which is the basis for
C     the integrated 9-3 potential.
C     However the integrations for configurational energy have
C     been done from the edge of the wall molecule.
C     Therefore it is necessary to translate the coordinate.
C     BETA is the distance from the edge of the wall
C     in reduced units

      SA=ZETA-0.5-BETA

      IF (BETA.LE.1.5) THEN
        A1=BETA+0.5
        A2=1.-1./SA**3
        A3=1./3.*A2
        A=AB*(A1+A3)*3./8.
      END IF

      IF(BETA.GT.(ZETA-1.5)) THEN
        A1=SA+1.
        A2=1.-1./(BETA-0.5)**3
```

```
      A3=A2/3.
      A=AB*(A1+A3)*3./8.
    END IF

    IF((BETA.GT.1.5).AND.(BETA.LE.(ZETA-1.5))) THEN
      A1=7./3.-1./3./(BETA-0.5)**3
      A2=1.-1./SA**3
      A3=A2/3.
      A=AB*(A1+A3)*3./8.
    END IF

    RETURN
    END

C   Use subroutine CUBIC as per flat wall program
```

```
C       PORE -PURE GAS
C     ******************************************************************
C234567
C     Program to calculate surface excess or adsorption isotherms
C
C
C     The program uses Peng-Robinson equation of state, with a modified
C     a to account for exclusion.  The strength of the adsorption
C     potential and its dependence on position is given by Psi.
C     The fluid-fluid potential uff = u total - u ads.
C     From this potential the various fluid properties are calculated.
C
C
C     The variables used are defined below.
C     All units used are SI unless otherwise stated.
C
      DIMENSION H90(30000),H91(30000),H92(30000),H93(30000),H94(30000)
      DIMENSION H3(30000),H31(30000),H32(30000),H33(30000),H34(30000)
      DIMENSION AC(30000),RHO(30000),DIST(30000)
      REAL TC,PC,R,PLIM,AB,A,BB,B,T,OMEGA,DELP

      COMMON R,TC,PC,OMEGA,AC

      PSI(ETA)=0.382*3.14159*3.14159*SIGFW*SIGFW*EPSFW*(3.*SIGFW**4*
     1(H3(K)*(RFW/(RFW*RFW-ETA*ETA*SIGMA*SIGMA))**4+H31(K)*((RFW+ALPHA)
     */((RFW+ALPHA)**2-ETA*ETA*SIGMA*SIGMA))**4+H32(K)*((RFW+
     *2.*ALPHA)/((RFW+2.*ALPHA)**2-ETA*ETA*SIGMA*SIGMA))**4+H33(K)
     **((RFW+3.*ALPHA)/((RFW+3.*ALPHA)**2-ETA*ETA*SIGMA*SIGMA))**4+
     *H34(K)*((RFW+4.*ALPHA)/((RFW+4.*ALPHA)**2-ETA*ETA*SIGMA*SIGMA))
     ***4)-63./32.*SIGFW**10*(H90(K)*(RFW/(RFW*RFW-ETA*ETA*SIGMA*SIGMA))
     ***10+H91(K)*((RFW+ALPHA)/((RFW+ALPHA)**2-ETA*ETA*SIGMA*SIGMA))
     ***10+H92(K)*((RFW+2.*ALPHA)/((RFW+2.*ALPHA)**2-ETA*ETA*SIGMA*
     *SIGMA))**10+H93(K)*((RFW+3.*ALPHA)/((RFW+3.*ALPHA)**2-ETA*ETA
     **SIGMA*SIGMA))**10+H94(K)*((RFW+4.*ALPHA)/((RFW+4.*ALPHA)**2-
     *ETA*ETA*SIGMA*SIGMA))**10))

      DO 10 I=1,81,1
        OPEN(UNIT=2,FILE='hyper5-9.dat',STATUS='UNKNOWN')
        READ(2,*) ET,F0,F1,F2,F3,F4
C     WRITE(*,*) ETA1
        J=ET*1000
        H90(J)=F0
        H91(J)=F1
        H92(J)=F2
        H93(J)=F3
        H94(J)=F4
C     WRITE(*,*) J,ET,H90(J),H91(J),H92(J),H93(J)
 10   CONTINUE

      DO 15 M=1,81,1
        OPEN(UNIT=4,FILE='hyper5-3.dat',STATUS='UNKNOWN')
        READ(4,*) ETA1,G0,G1,G2,G3,G4
        J=ETA1*1000
```

```
      H31(J)=G1
      H32(J)=G2
      H33(J)=G3
      H3(J)=G0
      H34(J)=G4
C     WRITE(*,*) J,ETA1,H3(J),H31(J),H32(J),H33(J)
 15   CONTINUE

      DO 6 MA=1,81,1
        OPEN(UNIT=3,FILE='ethdia5.dat',STATUS='UNKNOWN')
        READ(3,*) ETA1,ANEW
        J=ETA1*1000
        AC(J)=ANEW
C       WRITE(*,*) J,ETA1,AC(J)
 6    CONTINUE
C     write(*,*) AC(0)

C     R = Gas constant J/K/mol
C     Tc = Critical Temperature K
C     Pc = Critical Pressure   N/m2
C     OMEGA = Acentric Factor
C     SIGMA = Sigma fluid-wall in m.
C     T = Temperature K
C     FLIM = Bulk fugacity limit.
C     EPSFW = Fluid-wall potential well depth in K
C     SIGFW = Sigma fluid-wall in Angstroms
C     ALPHA = Spacing of graphite planes / Sigfw
C     SIGFF = Sigma fluid-fluid in Angstroms
C     SIGWW = Sigma wall-wall in Angstroms
C     AB = Bulk Peng-Robinson 'a'
C     BB = Bulk Peng-Robinson 'b'
C     ALPHA = Spacing of graphite planes / Sigfw
C     SIGFF = Sigma fluid-fluid in Angstroms

      WRITE(*,*)' Plim ,T,EPSILON'
      READ(*,*) PLIM,T,EPSFW

      R=8.314
      TC=282.4
      PC=50.4E5
      OMEGA=0.089
      SIGMA=4.22
      SIGWW=3.4
      ALPHA=3.35
      RFW=12.25
      SIGFW=(SIGWW+SIGMA)/2.
      SIGGS=SIGMA*1E-10

C     Write parameters to files
      OPEN(UNIT=7,FILE='denpro.dat',STATUS='UNKNOWN')
      OPEN(UNIT=8,FILE='adsorp.dat',STATUS='UNKNOWN')

      WRITE(7,*) ' Ethylene at ',T,' K with an epsilon of ',EPSFW
      WRITE(8,*) ' Ethylene at ',T,' K with an epsilon of ',EPSFW
```

```
      WRITE(8,*)' RFW is ',RFW, ' angstroms ', 'R is RFW - 1.7'
      WRITE(8,*)
      WRITE(8,*)'  P bar',',  ','Excess um/m2',',  ','Den moles/cc'
      WRITE(8,*)    0,',     ',   0,',     ',   0

      TR=T/TC
      FOMEG=0.37464+1.54226*OMEGA-0.26992*(OMEGA**2)

C     Calculate a bulk and b
      AB=0.45724*(R*TC*(1+FOMEG*(1-SQRT(TR))))**2/PC
      BB=0.07780*R*TC/PC

      PCB=PC/1.0E5
      IF(TR.GE.1) GOTO 2
      CALL FSAT(AB,BB,T,FUGS,PS,VV,VL)

 2    DELP=PLIM/40.

C     Loop for bulk fugacity
      PB=0.0E5
      J=0

C     FOR EACH BULK FUGACITY VALUE
 3    PB=PB+DELP
C     PB=PLIM
      B=BB
      A=AB

C     First calculate bulk density (DENB) and bulk pressure (BP)
      CALL BVCAL(A,B,T,PB,PS,V,FB)
      CALL PV(A,B,T,V,P)
      DENB=1.0/V
      BP=P
      WRITE(7,*)'P = ', P,' bar'
      WRITE(7,*)'DENB = ',DENB,' gmol/m3',' FB = ',FB,' bar'
      WRITE(7,*)
      WRITE(7,*) '   ETA',',    ',' DEN gmol/m3',',  ','Log(Fugacity)'

C     Start iterating in ETA
      DELETA=0.025
      ETA=2.025
      EXCESS=0.0
      AMOUNT=0.0
      AMOUNT1=0.0
      KDEL=25
      K=2025
      L=0
 5    ETA=ETA-DELETA
      K=K-KDEL

C     Calculate local fugacity
C     Use the following formula to get the local
C     fugacity (F), for a given position ETA.
C     F=FB*EXP(PSI(ETA)/T)
```

```
      ALNFB=ALOG(FB)
      ALNF=ALNFB+PSI(ETA)/T
      PSIV=PSI(ETA)/T

C     Calculate local a
C       WRITE(*,*)K,H3(K),H31(K),H32(K),H33(K)
C       WRITE(*,*)K,H90(K),H91(K),H92(K),H93(K),PSI(ETA)
C       WRITE(*,*) K, AC(K)
      AC(0)=0.9262953
      CALL ACALC(ETA,K,AB,A)

      IF(TR.GE.1.) GO TO 20
      CALL FSAT(A,B,T,FUGS,PS,VV,VL)

C     Using local parameters calculate V and local density DENL
 20   CALL VCALC(A,B,T,ALNF,BP,PS,V)
      DENL=1.0/V
C-----------------------------------------------------------------
C     Using Rectangular Rule:
      EXCESS=SIGGS*(DENL-DENB)*DELETA*1.E6+EXCESS
C     Amount is den*r*dr*2 Pi L; 2 Pi L = 988/Pore Radius.
C     Amt.=denl*siggs*eta*siggs*deleta*988/(2.5*siggs) [mmol/g]
      AMOUNT=SIGGS*DENL*ETA*DELETA*988/2.5*1.e3+AMOUNT
C-----------------------------------------------------------------
      RHO(L)=DENL
      DIST(L)=ETA

C     DENLG is the density in gmoles/cc
      DENLG=DENL/1.0E6
      WRITE (7,*)ETA,',',DENL,',',ALNF

      L=L+1
      IF(L.LT.81) GOTO 5

      CALL SIMP(RHO,DIST,EX1,AMT1,L,DENB,SIGGS,A3)

      BP=P/1.0E5
      DENBG=DENB/1.E6
      WRITE(8,*)  BP, ',', EX1, ',',AMT1,',',DENBG
      WRITE(6,*)  BP, ',', EXCESS, ',',AMOUNT,',',DENBG
      WRITE(6,*) BP, ',',EX1, ',', AMT1,A3
      J=J+1
      IF (J.LT.40) GOTO 3


 102  FORMAT(1X,F8.2,2X,F12.5,2X,F10.5)
      END

C*********************************************************************
C234567
C     SUBROUTINES
C*********************************************************************
C     THIS IS A SIMPSON'S RULE SUBROUTINE
```

```
      SUBROUTINE SIMP(RHO,DIST,EX1,AMT1,L,DENB,SIGGS,A3)
      DIMENSION RHO(30000),DIST(30000)

      E1=0
      A1=0
      E2=0
      A2=0

      DO 250 I=0,L-1
        A3=A3+SIGGS*RHO(I)*DIST(I)*0.025*988./2.5*1.E3
        E3=E3+SIGGS*(RHO(I)-DENB)*0.025*1.E6
  250 CONTINUE

      DO 200 I=1,L-2,2
        E1=E1+(RHO(I)-DENB)
        A1=A1+RHO(I)*(DIST(I)*SIGGS)
  200 CONTINUE

      DO 225 I=2,L-3,2
        E2=E2+(RHO(I)-DENB)
        A2=A2+RHO(I)*(DIST(I)*SIGGS)
  225 CONTINUE

      EX1=RHO(0)-DENB+RHO(L-1)-DENB+4.*E1+2.*E2
      EX1=0.025*SIGGS/3.*EX1*1.E6
      AMT1=0.025/3.*(DIST(L-1)*SIGGS*RHO(L-1)+4.*A1+2.*A2)
      AMT1=988./2.5*AMT1*1.E3
      RETURN
      END

C     Use subroutine VCALC as per flat wall program

C     Use subroutine DPDV as per flat wall program

C     Use subroutine V1CALC as per flat wall program

C     Use subroutine V3CALC as per flat wall program

C     Use subroutine PV as per flat wall program

C     Use subroutine ARANGE as per flat wall program

      SUBROUTINE ACALC(ETA,K,AB,A)

C     This subroutine calculates the van der Waals a term
C     after taking into account the effect of exclusion.
C     AB = Value of a in the bulk
C     ETA = reduced distance from the center of wall
C     The main program sends a reduced distance ETA from the
C     center of the wall molecule, which is the basis for
C     the integrated 9-3 potential.

      DIMENSION AC(30000)
```

```
      COMMON R,TC,PC,OMEGA,AC
      A=AB*AC(K)

      IF (AC(K).EQ.0.0) THEN
        K1=INT(K/100)
        K2=K1*100
        AK2=FLOAT(K/100.-K1)
        K3=(K1+1)*100
        AC(K) = AC(K2)+(AC(K3)-AC(K2))*AK2
        WRITE(*,*) K,K1,K2,AK2,K3,AC(K)
        A=AB*AC(K)
      ENDIF

      RETURN
      END

C     Use subroutine CUBIC as per flat wall program
```

```
C    PROGRAM FOR BINARY MIXTURES on SLITS

C     Define Psi as a statement function
C     Use a 10-4 potential where PSI is the negative of the
C     intermolecular potential.
C     SIGGS1 and SIGGS2 are  sigma fluid-wall for components 1 & 2, in Angstroms.
C     EPSGS1 & 2 are the fluid-wall potential in K
C     EXC1 & 2 are the excess in micro mol/m^2
C     AMT1 & 2 are the amount adsorbed in mmol/g
C     Y1 & 2 are the compositions of the two components in the adsorbed phase
C     P1 & 2 are the fugacity coefficients for the two components
C     F1 & 2 are the fugacities
C     p is the pressure in Mpa
C     TC, PC and W represent the critical temperature, pressure and omega's

*    This program is to calculate the adsorption in a mixture
      REAL K12
     CHARACTER RFILE*80


     PSI1(ETA)=4.0*3.1415926*0.382*SIGGS1*SIGGS1*EPSGS1*(-0.2
     1/ETA**10+0.5/ETA**4+0.5/(ETA+ALPHA)**4+0.5/(ETA+2.0*
     *ALPHA)**4+0.5/(ETA+3.0*ALPHA)**4+0.5/(ETA+4.0*ALPHA)
     ***4)

     PSI2(ETA)=4.0*3.1415926*0.382*SIGGS2*SIGGS2*EPSGS2*(-0.2
     1/ETA**10+0.5/ETA**4+0.5/(ETA+ALPHA)**4+0.5/(ETA+2.0*
     *ALPHA)**4+0.5/(ETA+3.0*ALPHA)**4+0.5/(ETA+4.0*ALPHA)
     ***4)

     PSI3(XI)=4.0*3.1415926*0.382*SIGGS1*SIGGS1*EPSGS1*(-0.2
     1/XI**10+0.5/XI**4+0.5/(XI+ALPHA)**4+0.5/(XI+2.0*
     *ALPHA)**4+0.5/(XI+3.0*ALPHA)**4+0.5/(XI+4.0*ALPHA)
     ***4)

     PSI4(XI)=4.0*3.1415926*0.382*SIGGS2*SIGGS2*EPSGS2*(-0.2
     1/XI**10+0.5/XI**4+0.5/(XI+ALPHA)**4+0.5/(XI+2.0*
     *ALPHA)**4+0.5/(XI+3.0*ALPHA)**4+0.5/(XI+4.0*ALPHA)
     ***4)

     PSIA(ETA)=PSI1(ETA)+PSI3(XI)
     PSIB(ETA)=PSI2(ETA)+PSI4(XI)


     SIGGS1=4.0
     SIGGS2=4.0
     ALPHA=3.35/SIGGS1


     R = 8.314

     TC2=282.4
     PC2=5.04
     W2=0.089
```

```
      TC1=364.9
      PC1=5.49
      W1=0.13
      K12=0

      PC2 = 1000000*PC2
      PC1 = 1000000*PC1
    2  PRINT*, 'ENTER T(K), P(MPA),EPS1, EPS2, WIDTH'
      READ*, T,P,EPSGS1,EPSGS2,ZETA
      P=1000000*P
    3  PRINT*, 'ENTER Y1'
      READ*, Y1
      EXC1=0.0
      EXC2=0.0
      AMT1=0.0
      AMT2=0.0
      TYPE'(X,A,$)','ENTER THE FILE NAME FOR RESULTS :'
      ACCEPT'(A)',RFILE
      OPEN(UNIT=2,NAME=RFILE,TYPE='UNKNOWN')

      Y2 = 1-Y1
      Y1IN = Y1
      Y2IN = Y2

      DDY1 = 1E-5
      DDY2 = 1E-5

      TR1 = T/TC1
      TR2 = T/TC2


* SET DELTA P FOR PARTIAL DERIVATIVES
C     DDP=.01*P

* CALCULATE COMPRESSIBILITY FACTOR (Z)
* CALCULATE A1,A2, THEN A

      CALL ACALC(R,W1,TC1,TR1,PC1,A11)
      CALL ACALC(R,W2,TC2,TR2,PC2,A22)
      CALL BCALC(B1,TC1,PC1,R)
      CALL BCALC(B2,TC2,PC2,R)
      A12 = SQRT(A11*A22)*(1-K12)
      CALL AMIX(Y1IN,Y2IN,A11,A22,A12,A)
      CALL ASTAR(A11,A22,A12,A,AS1,AS2,AS12,AS,P,R,T)
      CALL BMIX(Y1IN,Y2IN,B1,B2,B)
      CALL BSTAR(B1,B2,B,BS1,BS2,BS,P,R,T)

      CALL SCUBIC(AS,BS,R1,R2,R3,IFLAG)
      IF(IFLAG.EQ.1) Z=R1
      IF(IFLAG.EQ.2) THEN
        Z=R1
        IF(R2.GT.R1) Z=R2
      END IF
      IF(IFLAG.EQ.3) THEN
```

```
      CALL ARANGE(R1,R2,R3)
       Z=R1
     END IF

     CALL PH(Y1IN,Y2IN,AS1,AS12,AS2,AS,BS1,BS2,BS,Z,P1,P2)
C    WRITE(*,*) 'A & B star ',AS,BS,'FUG',P1,P2

     DENB=P/Z/R/T
     PBULK=P/1000000

     WRITE(2,*) 'T =',T,' K','P =', PBULK,' MPa'
     WRITE(2,*) 'BULK DEN =', DENB,' gmol/m^3',' Width = ',ZETA
     WRITE(2,*)'Epsilon 1 & 2 =', EPSGS1,EPSGS2
     WRITE(2,*) 'inital mol. frac. Y1 = ',Y1,' Y2 = ', Y2

     F1BULK=Y1IN*P1*P
     F2BULK=Y2IN*P2*P
     PETA=P
C-------------Start iterating in ETA-----------------------------------

     BETA=ZETA/2.+(ZETA/2.-0.5)/100.
     DELETA=(ZETA/2.-0.5)/100.
     L=0
     WRITE (2,102)

 5   BETA=BETA-DELETA
     ETA=(BETA*2.*SIGFF+SIGWW)/(SIGFF+SIGWW)
     XI=(ZETA*SIGFF+SIGWW/2.-BETA*SIGFF)/SIGGS1

*    SET DELTA P FOR PARTIAL DERIVATIVES
     DDP=.01*PETA

     GOLD=1E5
     K=0
     H = 0

     CALL AZCALC(BETA,A11,A1,ZETA)
     CALL AZCALC(BETA,A22,A2,ZETA)
     A12 = SQRT(A1*A2)*(1-K12)


     F1 = F1BULK*EXP(PSIA(ETA)/T)
     F2 = F2BULK*EXP(PSIB(ETA)/T)
     P=F1/P1+F2/P2
C    WRITE(*,*) 'F1,F2,P',F1,F2,P

 10  CALL AMIX(Y1,Y2,A1,A2,A12,A)

C    WRITE(*,*) 'A=', A
     CALL ASTAR(A1,A2,A12,A,AS1,AS2,AS12,AS,P,R,T)

     CALL BMIX(Y1,Y2,B1,B2,B)
C    WRITE(*,*) 'B=', B
```

```
      CALL BSTAR(B1,B2,B,BS1,BS2,BS,P,R,T)
      CALL SCUBIC(AS,BS,R1,R2,R3,IFLAG)
      IF(IFLAG.EQ.1) THEN
        Z1=R1
        CALL PH(Y1,Y2,AS1,AS12,AS2,AS,BS1,BS2,BS,Z1,P1,P2)
*     CALCULATE OBJECTIVE FUNCTIONS
        G1 = Y1*P1*P/F1-1
        G2 = Y2*P2*P/F2-1
        G3 = 1 - Y1 - Y2
        G0=SQRT(G1*G1+ G2*G2 + G3*G3)
        NROOT=1
        GOTO 25
      ENDIF

      IF(IFLAG.EQ.2) THEN
        Z1=R1
        Z2=R2
        IF(R2.GT.R1) THEN
          Z1=R2
          Z2=R1
        ENDIF
      ENDIF

      IF(IFLAG.EQ.3) THEN
        CALL ARANGE(R1,R2,R3)
        Z1=R1
        Z2=R3
      ENDIF

      CALL PH(Y1,Y2,AS1,AS12,AS2,AS,BS1,BS2,BS,Z1,P1A,P2A)

*     CALCULATE OBJECTIVE FUNCTIONS
      G1A = Y1*P1A*P/F1-1
      G2A = Y2*P2A*P/F2-1
      G3A = 1 - Y1 - Y2
      G0A=SQRT(G1A*G1A+ G2A*G2A+ G3A*G3A)
C     WRITE(*,*)'G1A,G2A',G1A,G2A

      G0=G0A
      G1=G1A
      G2=G2A
      G3=G3A
      Z=Z1
      P1=P1A
      P2=P2A
      NROOT=1
      IF(Z2.LT.BS) THEN
C     PRINT*, 'SKIPPING Z2'
        GOTO 25
      ENDIF
      CALL PH(Y1,Y2,AS1,AS12,AS2,AS,BS1,BS2,BS,Z2,P1B,P2B)

*     CALCULATE OBJECTIVE FUNCTIONS
      G1B = Y1*P1B*P/F1-1
```

```
      G2B = Y2*P2B*P/F2-1
      G3B = 1 - Y1 - Y2
      G0B=SQRT(G1B*G1B + G2B*G2B + G3B*G3B)

      IF(G0A.GT.G0B) THEN
        G0=G0B
        G1=G1B
        G2=G2B
        G3=G3B
        Z=Z2
        P1=P1B
        P2=P2B
        NROOT=2
      ENDIF
   25 CONTINUE
      PRINT*,'G0=',G0A,G0B,'NROOT=',NROOT,'IFG=',IFLAG

      F1CALC=Y1*P1*P
      F2CALC=Y2*P2*P
      YT=Y1+Y2
C     WRITE(*,*) F1CALC,F1,P
C     WRITE(*,*) F2CALC,F2,H
C     PRINT*, 'ETA,Y1',ETA,Y2
      IF (K.LT.5.AND.GOLD.LT.G0) THEN
        K=K+1
        Y1=Y1-DY1
        Y2=Y2-DY2
        P=P-DP
        DY1 = DY1/2
        DY2 = DY2/2
        DP = DP/2
        GOTO 100
      END IF
      K=0
      GOLD=G0
 9999 FORMAT(4G15.5,1X,I3)

C     IF(G0.LT.2E-2) THEN
      IF(G0.LT.1E-3) THEN
C     WRITE (*,*) 'Bubble Pressure Calculation'
C     WRITE (*,101)
C     WRITE (*,103) X1,X2,T

        DEN=P/Z/8.314/T
        PETA=P
        EXC1=SIGGS1*(Y1*DEN-Y1IN*DENB)*DELETA*1.E-4+EXC1
        AMT1=Y1*DEN*SIGGS1*DELETA*988.*1.E-7+AMT1

        EXC2=SIGGS1*(Y2*DEN-Y2IN*DENB)*DELETA*1.E-4+EXC2
        AMT2=Y2*DEN*SIGGS1*DELETA*988.*1.E-7+AMT2

        WRITE (*,104) Y1,DEN,P,BETA,H
        WRITE (2,104) Y1,DEN,P,BETA,H
  101   FORMAT(10X,'X1',10X,'X2',10X,'T-K')
```

```
102   FORMAT(4X,'Y1',7X,'DEN',9X,'PRESS',9X,'ETA',8X,'# ITER')
104   FORMAT(F8.5,2X,2G12.5,2X,G12.5,2X,F5.1)
      GO TO 200
     ENDIF

     YY1 = Y1 + DDY1
     YY2 = Y2 + DDY2
     PP = P + DDP

*    CALCULATE DERIVATIVES WRT P
     CALL ASTAR(A1,A2,A12,A,AS1,AS2,AS12,AS,PP,R,T)
     CALL BSTAR(B1,B2,B,BS1,BS2,BS,PP,R,T)
     CALL SCUBIC(AS,BS,R1,R2,R3,IFLAG)

     IF(IFLAG.EQ.1) THEN
       Z=R1
       CALL PH(Y1,Y2,AS1,AS12,AS2,AS,BS1,BS2,BS,Z,PN1,PN2)
       GOTO 30
     ENDIF

     IF(IFLAG.EQ.2) THEN
       BIG=R1
       SMALL=R2
       IF(R1.LT.R2) THEN
         BIG=R2
         SMALL=R1
       ENDIF
       R1=BIG
       R3=SMALL
     ENDIF
     IF(IFLAG.EQ.3) THEN
       CALL ARANGE(R1,R2,R3)
     ENDIF

     IF(NROOT.EQ.1) THEN
       Z=R1
       CALL PH(Y1,Y2,AS1,AS12,AS2,AS,BS1,BS2,BS,Z,PN1,PN2)
     ELSE

       Z=R3
       CALL PH(Y1,Y2,AS1,AS12,AS2,AS,BS1,BS2,BS,Z,PN1,PN2)
     ENDIF

30   D1DP = (Y1*PN1*PP-Y1*P1*P)/DDP/F1
     D2DP = (Y2*PN2*PP-Y2*P2*P)/DDP/F2
     D3DP = 0

*    CALCULATE DERIVATIVES WRT Y1

     CALL AMIX(YY1,Y2,A1,A2,A12,A)
     CALL BMIX(YY1,Y2,B1,B2,BV)
     CALL ASTAR(A1,A2,A12,A,AS1,AS2,AS12,AS,P,R,T)
     CALL BSTAR(B1,B2,B,BS1,BS2,BS,P,R,T)
     CALL SCUBIC(AS,BS,R1,R2,R3,IFLAG)
```

```
      IF(IFLAG.EQ.1) THEN
        Z=R1
        CALL PH(YY1,Y2,AS1,AS12,AS2,AS,BS1,BS2,BS,Z,PN1,PN2)
        GOTO 40
      ENDIF

      IF(IFLAG.EQ.2) THEN
        BIG=R1
        SMALL=R2
        IF(R1.LT.R2) THEN
          BIG=R2
          SMALL=R1
        ENDIF
        R1=BIG
        R3=SMALL
      ENDIF
      IF(IFLAG.EQ.3) THEN
        CALL ARANGE(R1,R2,R3)
      ENDIF

      IF(NROOT.EQ.1) THEN
        Z=R1
        CALL PH(YY1,Y2,AS1,AS12,AS2,AS,BS1,BS2,BS,Z,PN1,PN2)
      ELSE
        Z=R3
        CALL PH(YY1,Y2,AS1,AS12,AS2,AS,BS1,BS2,BS,Z,PN1,PN2)
      ENDIF

   40 D1D1 = (PN1*YY1*P-P1*Y1*P)/DDY1/F1
      D2D1 = (PN2*Y2*P-P2*Y2*P)/DDY1/F2
      D3D1 = -1

*     CALCULATE DERIVATIVES WRT Y2

      CALL AMIX(Y1,YY2,A1,A2,A12,A)
      CALL BMIX(Y1,YY2,B1,B2,B)
      CALL ASTAR(A1,A2,A12,A,AS1,AS2,AS12,AS,P,R,T)
      CALL BSTAR(B1,B2,B,BS1,BS2,BS,P,R,T)
      CALL SCUBIC(AS,BS,R1,R2,R3,IFLAG)

      IF(IFLAG.EQ.1) THEN
        Z=R1
        CALL PH(Y1,YY2,AS1,AS12,AS2,AS,BS1,BS2,BS,Z,PN1,PN2)
        GOTO 50
      ENDIF

      IF(IFLAG.EQ.2) THEN
        BIG=R1
        SMALL=R2
        IF(R1.LT.R2) THEN
          BIG=R2
          SMALL=R1
        ENDIF
        R1=BIG
```

```
      R3=SMALL
    ENDIF

    IF(IFLAG.EQ.3) THEN
      CALL ARANGE(R1,R2,R3)
    ENDIF

    IF(NROOT.EQ.1) THEN
      Z=R1
      CALL PH(Y1,YY2,AS1,AS12,AS2,AS,BS1,BS2,BS,Z,PN1,PN2)
    ELSE
      Z=R3
      CALL PH(Y1,YY2,AS1,AS12,AS2,AS,BS1,BS2,BS,Z,PN1,PN2)
    ENDIF


 50 D1D2 = (PN1*Y1*P-P1*Y1*P)/DDY2/F1
    D2D2 = (PN2*YY2*P-P2*Y2*P)/DDY2/F2
    D3D2 = -1

*   CALCULATE INCREMENTS

    CALL INV(D1DP,D2DP,D3DP,D1D1,D2D1,D3D1,D1D2,D2D2,D3D2,DET)

    DY1 = -G1*D1D1 - G2*D1D2 - G3*D1DP
    DY2 = -G1*D2D1 - G2*D2D2 - G3*D2DP
    DP = -G1*D3D1 - G2*D3D2 - G3*D3DP
    PRINT*, ETA,Y1,DY1,P,DP
    IF(ABS(DY1).GT.Y1) THEN
      PRINT*,'WARNING, LARGE DY',DY1
      DY1=0.5*Y1*DY1/ABS(DY1)
      DY2=-DY1
C   P=9.E7
C   DP=0
    END IF
100 Y1 = Y1 + DY1
    Y2 = Y2 + DY2
    P = P + DP
    IF(Y1.LT.0)Y1=0
    IF(Y1.GT.1)Y1=1.
    IF(Y2.LT.0)Y2=0
    IF(Y2.GT.1)Y2=1.

    H = H +1
    IF (H.LT.200) GO TO 10
    PRINT*, 'ITERATIONS EXCEEDED'
C   DDY1=1E-3
C   DDY2=1E-3
C   DDP=.01*P
C   GOTO 10
200 CONTINUE
    L=L+1
    IF(L.LT.101) GOTO 5
    WRITE(*,*) EXC1,EXC2,DENB,AMT1,AMT2
```

```
      WRITE(2,*) EXC1,',',EXC2,',',DENB
      WRITE(2,*) AMT1,',',AMT2

      PRINT*, 'ENTER 1 FOR SAME T, DIFFERENT X1'
      PRINT*, 'ENTER 2 FOR NEW T AND NEW X1'
      PRINT*, 'ENTER 0 TO QUIT'
      READ*, IDB
      IF (IDB.EQ.1) GO TO 3
      IF (IDB.EQ.2) GO TO 2
      END
*************************************************************************
* SUBROUTINES BELOW !!!!

      SUBROUTINE ACALC(R,W,TC,TR,PC,AN)
        FW = 0.37464 + 1.54226*W - .26992 * W**2
        AN = 0.45724*R**2*TC**2*(1+FW*(1-SQRT(TR)))**2/PC
      RETURN
      END

      SUBROUTINE AMIX(M1,M2,A1,A2,A12,AA)
      REAL AA, A1, A2, A12, M1, M2
        AA = M1**2*A1 + 2*M1*M2*A12 + M2**2 * A2
      RETURN
      END

      SUBROUTINE ASTAR(A1,A2,A12,A,AS1,AS2,AS12,AS,P,R,T)
        AS1 = A1*P/(R**2*T**2)
        AS2 = A2*P/(R**2*T**2)
        AS12 = A12*P/(R**2*T**2)
        AS = A*P/(R**2*T**2)
      RETURN
      END
C-------------------------------------------------------------------------
      SUBROUTINE BCALC(B,TC,PC,R)
        B = 0.07780*R*TC/PC
      RETURN
      END

      SUBROUTINE BMIX(M1,M2,B1,B2,BB)
      REAL BB, B1, B2, M1, M2
        BB = M1*B1 + M2*B2
      RETURN
      END

      SUBROUTINE BSTAR(B1,B2,B,BS1,BS2,BS,P,R,T)
        BS1 = B1*P/(R*T)
        BS2 = B2*P/(R*T)
        BS = B*P/(R*T)
      RETURN
      END
C-------------------------------------------------------------------------
      SUBROUTINE TM2(BS,T2)
        T2 = BS - 1
*      WRITE (*,*) T2
```

```
      RETURN
      END

      SUBROUTINE TM1(AS,BS,T1)
        T1 = AS - BS*(2+3*BS)
*       WRITE (*,*) T1
      RETURN
      END

      SUBROUTINE TM0(AS,BS,T0)
        T0 = BS*(BS**2 + BS - AS)
*       WRITE(*,*) T0
      RETURN
      END
C-----------------------------------------------------------------------
      SUBROUTINE PH(M1,M2,AS1,AS12,AS2,AS,BS1,BS2,BS,Z,P1,P2)
      REAL M1,M2
        Q = M1*AS1 + M2*AS12
        CALL PHICLC(BS1,AS,BS,Z,Q,P1)
        Q = M1*AS12 + M2*AS2
        CALL PHICLC(BS2,AS,BS,Z,Q,P2)
      RETURN
      END

C-----------------------------------------------------------------------
      SUBROUTINE PHICLC(B,AS,BS,Z,Q,PHI)
        TERM1 = (B/BS)*(Z-1)

        TERM1A = (2*Q/AS) - (B/BS)
        TERM1B = 2*Q/AS
        TERM2 = (2*Q/AS - B/BS)*(AS/(2*SQRT(2.0)*BS))

        TERM3 = 1/(Z-BS)

        TERM4 = ((Z-(SQRT(2.0)-1)*BS)/(Z+(SQRT(2.0)+1)*BS))
*       WRITE(*,*) BS, TERM1A, TERM1B
*       WRITE(*,*) TERM2, TERM3, TERM4

        PHI = TERM3*(TERM4**TERM2)*EXP(TERM1)
      RETURN
      END

C-----------------------------------------------------------------------
      SUBROUTINE SCUBIC(AS,BS,R1,R2,R3,IFLAG)
        CALL TM2(BS,T2)
        CALL TM1(AS,BS,T1)
        CALL TM0(AS,BS,T0)
*       WRITE (*,*) T2,T1,T0
        CALL CUBIC(T2,T1,T0,R1,R2,R3,C1,C2,C3,IFLAG)
*       WRITE(*,*) IFLAG
*       WRITE(*,*) 'R1  R2   R3'
*       WRITE(*,*) R1,R2,R3
      RETURN
      END
```

```
C-------------------------------------------------------------------------
      SUBROUTINE ARANGE(R1,R2,R3)

C     PROGRAM TO PUT 3 NUMBERS IN DESCENDING ORDER

      DO 20 J=1,3

       IF(R2.GT.R1) THEN
         TEMP=R1
         R1=R2
         R2=TEMP
       ENDIF

       IF(R3.GT.R2) THEN
         TEMP=R2
         R2=R3
         R3=TEMP
       ENDIF

 20     CONTINUE

      RETURN
      END
C-------------------------------------------------------------------------
       SUBROUTINE  AZCALC(BETA,AB,A,ZETA)

       SA=ZETA-0.5-BETA

       IF (BETA.LE.1.5) THEN
         A1=BETA+0.5
         A2=1.-1./SA**3
         A3=1./3.*A2
         A=AB*(A1+A3)*3./8.
       END IF

       IF(BETA.GT.(ZETA-1.5)) THEN
         A1=SA+1.
         A2=1.-1./(BETA-0.5)**3
         A3=A2/3.
         A=AB*(A1+A3)*3./8.
       END IF

       IF((BETA.GT.1.5).AND.(BETA.LE.(ZETA-1.5))) THEN
         A1=7./3.-1./3./(BETA-0.5)**3
         A2=1.-1./SA**3
         A3=A2/3.
         A=AB*(A1+A3)*3./8.
       END IF

       RETURN
       END

C-------------------------------------------------------------------------
```

```
      SUBROUTINE INV(D1DP,D2DP,D3DP,D1D1,D2D1,D3D1,D1D2,D2D2,D3D2,DET)
        CO11 = D2D2*D3DP-D3D2*D2DP
        CO12 = -(D2D1*D3DP-D2DP*D3D1)
        CO13 = D2D1*D3D2-D3D1*D2D2

        CO21 = -(D1D2*D3DP-D3D2*D1DP)
        CO22 = D1D1*D3DP-D3D1*D1DP
        CO23 = -(D1D1*D3D2-D3D1*D1D2)

        CO31 = D1D2*D2DP-D2D2*D1DP
        CO32 = -(D1D1*D2DP-D2D1*D1DP)
        CO33 = D1D1*D2D2-D2D1*D1D2

        DET = D1D1*CO11 + D1D2*CO12 + D1DP*CO13
*         WRITE(*,*) 'DET'
*         WRITE(*,*) DET
        D1D1 = CO11/DET
        D1D2 = CO21/DET
        D1DP = CO31/DET

        D2D1 = CO12/DET
        D2D2 = CO22/DET
        D2DP = CO32/DET

        D3D1 = CO13/DET
        D3D2 = CO23/DET
        D3DP = CO33/DET
      RETURN
      END

C     Use Subroutine CUBIC as per other
```

```
C       ACAL1.DOC
C   This is a program to calculate the value of the vanderwaals 'a'
C   in a cylindrical pore for r1 varies from R-3 sigma/2 to R-sigma/2

    IMPLICIT DOUBLE PRECISION(A-Z)
    INTEGER I,J,K

    WRITE(*,*) 'ETA1',' SIGMA',' PORE SIZE IN NUMBER OF SIGMA'
    READ(*,*) ETA1,SIGMA,P
    R1=SIGMA*ETA1
    R=SIGMA*P

    WRITE(*,*) R,R1
C   CASE 1 r1 varies from R-3 sigma/2 to R-sigma/2

    A1=0.0
    PI=3.1415926535897932

    Z1=(SIGMA*SIGMA-(R-SIGMA/2.-R1)**2)
    WRITE(*,*) Z1
    Z1=DSQRT(Z1)
    WRITE(*,*) Z1
    DO 10 I=0,1000
      Z=I*Z1/1000.
C       WRITE(*,*) Z
      B=R1*R1+SIGMA*SIGMA-Z*Z
      B1=(R-SIGMA/2.)*(R-SIGMA/2.)
      B2=SIGMA*SIGMA-Z*Z
C       WRITE(*,*) B2
      IF(B2.EQ.0.0) THEN
        WRITE(*,*) 'B2 EQ 0'
        GO TO 15
      ENDIF

      B3=DSQRT(B2)
      A=(B-B1)/2./R1/B3
C       WRITE(*,*) A
      IF(A.GT.1.0) THEN
        WRITE(*,*) 'A.GT.1.0 ',Z,A
        A=1.0
      ENDIF
      IF(A.LE.-1.0) THEN
        WRITE(*,*) Z,A
        A=-1.0
      ENDIF
         F=DACOS(A)
         GO TO 17
15    F=PI

17    A1=F*DSQRT(SIGMA*SIGMA-(R-SIGMA/2.-R1)**2)/1000.+A1

10  CONTINUE
    A1=A1/4./(SIGMA**4)
```

```
      WRITE(*,*) 'A1= ',A1

      DO 20 J=0,1000
        Z1=DSQRT(SIGMA*SIGMA-(R-SIGMA/2.-R1)**2)
        Z=J*Z1/1000.
        DO 30 K=0,1000
          B=R1*R1+SIGMA*SIGMA-Z*Z
          B1=(R-SIGMA/2.)*(R-SIGMA/2.)
          B2=SIGMA*SIGMA-Z*Z
          IF(B2.EQ.0.0) GO TO 25
          B3=DSQRT(B2)
          A=(B-B1)/2./R1/B3
          IF(A.GT.1.0) THEN
            WRITE(*,*) 'AA GT 1.0 ',Z,A
            A=1.0
          ENDIF
          IF(A.LT.-1.0) THEN
            WRITE(*,*) Z, A
            A=-1.0
          ENDIF
          GO TO 27
   25     A=-1.0
   27     THETA=DACOS(A)*K/1000.
C          WRITE(*,*) Z, A,THETA

          C=R1*DCOS(THETA)
          C1=(R-SIGMA/2.)*(R-SIGMA/2.)
          C2=R1*R1*DSIN(THETA)*DSIN(THETA)
          C3=DSQRT(C1-C2)
          C4=C+C3
          F1=C4*C4+Z*Z
          F=1./F1/F1

          AA=F*Z1/1000.*DACOS(A)/1000.+AA

   30   CONTINUE
   20 CONTINUE

      AA=AA/4.
      WRITE(*,*) 'AA= ',AA

      Y=DSQRT(SIGMA*SIGMA-(R-SIGMA/2-R1)**2)

      DO 50 K=0,1000
        THETA=PI*K/1000.
        C=R1*DCOS(THETA)
        C1=(R-SIGMA/2.)*(R-SIGMA/2.)
        C2=R1*R1*DSIN(THETA)*DSIN(THETA)
        C3=DSQRT(C1-C2)
        C4=C+C3
        C5=C4*C4

        F1=SIGMA/2./C5/(C5+SIGMA*SIGMA)
        F2=Y/2./C5/(C5+Y*Y)
```

```
      F3=DATAN(SIGMA/C4)/2./C5/C4
      F4=DATAN(Y/C4)/2./C5/C4
      F=F1-F2+F3-F4
      AB=F*PI/1000.+AB

 50  CONTINUE

     AB=PI*(SIGMA-Y)/4./SIGMA**4-AB/4.
     WRITE(*,*) 'AB = ',AB


C    PART 2 i.e. z going from sigma to infinity

     DO 40 I=0,1000
       THETA=I*PI/1000.
       B=R1*DCOS(THETA)
       B1=(R-SIGMA/2.)*(R-SIGMA/2.)
       B2=R1*R1*DSIN(THETA)*DSIN(THETA)
       B3=DSQRT(B1-B2)
       A=B+B3
       F1=PI/4./A/A/A
       F2=SIGMA/2./A/A/(A*A+SIGMA*SIGMA)
       F3=DATAN(SIGMA/A)/2./A/A/A
       F=F1-F2-F3
C      WRITE(*,*) F1,F2,F3

       A2=F*PI/1000.+A2

 40  CONTINUE
     A2=A2/4.
     A3=PI/12./SIGMA/SIGMA/SIGMA-A2

     WRITE(*,*) A2,A3
     A4=A1-AA+AB+A3
     A5=A4*3.*SIGMA*SIGMA*SIGMA/PI
     WRITE(*,*) 'A/ABULK= ', A5,A4

     END
```

```
C       ACAL2.F
C    This is a program to calculate the value of the vanderwaals 'a'
C    in a cylindrical pore r1 varies from 0 to R-3sigma/2

     IMPLICIT DOUBLE PRECISION(A-Z)
     INTEGER I

     WRITE(*,*) 'ETA1',' SIGMA',' PORE SIZE IN NUMBER OF SIGMA'
     READ(*,*) ETA1,SIGMA,P
     R1=SIGMA*ETA1
     R=SIGMA*P

     WRITE(*,*) R,R1
C    CASE 2 r1 varies from 0 to R-3sigma/2

     A1=0.0
     PI=3.1415926535897932

     DO 10 I=0,1000
       THETA=I*PI/1000.
       B=R1*DCOS(THETA)
       B1=(R-SIGMA/2.)*(R-SIGMA/2.)
       B2=R1*R1*DSIN(THETA)*DSIN(THETA)
       B3=DSQRT(B1-B2)
       A=B+B3
       F1=A*A*A
       F=1./F1
C        WRITE(*,*) THETA,A,F
C        F3=2.*A*A*A
C        F=F1+F2/F3
      .A1=F*PI/1000.+A1

 10  CONTINUE

     A2=1./3.-SIGMA*SIGMA*SIGMA/16.*A1
     A3=A2*3.
     WRITE(*,*) 'A/ABULK ', A3,A1,A2

     END
```

```
C       ACAL3.F
C   This is a program to calculate the value of the vanderwaals 'a'
C   in a cylindrical pore r1 =  R-sigma/2

    REAL ETA1,SIGMA,P,R,R1,A,A1,A2

    WRITE(*,*) 'ETA1',' SIGMA',' PORE SIZE IN NUMBER OF SIGMA'
    READ(*,*) ETA1,SIGMA,P
    R1=SIGMA*ETA1
    R=SIGMA*P

    WRITE(*,*) R,R1
C   CASE 3 r1 =  R-sigma/2

    A1=0.0
    PI=3.1415927

    DO 10 I=0,100
      Z=I*SIGMA/100.
      B=SIGMA*SIGMA-Z*Z
      B1=SQRT(B)
      THETA=ACOS(B1/2./R1)

      F=THETA/4./SIGMA**4

C       WRITE(*,*) Z,A,F

      A1=F*SIGMA/100.+A1

 10  CONTINUE

    WRITE(*,*) 'A1= ',A1

    DO 20 J=1,100
      Z=J*SIGMA/100.
      B=SIGMA*SIGMA-Z*Z
      B1=SQRT(B)
      THETA=ACOS(B1/2./R1)

      C=2.*R1*R1+Z*Z
      C1=4.*R1*R1+Z*Z
      C2=C1**1.5
      C3=C/C2/Z/Z/Z
      write(*,*) C,C1,C2,C3
      IF(Z.EQ.SIGMA) GO TO 25
      C4=Z*TAN(THETA)/SQRT(C1)
      C5=ATAN(C4)
      GO TO 27
 25    C5=PI/2.
 27    C6=C3*C5
C       write(*,*) C3,C5,C6

      D1=R1*R1*SIN(2*THETA)
      D2=Z*Z*C1*(2.*R1*R1+Z*Z+2.*R1*R1*COS(2.*THETA))
```

```
      D3=D1/D2
C       WRITE(*,*) D1,D2,D3

      F=C6-D3

      A2=F*SIGMA/100.+A2
C         WRITE(*,*) Z, A,THETA

 20  CONTINUE
     A2=A2/4.

     AA=A1-A2
     WRITE(*,*) 'A2= ',A2,' AA= ',AA

C    PART 2 i.e. z going from sigma to infinity

     DO 40 I=0,2000
       Z=SIGMA+I*SIGMA/100.
       B=R1*R1+Z*Z
       B1=4.*R1*R1+Z*Z
       B2=B1**1.5

       F=B/B2/Z/Z/Z
       A3=F*SIGMA/100.+A3

 40  CONTINUE
     A3=A3*PI/8.
     A4=PI/24./SIGMA/SIGMA/SIGMA
     A5=A4-A3

     WRITE(*,*) A3,A4,A5
     A6=AA+A5
     A=A6*SIGMA*SIGMA*SIGMA*3./PI

     WRITE(*,*) 'A/ABULK= ', A6,A

     END
```

Appendix 3 - Properties of Gases

Table: Appendix 3 -1 Supercritical Ethylene

40 F				
P(Psia)	V(ft3/lb)	P(MPa)	V(cm3/mol	V (PR)
500	0.26035	3.447367	455.9669	443.6109
600	0.18181	4.13684	318.415	307.7956
700	0.04754	4.826313	83.2597	93.08558
800	0.04511	5.515787	79.0039	85.36646
900	0.04368	6.20526	76.49945	81.0538
1000	0.04267	6.894733	74.73058	78.03798
1100	0.04187	7.584207	73.32949	75.72067
1200	0.04122	8.27368	72.1911	73.84304
1300	0.04067	8.963153	71.22785	72.26802
1400	0.04019	9.652627	70.3872	70.91416
1500	0.03977	10.3421	69.65163	69.72904

60 F				
P(Psia)	V(ft3/lb)	P(MPa)	V(cm3/mol	V (PR)
500	0.29183	3.447367	511.0997	498.076
600	0.21835	4.13684	382.4097	371.1377
700	0.16006	4.826313	280.3229	271.7131
800	0.10129	5.515787	177.3954	175.101
900	0.05804	6.20526	101.649	109.1489
1000	0.05119	6.894733	89.65217	95.9797
1100	0.04821	7.584207	84.43312	89.38151
1200	0.04637	8.27368	81.21061	85.037
1300	0.04506	8.963153	78.91633	81.82833
1400	0.04404	9.652627	77.12994	79.3
1500	0.04322	10.3421	75.69383	77.225

Table: Appendix 3 -1 Supercritical Ethylene

80 F				
P(Psia)	V(ft3/lb)	P(MPa)	V(cm3/mol	V (PR)
500	0.31926	3.447367	559.1395	545.9039
600	0.24619	4.13684	431.1676	419.54
700	0.19172	4.826313	335.7709	326.25
800	0.14789	5.515787	259.0088	252.5661
900	0.11013	6.20526	192.8774	191.167
1000	0.08024	6.894733	140.5292	143.56
1100	0.06464	7.584207	113.208	117.688
1200	0.05726	8.27368	100.2829	104.796
1300	0.05314	8.963153	93.06733	97.089
1400	0.05049	9.652627	88.42622	91.807
1500	0.0486	10.3421	85.11615	87.86828
100 F				
P(Psia)	V(ft3/lb)	P(MPa)	V(cm3/mol	V (PR)
500	0.34426	3.447367	602.9236	589.77
600	0.27016	4.13684	473.1477	461.53
700	0.21611	4.826313	378.4866	368.65
800	0.17436	5.515787	305.3673	297.77
900	0.14072	6.20526	246.4515	241.692
1000	0.11315	6.894733	198.1665	196.747
1100	0.09162	7.584207	160.4597	161.9475
1200	0.079677	8.27368	139.5432	137.3667
1300	0.06737	8.963153	117.9892	121.2451
1400	0.06131	9.652627	107.3759	110.5723
1500	0.0572	10.3421	100.1779	103.106

Table: Appendix 3-2 Supercritical Methane

0 F				
P(Psia)	V(ft3/lb)	P(MPa)	V(cm3/mol	V (PR)
400	0.70345	2.757893	702.642	602.89
500	0.54934	3.447367	548.709	542.64
600	0.44659	4.13684	446.077	503.81
700	0.37323	4.826313	372.8013	476.417
800	0.31829	5.515787	317.9244	455.814
900	0.27569	6.20526	275.3733	439.614
1000	0.2418	6.894733	241.5223	426.457
1100	0.21431	7.584207	214.0638	415.5051
1200	0.1917	8.27368	191.4798	406.211
1400	0.15722	9.652627	157.0394	391.2046
1600	0.13293	11.03157	132.7773	379.533
1800	0.11561	12.41052	115.4772	370.137
120 F				
P(Psia)	V(ft3/lb)	P(MPa)	V(cm3/mol	V (PR)
400	0.9341	2.757893	933.0271	868.8
500	0.74051	3.447367	739.6594	738.296
600	0.61165	4.13684	610.9475	657.42
700	0.51978	4.826313	519.183	602.418
800	0.45106	5.515787	450.5419	562.4746
900	0.39777	6.20526	397.3131	532.0424
1000	0.3553	6.894733	354.8919	508
1100	0.3207	7.584207	320.3316	488.47
1200	0.29202	8.27368	291.6846	472.25
1400	0.24737	9.652627	247.0859	446.74
1600	0.21439	11.03157	214.1438	427.5
1800	0.18923	12.41052	189.0126	412.38

Table: Appendix 3-3 CO2

TC=	304.2	K		0.4576						
PC=	7.382	MPa		0.259						
OMEGA=	2.28E-01			44						
T	PSAT	VAPOR	LIQUID		density	density	Tr	Table: App	FUGV	FUGL
K	MPa	CM3/MOL	CM3/MOL		calc	exp		% error	MPa	MPa
250	1.761	961.51	41.08	42.12739	0.024343	0.023738	0.821828	2.549632	1.483	1.483
260	2.394	692.26	43.6	44.14209	0.022936	0.022654	0.854701	1.243327	1.937	1.937
270	3.182	500.83	46.92	46.6386	0.021313	0.021441	0.887574	-0.59974	2.463	2.463
280	4.149	360.28	51.58	49.92432	0.019387	0.02003	0.920447	-3.20992	3.058	3.058
290	5.32	252.72	58.92	54.76832	0.016972	0.018259	0.95332	-7.04631	3.716	3.716
295	5.99	206.55	64.79	58.48413	0.015434	0.017099	0.969757	-9.73278	4.067	4.067
300	6.721	161.64	74.5	64.62157	0.013423	0.015475	0.986193	-13.2596	4.431	4.43

Table: Appendix 3-4 Argon

TC=	150.9	K		0.5082						
PC=	4.898	MPa		0.2735						
OMEGA=	-4.00E-03			39.948						
T	PSAT	VAPOR	LIQUID		density	density	Tr		FUGV	FUGL
K	MPa	CM3/MOL	CM3/MOL		calc	exp		% error	MPa	MPa
120	1.221	655.59	31.19	34.47949	0.032062	0.029003	0.795229	10.54663	1.017	1.017
130	2.039	376.95	35.02	37.61764	0.028555	0.026583	0.861498	7.417602	1.58	1.58
140	3.189	215.42	41.75	42.62994	0.023952	0.023458	0.927767	2.107632	2.272	2.272
145	3.909	156.86	48.05	47.0394	0.020812	0.021259	0.960901	-2.10322	2.66	2.66
148	4.393	124.22	54.76	51.69137	0.018262	0.019346	0.980782	-5.60378	2.905	2.904
149	4.564	112.63	58.26	54.21695	0.017164	0.018444	0.987409	-6.93967	2.988	2.988
149.5	4.652	106.33	60.53	55.92608	0.016521	0.017881	0.990722	-7.60601	3.03	3.03

Table: Appendix 3-5 Propane

TC=	369.8	K		0.2204						
PC=	4.249	MPa		0.2753						
OMEGA=	1.52E-01			44.097						
T	PSAT	VAPOR	LIQUID		density	density	Tr		FUGV	FUGL
K	MPa	CM3/MOL	CM3/MOL		calc	exp		% error	MPa	MPa
273.15	0.4741	4278.3	78.78	83.06138	0.012694	0.012039	0.738643	5.434606	0.4281	0.4281
323.15	1.721	1126.5	97.55	97.97961	0.010251	0.010206	0.873851	0.440396	1.344	1.344
343.15	2.605	672.61	113.6	108.8859	0.008803	0.009184	0.927934	-4.14977	1.884	1.884
363.15	3.784	359.3	152.4	132.8868	0.006562	0.007525	0.982017	-12.8039	2.508	2.508

Table: Appendix 3-6 Methane

TC=	190.6	K		0.1611						
PC=	4.604	MPa		0.2877						
OMEGA=	1.10E-02			16						
T	PSAT	VAPOR	LIQUID		density	density	Tr	% error	FUGV	FUGL
K	MPa	CM3/MOL	CM3/MOL		calc	exp			MPa	MPa
150	1.048	970.57	41.24	44.5861	0.024248	0.022429	0.786988	8.113728	0.8827	0.8826
160	1.605	619.51	44.88	47.44554	0.022282	0.021077	0.839454	5.716443	1.279	1.279
170	2.348	399.33	50.25	51.34437	0.0199	0.019476	0.89192	2.177859	1.757	1.757
180	3.31	250.57	59.53	57.54882	0.016798	0.017377	0.944386	-3.32804	2.308	2.308
185	3.883	190.43	68.12	63.02782	0.01468	0.015866	0.970619	-7.47531	2.608	2.607
189	4.391	140.94	82.14	72.26927	0.012174	0.013837	0.991605	-12.017	2.857	2.857
190	4.526	123.46	89.56	78.10836	0.011166	0.012803	0.996852	-12.7866	2.921	2.921

Table: Appendix 3-7 Ethylene

TC= 282.4 K
PC= MPa
OMEGA=

T K	density calc	density exp	Tr	% error
269	0.012189	0.012938	0.95255	-5.78915
255	0.014574	0.014641	0.902975	-0.45762
241	0.016372	0.015908	0.853399	2.916771
225	0.018031	0.017078	0.796742	5.580279
211	0.019248	0.017965	0.747167	7.141664

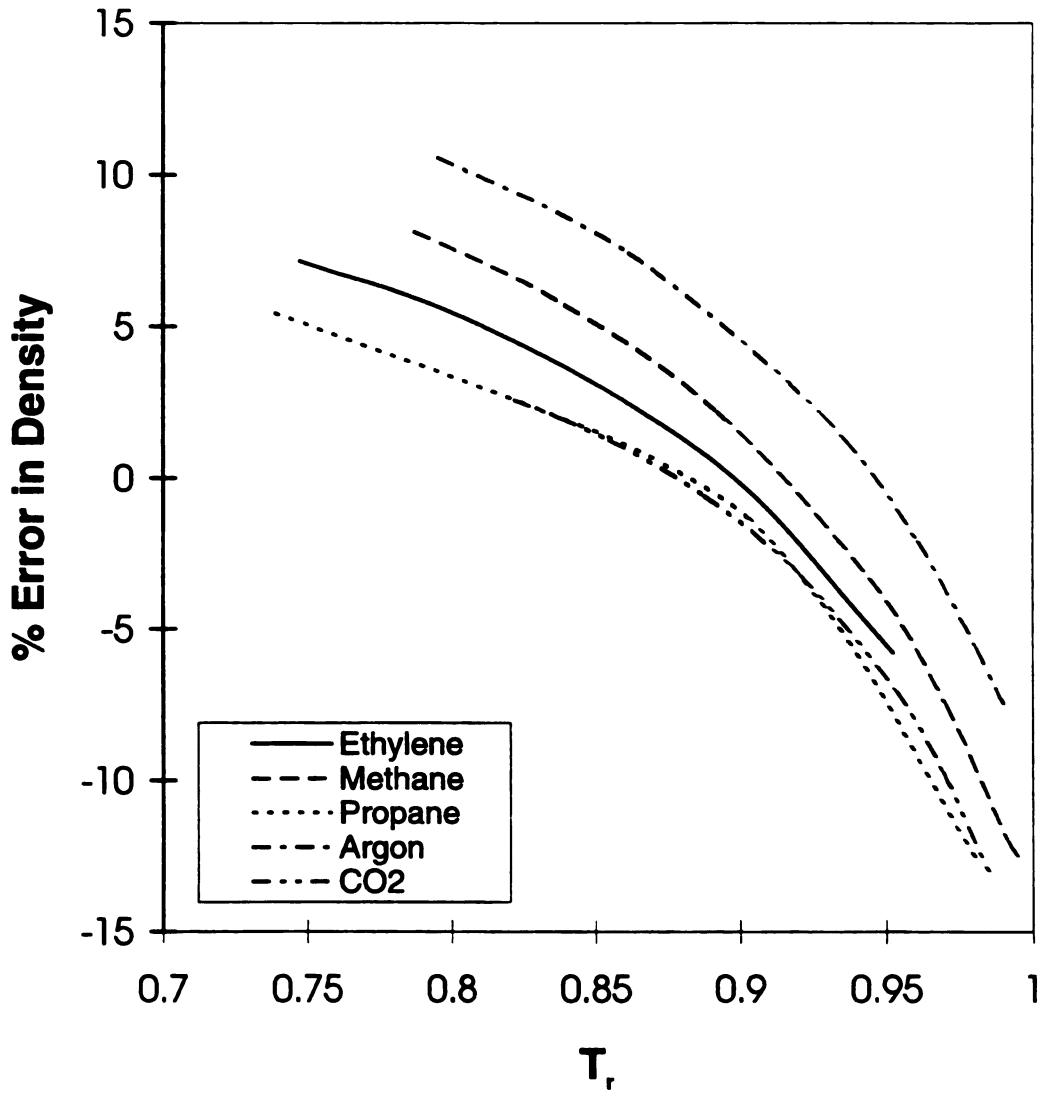

Figure Appendix 3-1: Error in the Peng-Robinson Calculation of Saturation Density

LIST OF REFERENCES

LIST OF REFERENCES

Abraham, F. F.; Singh, Y. *J. Chem. Phys.* **1978**, *68*, 4767.

Angus, S.; Armstrong, B.; de Reuck, K. M.; Featherstone, W.; Gibson, M. R. Eds., *International Union of Pure and Applied Chemistry*; Butterworths: London, **1974**, 39.

Asselineau, L.; Bogdanic G.; Vidal, J., *Fluid Phase Equil.* **1979**, *3*, 273.

Barrer, R. M.; Robins, A. B., *Trans. Faraday Soc.* **1951**, *47*, 773.

Barton, S. S.; Dacey, J. R.; Quinn, D. F. In *Fundamentals of Adsorption*, Myers, A. L.; Belfort, G. Eds., Engineering Foundation: New York, **1983**, 65.

Berenyi, L. *Z. Phys. Chem.*, **1923**, *105*, 55.

Bienfait, M. In *Phase Transitions in Surface Films*, Dash, J. G.; Ruvalds, J. Eds., Plenum Press: New York, **1980**, 29.

Brennecke, J. F.; Eckert, C. A. In *Supercritical Fluid Science and Technology;* Johnston, K. P.; Penninger, M. L. Eds., *ACS Symposium Series 406*, American Chemical Society: Washington DC, **1989**,14.

Brennecke, J. F. *Ph. D. Thesis,* University of Notre Dame, **1989**.

Brennecke, J. F.; Tomasko, D. L.: Peshkin, J.; Eckert, C. A. *Ind. Eng. Chem. Res.* **1990**, *29*, 1682.

Brunauer, S. *The Adsorption of Gases and Vapors Vol. 1*, Princeton University Press, Princeton: New Jersey, **1945**.

Davis, H. T.; Scriven, L. E. In *Advances in Chemical Physics*, Prigogine, I., Rice, S. A., Wiley: New York, **1982**, *49*, 357.

Debenedetti, P. G. *Chem. Eng. Sci.* **1987**, *42*, 2203.

de Boer, J. H. *The Dynamical Character of Adsorption*, Clarendon Press: Oxford, **1953**.

Defay, L.; Prigogine, I., *Surface Tension and Adsorption*, John Wiley, New York, **1966**.

Denbigh, K. *The Principles of Chemical Equilibrium*, 4th ed., Cambridge University Press: Cambridge, **1981**.

Dubinin, M. M. *Proc. Acad. Sci. USSR.* **1947**, *55*, 331.

Dubinin, M. M. *Progr. Surf. Membrane Sci.* **1975**, *9*, 1.

Eckert, C. A.; Ziger, D. H.; Johnston, K. P.; Ellison, T. K. *J. Phys. Chem.* **1986**, *90*, 2798.

Evans, R. *Advances in Physics* **1979**, *28*, 143.

Findenegg, G. H. In *Fundamentals of Adsorption*, Myers, A. L., Belfort, G. Eds., Engineering Foundation: New York, **1983**, 207.

Fisher, B. B., McMillan, W. G. *J. Am. Chem. Soc.*, **1957**, *79*, 2969.

Fisher, J.; Methfessel, M. *Phys. Rev. A.* **1980**, *22*, 2836.

Gregg, S. J.; Sing, K. S. W. *Adsorption, Surface Area and Porosity*, Academic Press: London, **1982**.

Guggenheim, *Thermodynamics*, 5th ed., North-Holland Publishing: Amsterdam, **1967**.

Henderson, D. *Fundamentals of Inhomogeneous Fluids*; Marcel Dekker: New York, **1992**.

Hill, T. L. *J. Chem. Phys.* **1946**, *14*, 441.

Hill, T. L. *J. Chem. Phys.* **1947**, *15*, 767.

Hill, T. L. *J. Chem. Phys.* **1948**, *16*, 181.

Hill, T. L. *J. Phys. Chem.* **1950**, *54*, 1186.

Hill, T. L. *J. Chem. Phys.* **1951**, *19*, 261.

Hill, T. L. In *Advances in Catalysis*, Frankenburg, W. G.; Rideal, E. K.; Komarewsky, V. I. Eds., Academic Press: New York, **1952**, *4*, 211.

Johnston, K. P.: Kim, S.; Combs, J. In *Supercritical Fluid Science and Technology;* Johnston, K. P.; Penninger, M. L. Eds. ACS Symp. Ser. 406, American Chemical Society: Washington DC, **1989**.

Kierlik E.; Rosinberg, M. L. *Phys. Rev. A*. **1990**, *42*, 3382.

Kierlik E.; Rosinberg, M. L. *Phys. Rev. A*. **1991**, *44*, 5025.

Kim, S.; Johnston, K. P. *Ind. Eng. Chem. Res*. **1987a**, *26*, 1206.

Kim, S.; Johnston, K. P. *AIChE J.* **1987b**, *33*, 1603.

Kung, W. C.; Scriven, L. E., Davis, H. T. *Chem. Phys.* **1990**, *149*, 141.

Lee, L. L. *Molecular Thermodynamics of Non-Ideal Fluids*; Butterworths: Stoneham, MA, **1988**.

Lee, L. L.; Debenedetti, P. G.; Cochran, H. D. In *Supercritical Fluid Technology: Reviews in Modern Theory and Applications*, Bruno, T. J.; Ely, J. F. Eds., CRC Press: Boca Raton, Fl, **1991**, 193.

Lennard-Jones, J. E.; Devonshire A. F. *Proc. Royal Soc. A* **1937**, *163*, 132.

Maslan. F. D.; Altman, M.; Abereth, E. R. *J. Phys. Chem.* **1953**, *57*, 106.

McQuarrie, D. A. *Statistical Mechanics*; Harper & Row: New York, **1976**.

Myers, A. L.; Prausnitz, J. M. *AIChE J.* **1965**, *11*, 121.

Nicholson, D.; Parsonage, N. G. *Computer Simulation and Statistical Mechanics of Adsorption*, Academic Press: New York, **1982**.

Peng, D. Y.; Robinson, D. B. *Ind. Eng. Chem. Fund.* **1976**, 15, 59.

Polyani, M. *Trans. Faraday Soc.* **1932**, *28*, 316.

Powles, J. G.; Rickvayzen, G.; Williams M. L., *Mol. Phys.* **1988**, *64*, 33.

Prausnitz, J. M. *Proceedings of the 2nd International Conference*, EFCE, DECHEMA: Berlin, **1980**.

Prausnitz, J. M., Liechtenthaler, R. N., de Azvedo, E. G. Molecular Thermodynamics of Fluid Phase Equilibria, Prentice-Hall, Englewood-Cliffs: New Jersey, **1986**.

Pyada, H. *Masters Thesis*, Michigan State University, **1994**.

Radke C. J., Prausnitz, J. M. *AIChE J.* **1972**, *18*, 761.

Rangarajan, B.; Lira, C. T. In *Better Ceramics Through Chemistry V*, Hampden-Smith, M. J., Kemperer, W. G., Brinker, C. J. Eds. , Materials Research Society: Pittsburgh, PA, **1992**, 559.

Rangarajan, B.; Lira, C. T.; Subramanian, R. *AIChE J.* **1995**, *41*, 838.

Reich, R., Ziegler, W. T., Rogers, K. A. *Ind. Eng. Chem. Proc. Des. Dev.***1980**, *19*, 336.

Reid, R. C.; Prausnitz, J. M.; Poling, B. *The Properties of Gases and Liquids*, 4th ed., McGraw-Hill: New York, **1987**.

Ross, S., Clark H., *J. Am. Chem. Soc.* **1954**, 76, 4291.

Ross, S.; Olivier, J. P. *On Physical Adsorption*, Interscience Publishers: New York, **1964**.

Rowlinson, J. S.; Widom, B. *Molecular Theory of Capillarity*, Clarendon Press: Oxford, 1982.

Saam, W. F.; Ebner, C. *Phys. Rev. A.* **1978**, *17*, 1768.

Sandler, S. L. *Chemical and Engineering Thermodynamics*, 2nd ed., Wiley: New York, **1989**.

Snook, I. K.; Henderson, D. *J. Chem. Phys.* **1978**, *68*, 2134.

Specovius J.; Findenegg, G. H. *Ber. Bunsenges Phys. Chem.* **1978**, *82*, 174.

Specovius J.; Findenegg, G. H. *Ber. Bunsenges Phys. Chem.* **1980**, *84*, 690.

Steele, W. A. In *The Solid-Gas Interface Vol 1*, Flood, E. A. Ed., Marcel Dekker: New York, **1967**, 307.

Steele, W. A. *The Interaction of Gases with Solid Surfaces*, Pergamon Press: Oxford, **1974**.

Strubinger, J. R.; Parcher, J. F. *Anal. Chem.* **1989**, *61*, 951.

Subramanian, R.; Pyada H.; Lira, C. T. *Ind. Eng. Chem. Res.* (in press).

Sullivan, D. E. *Phys Rev. B.* **1979**, *20*, 3991.

Tan, C. -S.; Liou, D. -C. *Ind. Eng. Chem. Res.* **1988**, *27*, 988.

Tan, C. -S.; Liou, D. -C. *Ind. Eng. Chem. Res.* **1990**, *29*, 1412.

Tan, Z.; Gubbins, K. E. *J. Phys. Chem.* **1990**, *94*, 6061.

Tarazona, P.; Evans, R. *Mol. Phys.* **1983**, *48*, 799.

Teletzke, G. F.; Scriven, L. E.; Davis, H. T. *J. Colloid Interface Sci.* **1982a**, *87*, 550.

Teletzke, G. F.; Scriven, L. E.; Davis, H. T. *J. Chem. Phys.* **1982b**, *77*, 5794.

Telo de Gama, M. M.; Evans, R. *Mol. Phys.* **1983**, *48*, 687.

Tjatopolous, G. J.; Feke, D. L.; Adin Mann, Jr., J. *J. Phys. Chem.* **1988**, *192*, 4006.

Valenzuela, D. P., Myers, A. L. *Adsorption Data Handbook*, Prentice-Hall, Englewood-Cliffs: New Jersey, **1989**.

Vanderlick, T. K.; Scriven, L. E.; Davis, H. T. *J. Chem. Phys.* **1989**, *90*, 2422.

van Megen, B.; Snook, I. K. *Mol. Phys.* **1982**, *45*, 629.

van Megen, B.; Snook, I. K. *Mol. Phys.* **1985**, *54*, 741.

Vera, J. H.; Prausnitz, J. M. *Chem. Eng. J.* **1972**, *3*, 1.

Wu, R. -S.; Lee, L. L.; Cochran, H. D. *Ind. Eng. Chem. Res.* **1990**, *29*, 977.

Yang, R. T. *Gas Separation by Adsorption Processes*, Butterworths, Stoneham, MA, **1987**.

Young, D. M.; Crowell, A. D. *Physical Adsorption of Gases*, Butterworths, London, **1962**.

MICHIGAN STATE UNIV. LIBRARIES
31293014107431